Metabolism of Nicotine and the Tobacco Carcinogen 4-(methylnitrosamino)-1-(3-pyridyl)-1-butanone (NNK): Genetic and Phenotypic Variation

A DISSERTATION
SUBMITTED TO THE FACULTY OF THE GRADUATE SCHOOL
OF THE UNIVERSITY OF MINNESOTA
BY

Jeannette Zinggeler Berg

IN PARTIAL FULFILLMENT OF THE REQUIREMENTS
FOR THE DEGREE OF
DOCTOR OF PHILOSOPHY

Sharon E. Murphy, PhD; Advisor

October 2009

ACKNOWLEDGEMENTS

First and foremost, I thank Dr. Sharon Murphy -- I am thankful and honored that you indulged me with your wisdom and guidance. You've shared your bountiful knowledge of enzymes, metabolism, and analytical approaches with me and have challenged me to think and communicate as a biochemist. From deciding on which scientific questions to pursue to the design and execution of specific experiments you've allowed me to make mistakes and have patiently helped me to learn from them, thus substantially developing my independence as a research scientist. Also, I have learned from how you lead your laboratory: you ask probing questions about the experiments being conducted, have reasonable expectations, and care about each person as an individual.

In addition, I thank my PhD thesis committee members Dr. John Lipscomb (chair), Dr. Alex Lange, and Dr. Tim Tracy for their academic guidance, insightful scientific feedback, as well as time contributed to meeting with me, attending seminars, and reading this thesis.

I thank present and former members of the Murphy lab for their unwavering camaraderie. The many hours I've spent in the lab have been particularly enjoyable because it is a fun and interesting group. To Linda, Kari, and Gwen: thank you also for answering my questions, offering the occasional unsolicited but needed advice, and sharing protocols, reagents, and lab duties. Linda you have been a steadfast supporter and a wonderful friend throughout; thanks for everything, from guiding me through LC/MS experiments to unexpectedly landing me a beautiful horse! Val, we were thrilled that you joined our group, and I hope you may have another counterpart soon ☺ I've had help from a truly amazing group of undergraduates and pre-meds -- I thank Katie Lee, Jodi Blustin, Jessica van Lengerich, and Natalie Weisensel (what a powerhouse of energy and intellect!) I owe a huge debt of gratitude to Elizabeth Thompson, Katie Wickham, and Nicole Thomson for their leading roles in analyzing and organizing several hundred samples for the nicotine metabolism studies. I thank Cassie Retzlaff for spending a good part of her summer in the lab, and quickly becoming a knowledgeable and productive member of the TTURC group. Also, I thank Greg Blaufuss and Aleks Knezevich for assisting with analyzing samples. I thank Angela Boettcher for expertly managing the nicotine patch data before moving on to sunny California. The *in vivo* metabolism studies are definitely the 'team sport' of the Murphy lab and we've got a strong pass, shoot, score, game.

I am grateful for the friendship and generous support of *many* cancer center neighbors! I especially acknowledge and thank Drs. Chris Pennell, Stephen Hecht, and Tucker LeBien for being fantastic scientific role-models and also for kindly allowing me frequent use of their space, instrumentation, and occasional reagents. I thank Peter Villalta and Brock Matter, Steve Carmella, Brad Hochalter, Michelle Jund, and Sonja Nodland for their expert advice in mass spectrometry, HPLC, chemistry, molecular biology, and cell biology respectively. I thank Bob Carlson for helping me at a

moment's notice, whether it's to solve a computer problem, to edit a document, or to clarify an order issue. I thank Sabine Fritz for being quick and resourceful about addressing any facility issue. The Cancer Center is a remarkable place, and it seems to me that under the leadership of Dr. John Kersey, a culture of scientific altruism developed and it is flourishing.

I thank Dr. Hatsukami for her interest in and support of the nicotine metabolism biomarker studies. I thank Joni Jensen for promptly answering my questions about study participants, protocols, and for helping me to find data.

I thank Drs. Tim Tracy and Rory Remmel and their lab members for welcoming Val and I to friday journal club; I always learn from discussions with your group! I also thank Dr. Tracy for kindly allowing me to come to the lab to perform reduced CO difference spectra and for the gift of chaperone plasmids.

I thank the University of Minnesota MD/PhD program for encouragement throughout the PhD phase: Dr. Tucker LeBien, Dr. Peter Bitterman, Susan Shurson, Nick Berg, and Sandi Sherman. MSTP (T32-GM08244)

There are several labs beyond the University of Minnesota that have generously provided me with biologic reagents. I thank Dr. Emily Scott and Natasha DeVore, Univ. of Kansas, for collaborating with us on assessing CYP2A7 activity and for our discussions relating to this effort. I thank Dr. Philip Lazarus, Penn State Univ., for UGT2B7-expressing HEK cells; Dr. Robert Tukey, Univ. of California San Diego, for UGT1A9 plasmid; and Dr. Moshe Finel, Univ. of Helsinki, for UGT2B17 plasmid.

I acknowledge funding support from: (1) Ruth L. Kirschtein National Research Service Award Individual Fellowship, Title: P450-mediated Nicotine Metabolism (F30DA020968), National Institute on Drug Abuse; (2) Biochemistry, Molecular Biology, and Biophysics; (3) Dr. Jasjit Ahluwalia, Office of Clinical Research.

I acknowledge the encouragement of my husband and family to pursue my dreams. I am deeply grateful to my parents, Margrit and Robert, for nurturing my interest in all things biological, and for emphasizing education as a critical means to understanding the living world better. Bringing home toads and turtles turned into trips to the herpetological society meetings and other opportunities, such as looking at whatever would fit (and stay) on the slide of our microscope. Therefore, I especially acknowledge your long-standing support of my science education. My brother Yves is always an inspiration to me, in no small part for being unequivocally more focused, organized, disciplined, and ambitious. To my husband, I thank you for believing in me, for valuing my goals, and for being selflessly accommodating. I couldn't imagine being more in love or feeling more loved and this is a deep source of happiness for me – you are a miracle in my life.

DEDICATION

To my loving husband Michael Berg, in memory of Russell Berg, for sharing with me the hope and expectation that research will yield insights to better prevent and treat lung cancer

ABSTRACT

Nicotine is the addictive agent in tobacco and differences in nicotine metabolism may affect tobacco use, and consequently exposure to tobacco carcinogens. A lung procarcinogen in tobacco is 4-(methylnitrosamino)-1-(3-pyridyl)-1-butanone (NNK) and its carcinogenic effect is dependent on metabolic activation and is counter-balanced by metabolic detoxification. Nicotine and NNK are structurally related and both are metabolized by cytochrome P450 (P450), UDP-glucuronosyltransferase (UGT), and flavin-monoxygenase (FMO) enzymes. The goal of this thesis research was to explore variation in nicotine metabolism *in vivo* and to probe specific enzyme-catalyzed reactions of NNK *in vitro*.

The role of glucuronidation on variation in nicotine metabolism and smoking behavior is not well characterized. In a controlled dose study of ethnic differences in nicotine metabolism (n= 93 smokers), African Americans excreted 30-40 % less nicotine and cotinine as their glucuronide conjugates than European Americans. This difference in glucuronidation explained the higher free cotinine concentrations observed in African Americans compared to European Americans in the controlled dose setting. The most efficient *in vitro* catalyst of nicotine and cotinine glucuronidation is UGT2B10. In human liver microsomes (n=28), UGT2B10 genotype for the Asp67Tyr polymorphism was a better predictor of glucuronidation than ethnicity. Subsequently, we demonstrated that UGT2B10 contributes to *in vivo* nicotine metabolism in a genotype-phenotype analysis of 325 smokers. Individuals who were heterozygous for the UGT2B10 Asp67Tyr allele excreted less nicotine or cotinine as their glucuronide

conjugates than wild-type; the ratio of cotinine glucuronide:cotinine was decreased by 60 %, while increases in urinary and plasma cotinine and trans-3'-hydroxycotinine were observed. Strikingly, a robust biomarker of nicotine intake, nicotine equivalents, were lower among Asp67Tyr heterozygotes compared to individuals without this allele; 58.2 nmol/ml (95 % CI, 48.9 – 68.2) versus 69.2 nmol/ml (95 % CI, 64.3 – 74.5). Individuals with low activity UGT2B10 may smoke less intensely, as reported for individuals with CYP2A6 polymorphisms that cause decreased nicotine C-oxidation.

In contrast to nicotine, NNK is a carcinogen. It is metabolized to reactive intermediates that can form DNA and protein adducts, or it is detoxified by glucuronidation. P450 2A13 is the most efficient catalyst of NNK oxidation. We explored the effect of an active site mutant, Asn297Ala, on enzyme function and found that loss of hydrogen bonding to substrate in the active site affected substrate orientation and product formation. The orphan P450 2A7 was considered as a potential catalyst for NNK oxidation, but expression of wild-type or two naturally-occurring variants failed to yield protein with a P450 spectra and no appreciable activity towards P450 2A substrates was observed. Preliminary experiments were conducted to search for the glucuronide conjugate formed from the unstable oxidation product α-hydroxymethyl NNK, which has not been identified in any human system.

The extent to which variation in metabolism mediates smoking behavior and cancer risk warrants consideration. The enzymes involved are potential drug targets for smoking cessation pharmacotherapy and cancer chemoprevention.

TABLE OF CONTENTS

LIST OF FIGURES

LIST OF TABLES

CHAPTER 1

Introduction

1.1 Tobacco use and health consequences

Tobacco use is a global public health problem that leads to over 5 million deaths per year and shortens life expectancy by an average of 15 years (1). Smoking increases risk of several cancers, chronic obstructive pulmonary disease, respiratory infections, asthma, ischemic heart disease, and cerebrovascular disease (2). There is growing recognition that smokeless tobacco use also increases risk of cancers, ischemic heart disease, and cerebrovascular disease. Importantly, health risks are attenuated after quitting, even after years of tobacco use (3) Health risks from secondhand smoke exposure are lower than for smokers but also result in smoking-associated diseases, as listed above (4;5). Tobacco is considered a major preventable cause of morbidity and mortality, but it is a challenging problem. Preventing or successfully treating addiction to tobacco products is imperative.

There are more than a billion smokers worldwide. In developed countries, 35 percent of men and 22 percent of women smoke (6). In developing countries, 50 percent of men and 9 percent of women smoke (6). Also, children and adolescents use tobacco and very few people take up smoking after age 21 (1). The tobacco industry spends over 10 billion dollars on product promotion and aggressively targets new and

expanding markets (6). Broadly, these potential markets include youth, women, developing countries, and smokeless products in areas with smoke-free policies. Current approaches to decrease tobacco use include smoke-free legislation, taxes on tobacco products to raise prices, bans on product promotion, education outreach, warning labels, and accessible quit programs.

Anti-smoking policies and increased awareness of health risks have resulted in a decrease in tobacco use in the United States, though ~20 % of the population continues to use tobacco regularly (7). Notably, 20 % of high school students smoke, based on the number of students who reported smoking at least 20 days per month in 2007 (8). Half of adults who have a history of smoking have succeeded in quitting (3). Indeed, the majority of smokers are interested in quitting and around 70 % of smokers report a quit attempt in the past year (9;10) However, only 58 % of smokers who tried quitting were abstinent for more than a single day and less than 20 % maintained abstinence at six months (9)!

There are several challenges to further decreasing tobacco use in the U.S. Only 1 of every 5000 dollars collected in tobacco tax revenue is spent on tobacco control (1). Meanwhile, tobacco companies are actively developing new products and marketing strategies to promote tobacco use. Adolescents continue to access tobacco products, and later encounter the difficulties of quitting (11). Pharmaceuticals to aid cessation are only moderately effective as currently used. Health insurance companies are reluctant to consider tobacco use as a chronic condition requiring long term treatment (12).

Addressing the tobacco problem also involves developing approaches to reduce disease in tobacco users, former users, and individuals exposed to environmental tobacco smoke. In the US, 81 billion dollars per year are currently spent on taking care of tobacco-associated diseases (1). The cost of routine care is a significant challenge, and yet investment in novel diagnostic and treatment modalities could improve health outcomes significantly.

1.2 Tobacco use and cancer

The International Agency for Research on Cancer (IARC) of the World Health Organization reviewed reports from laboratory animal toxicology studies to epidemiology studies and concluded that tobacco increases the risk of several cancers. There is sufficient evidence that cancers of the lung, larynx, nasal cavity, oral cavity, esophagus, liver, pancreas, bladder, cervix, and leukemia are associated with tobacco use (13). The US Surgeon general reported that smoking was the primary causal factor in 30 % of cancer deaths (2). Over 60 known carcinogens are present in tobacco smoke (14). Tobacco smoke is a complex mixture, and yet certain constituents have a remarkable predilection for causing specific cancers in laboratory animals.

About 90 % of lung cancers are attributable to smoking (2). Lung cancer is the second most common cancer and the leading cause of cancer death in the United States (15). In 85 % of cases, lung cancer is diagnosed after regional spread or metastasis has occurred. Risk of lung cancer increases with the number of cigarettes smoked per day

and with more years of smoking. Overall, about 16-18 % of lifelong smokers develop lung cancer (16;17). An estimated 3000 deaths from lung cancer per year also occur in nonsmokers exposed to secondhand smoke in the U.S. (5). Lung cancer is a well-recognized risk of smoking among the US public, though young people in particular underestimate risk of dying from lung cancer (18).

1.3 Nicotine and tobacco use

Nicotine is the addictive agent in tobacco products and it is the primary reason why people continue their use. Nicotine accumulates in tobacco plant leaves to up to 3 % of the dry weight. It serves the plant as a natural pesticide; nicotine is an alkaloid that acts as an acetylcholine analog that is toxic to insects (19). In laboratory animals and human smokers and nonsmokers, nicotine has psychoactive effects that reinforce its use (20;21). Smokers will self-administer intravenous nicotine over placebo (22). When switched to low nicotine cigarettes, smokers extract more nicotine per cigarette and smoke more cigarettes (23-25). Abstinent smokers who receive the nicotine patch have less craving than those who received placebo (26). The pharmacologic effects of nicotine were investigated, in part, by the tobacco industry and in a 1971 Phillip Morris document it was stated, "the cigarette should be conceived not as a product but as a package. The product is nicotine."

The effects of nicotine are related to blood levels of nicotine and the kinetics of exposure. Rapid delivery of nicotine to the brain causes the effects that tobacco users

seek, namely relaxation, reduced stress, and pleasant mood (27). In the case of smoking, nicotine is efficiently absorbed into the pulmonary circulation and it reaches the brain in 10-20 seconds where it binds nicotinic cholinergic receptors (27). Due to widespread distribution of receptors and the existence of various receptor subtypes, the effects of nicotine in the brain are complex and are mediated by dopinergic and non-dopinergic neurons (28). As nicotine levels fall, withdrawal symptoms arise and these include nervousness, restlessness, irritability, and anxiety (29). Though smokers seek the favorable effects of nicotine that occur when nicotine levels peak, their smoking behavior more closely corresponds to maintaining a threshold concentration in blood (30). Maintaining a nicotine threshold alleviates development of withdrawal symptoms. Since the half-life of nicotine is relatively short, about 2 hours, smokers use cigarettes repeatedly during the day and awaken in the morning with an urge to smoke (29).

The rate of decline in nicotine concentrations is predominantly a function of metabolism, as well as renal clearance. Less than 5% of nicotine is protein-bound (29). Nicotine is metabolized rapidly and extensively in the liver, though some metabolism occurs in other tissues including the lungs and kidneys (29). Enzymes capable of metabolizing nicotine are also present in brain (31). Nicotine is metabolized by C-oxidation, N-oxidation, or glucuronidation and these metabolic pathways are described in detail in Chapter 2. The major metabolites do not have psychoactive properties. Nicotine and its metabolites are predominantly excreted in urine. Typically, 10 % of nicotine is excreted unchanged in a 24-hour period (32). Higher concentrations of nicotine are excreted in urine shortly after smoking. The rate of nicotine metabolism and the distribution of metabolites vary among different individuals (33).

1.4 4-(methylnitrosamino)-1-(3-pyridyl)-1-butanone (NNK)

NNK is structurally related to nicotine, as it is a nitrosated product of nicotine formed during the tobacco curing process (Figure 1-1). NNK is an abundant nitrosamine in processed tobacco, albeit 1000-fold lower than nicotine (10 μg NNK/cigarette compared to 10 mg nicotine/cigarette) (14). NNK is found only in tobacco and it is therefore referred to as a tobacco-specific nitrosamine.

NNK is designated a class I carcinogen by the IARC, indicating that it is a likely carcinogen in humans. In contrast, nicotine is not a carcinogen. NNK induces tumors in lung, liver, pancreas, and nasal cavity in various species of rodents (34). In rats, induction of lung adenocarcinomas occur independent of route of administration including exposure through treated drinking water (35). Metabolism of NNK is required for carcinogenesis, which is described in detail in Chapter 6. NNK exposure has been documented by the detection of NNK metabolites in smokers' urine and toenails, as well as in urine samples from populations exposed to environmental tobacco smoke (e.g. casino workers, children of smokers) (36-39). DNA adducts that would be consistent with electrophilic attack from an NNK metabolite have been detected at higher levels in clinical lung cancer samples than in controls (40). Overall, NNK exposure is predicted to have a cumulative effect, with decades of low exposure translating to an increased cancer risk in susceptible individuals (14).

Figure 1-1. Structure of nicotine and NNK

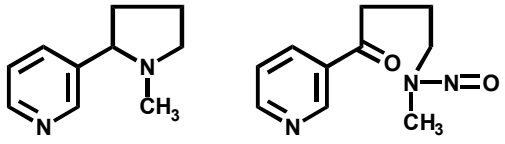

Nicotine **NNK**

1.5 Other tobacco constituents

Tobacco contains thousands of chemicals, that are either naturally present or have been added during processing. A few of these tobacco constituents are worth highlighting. Additives like menthol influence brand preference and possibly other aspects of smoking behavior (e.g. depth of inhalation) (41;42). Some constituents may induce or inhibit the enzymes that metabolize nicotine and NNK (e.g. polyaromatic hydrocarbons, menthofuran, carbon monoxide)(43-45). Co-exposure to various chemicals in tobacco may modify the biological outcomes. There are about 60 carcinogens in tobacco smoke tobacco including benzo[a]pyrene, *N*'-nitrosonornicotine, benzene, formaldehyde, 4-aminobiphenyl, vinyl chloride, arsenic, and cadmium (13). Levels of several tobacco constituents vary substantially between different tobacco products and are not regulated (46).

1.6 Cytochrome P450 Enzymes (P450s)

Nicotine and NNK are metabolized by enzymes which are members of the cytochrome P450 (P450) superfamily. An overview of these enzymes is provided here

and discussion of the specific enzymes involved in nicotine and NNK metabolism is covered in later chapters.

P450 enzymes are heme monoxgenases that catalyze diverse oxidation reactions and are biologically important for their roles in the metabolism of both exogenous and endogenous small molecules. Broadly, cytochrome P450 enzymes (P450s) biosynthesize endogenous molecules, inactivate/activate compounds with biological activity, and increase the hydrophilicity of compounds which facilitates their excretion and prevents toxic accumulation (47;48). This ancient family includes more than 8500 genes that have been identified in animals, plants, fungi, unicellular eukaryotes, and bacteria. Sequence homology is used to classify enzymes into families and subfamilies, greater than 59 % and 70 % similarity, respectively (49). Some cytochrome P450 enzymes (P450s) fulfill a vital role for the organism and thus their disruption is lethal (50). The disruption of other enzymes can have negligible effects; the enzyme may protect the organism only under certain exposure conditions or redundancy in metabolic pathways may prevent any toxicity (51). Nonfunctional P450 pseudogenes have also been identified, particularly as evolutionary relics among higher eukaryotes (49).

Human cytochrome P450s contribute to normal development and homeostasis by metabolizing lipids, steroids, vitamins, eicosanoids, retinoids, prostaglandins, and xenobiotics (52). There are 57 cytochrome P450 genes (CYP) as well as 58 pseudogenes that have evolved from several gene duplication and deletion events (53;54). The enzymes are membrane-bound in the endoplasmic reticulum, though six are exclusively found in mitochondria (55). Regulatory networks including nuclear

receptors and transcription factors define the tissue-specific distribution of individual P450s, and modulate constitutive and inducible expression (56-59). Xenobiotic-metabolizing P450s are highly polymorphic and this leads to variation in the levels of enzymes and catalytic function. Furthermore, P450 activity is affected by exposure to inhibitors. Over 90 % of drugs on the market are metabolized by a relatively small number of cytochrome P450s, listed here in order of their relative contribution to drug metabolism: 3A4/3A5 > 2D6 > 2C9 > 2C19 > 2E1 ≈ 1A2 (55;60). The role of these enzymes is widely studied to predict the potential for adverse reactions and variation in drug efficacy.

Cytochrome P450s have characteristic absorbance spectra. P450 refers to a pigment absorbing at 450 nm which can be observed for these heme-containing proteins when carbon monoxide is bound to reduced enzyme (61). The absorption maximum at 450 nm depends on properly incorporated heme, with the heme iron coordinated to the P450 protein through a cysteine thiolate and stabilized by interactions between the heme and other P450 residues. Carbon monoxide difference spectra are routinely used to quantify the amount of P450 enzyme that is grossly intact from a catalytic perspective. Substrate binding to P450s can be analyzed by following changes in the UV-vis heme Soret spectrum that result from displacement of water or an amino acid ligand from the heme iron (type I spectrum), or from direct coordination of substrate to the heme iron (type II spectrum) (62) .

Cytochrome P450s catalyze a range of oxidative reactions. The heme iron-mediated chemistry of catalysis, the role of key amino acids, and the mechanisms of specific

P450 reactions have challenged many investigators. Reactions catalyzed by P450s include hydrocarbon hydroxylation, heteroatom oxidation and dealkylation (heteroatom release), aromatic ring oxidation, acetylene oxidation, dehydrogenation, carbon-carbon bond cleavage, and radical cross-linking of substrates (63;64).

A general catalytic cycle for cytochrome P450s is depicted in Figure 1-2 and is summarized below. Binding of substrate in a productive orientation displaces the 6^{th} axial ligand of the heme iron (e.g. a water molecule) generating a penta-coordinated iron-heme-thiolate complex (**2**) that is a better electron acceptor than the resting species (**1**). Also, changes in the spin state can result in a more positive redox potential (65). Catalysis requires the transfer of two electrons to the P450 enzyme, and in nature NADPH is the electron source and P450 oxidoreductase transfers the electrons. Cytochrome b5 can also transfer the second electron. However, recently the transfer of electrons from a gold electrode to bonded purified P450 was achieved and conversion of substrate to product was observed (66). Of note, substrate can bind and dissociate at different stages of the catalytic cycle (67;68). Futile cycling and generation of hydrogen peroxide can also occur (69).

Through a series of steps an oxygen atom derived from molecular oxygen is transferred to the substrate. Molecular oxygen binds readily to the ferrous heme species (**3**) in an end-on complex (**4**). A second electron reduction generates ferric-dioxygen which is a strong base that undergoes protonation by a water molecule to form a Fe^{3+}-hydroperoxy complex (**5**). A local network of amino acids facilitate further protonation, cleavage of the O-O bond, and formation of water and a reactive iron-oxo intermediate

(**6**). The heme contributes to shuttling protons and accepting electrons. The substrate is activated – the mechanism depends on its structure– and oxygen is transferred to the substrate (**7**). For instance, a typical hydroxylation reaction may occur by abstraction of hydrogen from the substrate, formation of a short-lived radical, substrate reorientation and rebound that results in transfer of oxygen to the substrate (70). Subsequent rearrangements may occur, and finally the product is released.

Figure 1-2. Cytochrome P450 catalytic cylcle

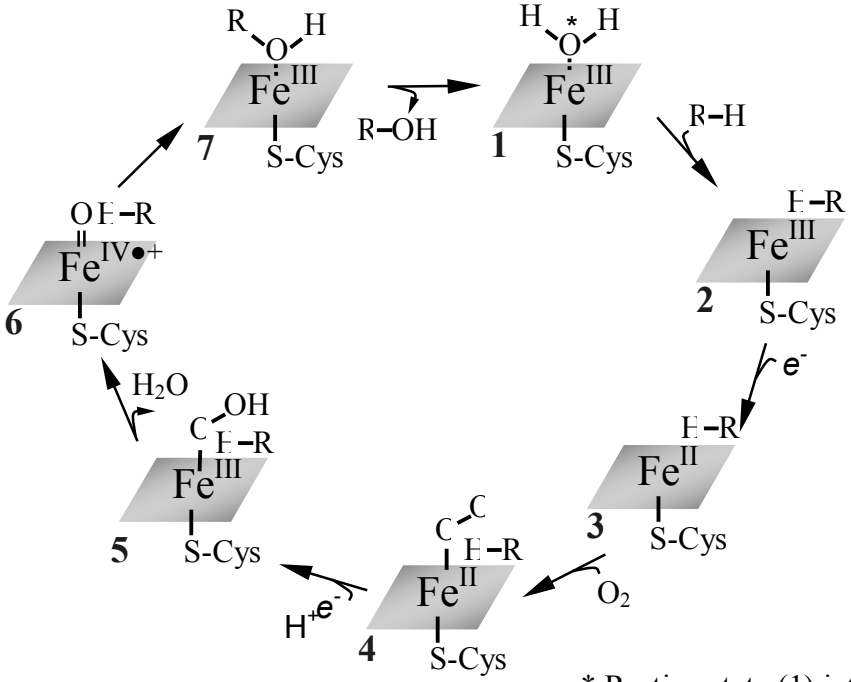

* Resting state (1) interacting with water molecule or a.a. residue

Different P450 enzymes, even enzymes that are > 90 % identical, have unique catalytic properties and catalyze specific arrays of reactions. A variety of empiric

studies are conducted to identify and compare enzyme substrates and resulting products, as theoretical prediction of enzyme activity and product distribution is still very limited. *In vitro* analyses are greatly facilitated by studying individual P450s that have been heterologously expressed (e.g. in *E. Coli*). Substrate binding spectra, product characterization, kinetics, and structural determination provide substantial information about an enzyme-substrate pair.

1.7 UDP-glucuronsyltransferase enzymes (UGTs)

Uridine diphosphate glucuronsyl transferase (UGTs) enzymes also metabolize nicotine, its metabolites, and metabolites of NNK. These enzymes in particular serve an inactivation and detoxification function (71). Overall, less is known about human UGTs than P450s, due in part to later recognition of their importance in xenobiotic metabolism and because UGTs have been difficult to characterize *in vitro* (e.g. including not being amenable to purification).

Human UGTs belong to the GT1 superfamily of glycosyltransferases. The predominant system to classify enzymes is based on amino acid sequence similarity (72;73). The GT1 superfamily includes enzymes found in archaea, bacteria, and eukaryotes; there are over 2800 entries for the GT1 superfamily in the Carbohydrate Active Enzymes database (CAZy; www.cazy.org). GT1 enzymes catalyze glycosyl transfer by an inverted mechanism in which the configuration of the sugar is changed

from an α- to β- linkage (74). Overall domain structure is also shared among GT1 enzymes despite relatively low sequence similarity.

There are 19 human UGTs that are classified into three subfamilies, UGT1A, UGT2A, and UGT2B (73). Sequence identity between subfamilies is less than 50 %. A unique feature of the UGT1A subfamily is that all UGT1As are transcribed from a single gene locus that spans 200 kb by a process similar to alternative splicing (75). Each enzyme has an independent promoter region and first exon that is spliced to shared exon 2-5 sequence. Thus, the C'-terminal 240 amino acids are identical among UGT1A enzymes. For all UGTs, the C-terminal domain is highly conserved and several residues in this domain interact with the sugar donor (76). The N-terminus contributes significantly to substrate specificity (77).

UGTs catalyze the transfer of a sugar moiety to a nucleophilic group on the substrate, forming a glycosidic bond (72;76). Human UGTs utilize uridine diphosphate glucuronic acid (UDPGA), but uridine diphosphate glucose can also serve as the sugar donor in some situations. Substrates are structurally diverse small molecules that are typically lipophilic. UGTs can catalyze the formation of O-, N-, S- or rarely C-glycosidic linkages (78). In humans, UGTs metabolize the endogenous substrates bilirubin, bile acids, steroids, hydroxylated eicosanoids, and leukotrienes (79). In addition, UGTs metabolize a number of xenobiotics and contribute to the metabolism of an estimated 20 % of drugs on the market (80). The addition of a sugar molecule confers increases hydrophilicity of substrates leading to increased excretion in urine and bile (81;82).

The predicted catalytic mechanism is that a nucleophilic substrate attacks the C1-carbon of glucuronic acid in an S_N2-like reaction (83) An example of an UGT-catalyzed N-glucuronidation reaction is presented in Figure 1-3; an aspartate may stabilize the positive charge on the nitrogen (84). For hydroxylated substrates, a histidine residue is proposed to act as a base that activates the substrate by deprotonation (76). Mutation of the active site histidine to alanine results in substantially decreased O-linked but not N-linked glucuronidation (84). The nucleophilic group on the substrate then attacks the sugar moiety, with uridine diphosphate as the leaving group. The product has inverted configuration at the C-1 carbon from an α- to β- linkage as mentioned previously.

Figure 1-3. UGT-catalyzed conjugation reaction: an example of *N*-glucuronidation

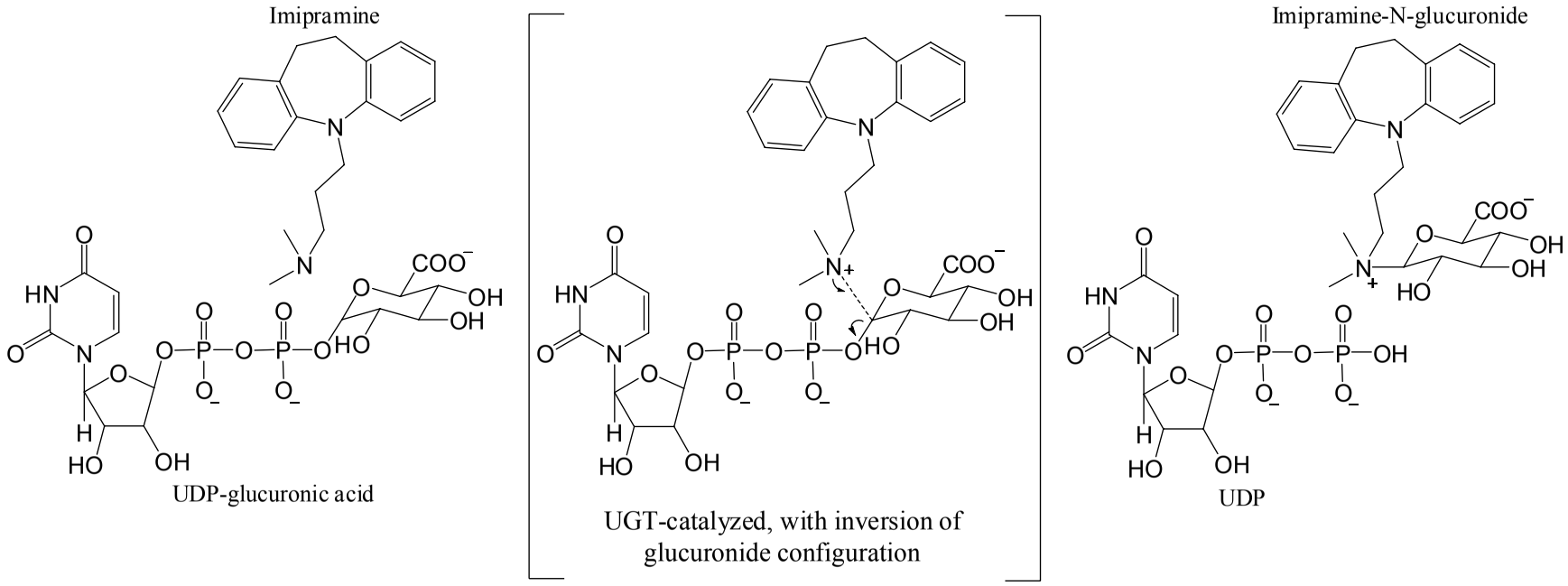

Human UGTs are embedded in the membrane of the endoplasmic reticulum. In addition to a transmembrane helix, the enzymes are closely associated with the membrane and the active site faces away from the cytosolic side of the membrane (79;85). Purification of heterologously-expressed full-length UGTs has failed with the exception of UGT1A9, but the purified form of this UGT has different substrate specificity and kinetics than UGT1A9 microsomes (86). Currently, the activity of individual UGTs is characterized using cell lysate or the membrane fraction from heterologously-expressed enzyme. Unlike with P450s, the amount of UGT protein is difficult to quantify. Addition of a his-tag and immunoblotting has been useful to compare the activities of different heterologously-expressed UGTs (87). Expressed UGTs have significantly lower activity than is observed with liver microsomes. A limited repetoire of selective inhibitors and antibodies have also been used to characterize enzyme activity in tissue preparations.

1.8 Flavin-containing monooxygenases (FMOs)

Flavin-containing monoxygenases (FMO) contribute to minor pathways of nicotine and NNK metabolism. In some individuals with decreased P450 activity, and perhaps decreased UGT activity, these enzymes have a more prominent role (88).

FMOs catalyze the oxidation of small molecules at nucleophilic heteroatoms including nitrogen, sulfur, phosphorus, and selenium (89). Similar to cytochrome P450-catalyzed metabolism, oxidation of typical lipophilic substrates generates products that

are more hydrophilic and therefore more readily excreted. In the Univeral Protein Resource (UniProt; www.uniprot.org) database, there are currently a total of 999 FMO protein sequence entries reflecting the presence of FMOs in viruses, bacteria, and eukaryotes. There are five active FMO enzymes in humans, FMO1-5, with 52-60 % sequence identity (90). There are also 6 pseudogenes for which no activity has been demonstrated. Human FMOs have a broad substrate range and contribute to xenobiotic detoxification (90). It is unclear if FMOs also have a role in endogenous biosynthetic or catabolic pathways. Ziegler *et al.* proposed that FMOs may catalyze endogenous disulfide bond formation through cysteamine oxidation (91). FMOs are localized to the endoplasmic reticulum membrane, and are abundantly expressed in adult liver (FMO3) and kidney (FMO1) (92).

Human FMOs have a unique catalytic cycle in which substrate affinity does not drive the velocity of the reaction (Figure 1-4) (91). FMOs bind NADPH resulting in a two electron reduction of flavin (**1**). Molecular oxygen binds the reduced flavin and C4α peroxyflavin is rapidly formed (**2**). Remarkably, this species is stable for minutes to hours and thus the enzyme is primed for catalysis prior to substrate binding (93). Ability of substrates to pass through the substrate access channel, depending on size and charge state, largely determine which molecules are metabolized by FMOs (90;94). When a substrate enters the active site, a nucleophilic moiety can react with the flavin peroxide (**3**). An oxygen atom is then incorporated into the substrate and a molecule of water is formed. Release of water is predicted to be the rate-limiting step (**4**). NADP leaves the active site at the end of the catalytic cycle (**5**). FMOs are resistant to inactivation by electrophiles, and there are no known examples of an FMO-generated

reactive intermediate leading to FMO inactivation. However, reactive FMO products can inactivate P450s (95).

Figure 1-4. Flavin monooxygenase catalytic cycle

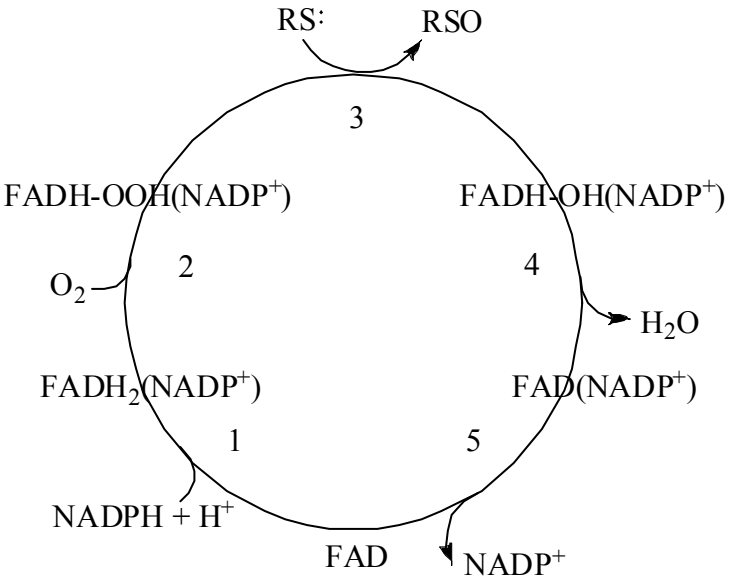

RS = Substrate with nucleophilic heteroatom

A number of xenobiotics are substrates for both FMOs and P450s and the tissue distribution of these enzymes also overlaps. Products of FMO- versus P450- mediated metabolism of a substrate are often different. Overall, substrate turnover is slower for FMOs than P450s, 30-60 min^{-1} versus 1-20 min^{-1} (96). Despite slower turnover, FMOs contribute to metabolism of many P450 substrates because of their relatively high abundance. In the liver, FMO3 is present to levels of ~60 % of the most abundant P450, and more FMO1 than P450s is present in the kidney (92). FMO activity is not thought to vary significantly in response to environmental exposures, as there is no

evidence for enzyme induction and only competitive inhibition has been observed (90). Nevertheless, genetic factors do cause inter-individual variation in FMO-mediated metabolism, and these include FMO polymorphisms and other genes that mediate age and gender differences in FMO expression. A note of caution is warranted in predicting the *in vivo* contribution of P450- versus FMO- mediated metabolism from *in vitro* experiments, as incubation conditions (ie. pH, buffer selection, timing of NADPH addition) can favor one metabolic pathway over the other in microsomal studies, and also influence the activity of individually-expressed enzymes. Heat inactivates FMOs at a lower temperature than P450s and this can be useful to distinguish between P450- and FMO- catalyzed reactions *in vitro* (97).

1.9 Regulation of P450s, UGTs, and FMOs

Regulation of P450s, UGTs, and FMOs may underlie some of the phenotypic variation observed in nicotine metabolism among smokers that is discussed in subsequent chapters, and is relevant to hypotheses generated about *in vivo* metabolism.

Regulatory mechanisms determine the amount and distribution of P450s, UGTs, and FMOs, in an individual. Gene knock out models and chemical induction studies have been instrumental to studying regulation. There are differences in the regulation of these xenobiotic metabolizing enzymes in mice and rats compared to humans, and therefore mice that are transgenic for various human genes (e.g. nuclear hormone receptors, UGT1A locus) are being generated to better assess regulatory networks (98).

Much of what we know is based on regulation of gene transcription. The arylhydrocarbon receptor (Ahr) and the nuclear hormone receptors, constitutive androstane receptor (CAR), pregnane X receptor (PXR), and peroxisome proliferator activated receptor (PPAR), are involved in upregulation of both P450s and UGTs (99-101). Upon activation by ligands, these receptors are translocated to the nucleus where they bind promoter gene elements and recruit transcription factors, such as the hepatocyte nuclear factors (56). There is cross-talk between the different receptor pathways in animal models. A number of P450s, UGTs, and FMOs, do not undergo substantial induction. For example, mouse P450 2A5 that shares high sequence identity with human P450 2A6 is induced through the arylhydrocarbon receptor (AhR) 3-fold while P450 1A1 is induced over 1500-fold (102). In smokers P450 1A1 is induced by polyaromatic hydrocarbons in tobacco smoke, but an effect on P450 2A6 has not been demonstrated (103). A number of other factors may influence regulation such as DNA methylation, transcriptional co-activators, and alternative splice variants.

In vitro enzymatic kinetics combined with estimates of *in vivo* expression are used to make hypotheses about the role of an enzyme in *in vivo* metabolism. Determining which enzyme(s) catalyzes a specific reaction can provide critical information about exposure risks to a xenobiotic agent and potential adverse drug reactions. While this provides a useful framework to consider the role of an enzyme, it is often not sufficient to make conclusions about *in vivo* metabolism. Human pharmacokinetic studies can provide specific information about the absorption, metabolism, distribution, and elimination of a compound though these studies are expensive, and also, are frequently not an option for studying carcinogens. Quantifying metabolites in body fluids of

exposed, and non-exposed, individuals is a mainstay for evaluating metabolism in population-based studies. Genotype-phenotype analyses can provide information about the role of an enzyme in *in vivo* metabolism. Gene-environment interactions, especially with factors like diet which are difficult to measure or control, can be a complicating factor. Overall, it is a challenge to assess factors that affect *in vivo* metabolism.

1.10 Goals of thesis research

The goals of the thesis were to better understand the role of specific enzymes in nicotine and NNK metabolism, to consider metabolic flux through more than one enzymatic pathway, and to improve the scientific basis of using selected tobacco biomarkers.

CHAPTER 2

Ethnic differences in nicotine metabolism

2.1 Introduction

African Americans have higher rates of lung cancer than European Americans despite consistently reporting smoking fewer cigarettes per day (cpd) (104;105). Yet higher levels of the nicotine metabolite cotinine have been documented in African Americans at all levels of smoking during the last 20 years (41;106-109). In the National Health and Nutrition Examination Survey III (NHANES III), cotinine was also higher in African American nonsmokers than European American nonsmokers who reported similar environmental tobacco smoke exposure (106). Higher cotinine among African American compared to European American smokers likely reflects higher exposure per cigarette, differences in nicotine metabolism, or a combination of both. A difference in nicotine metabolism could impact cancer risk through an effect on smoking behavior or because some of the same enzymes that metabolize nicotine also metabolize carcinogens in tobacco smoke.

Nicotine is extensively metabolized into pharmacologically inactive metabolites by C-oxidation, glucuronide conjugation, and N-oxidation (Fig. 2.1) (32;110;111). Typically, only ~10 % of the nicotine dose is excreted unchanged in urine (32). There is significant interindividual variation in the contribution of the three pathways to nicotine metabolism, albeit in most people C-oxidation is the major pathway and 80 % of nicotine is metabolized initially to cotinine (112). This metabolite is frequently used as a biomarker of nicotine exposure, since nicotine itself has a short half-life of 1-2 hours compared to 16 hours for cotinine, and nicotine levels spike immediately after smoking (113-115). Moreover, individuals who are not exposed to tobacco have virtually no cotinine in their body fluids as nicotine intake from other sources (e.g. eggplant) is insignificant (116;117). In urine, more than 40 % of nicotine and its oxidation metabolites, cotinine and *trans*-3'-hydroxycotinine, are present as glucuronide conjugates (111;112;118). *N*-oxidation is a minor metabolic pathway that typically accounts for less than 10 % of nicotine metabolism (119).

Quantifying the sum of nicotine and its major metabolites in urine reflects nicotine intake and can be used to assess the molar distribution of urinary metabolites (Table 2-1). The sum of nicotine, nicotine-*N*-glucuronide, cotinine, cotinine-*N*-glucuronide, *trans*-3'-hydroxycotinine, and *trans*-3'-hydroxycotinine glucuronide has been referred to as nicotine equivalents (120). This sum, with or without additional quantification of nicotine-*N*-oxide and cotinine-*N*-oxide, has been used in pharmacokinetic studies to quantify recovery of the administered nicotine dose. Furthermore, Benowitz *et al.* reported that nicotine equivalents in 24 hour urine accounted for an average of 90 % of the systemic nicotine intake from smoking or from the nicotine patch (32). In this

pharmacokinetics study, a 24-hour infusion of deuterium-labeled nicotine was used to assess nicotine clearance while unlabeled nicotine was quantified to calculate the AUC_{nic} from smoking or the patch. Systemic dose was then estimated as dose = AUC_{nic} * $Clearance_{D2\text{-}nic}$. Notably, the range of percent dose recovered was 51 – 124 % of the estimated systemic intake; the contribution of error(s) in estimating systemic dose and quantification of labeled and unlabeled analytes is not clear.

Figure 2-1. Pathways of nicotine metabolism in humans that result in the most abundant urinary metabolites

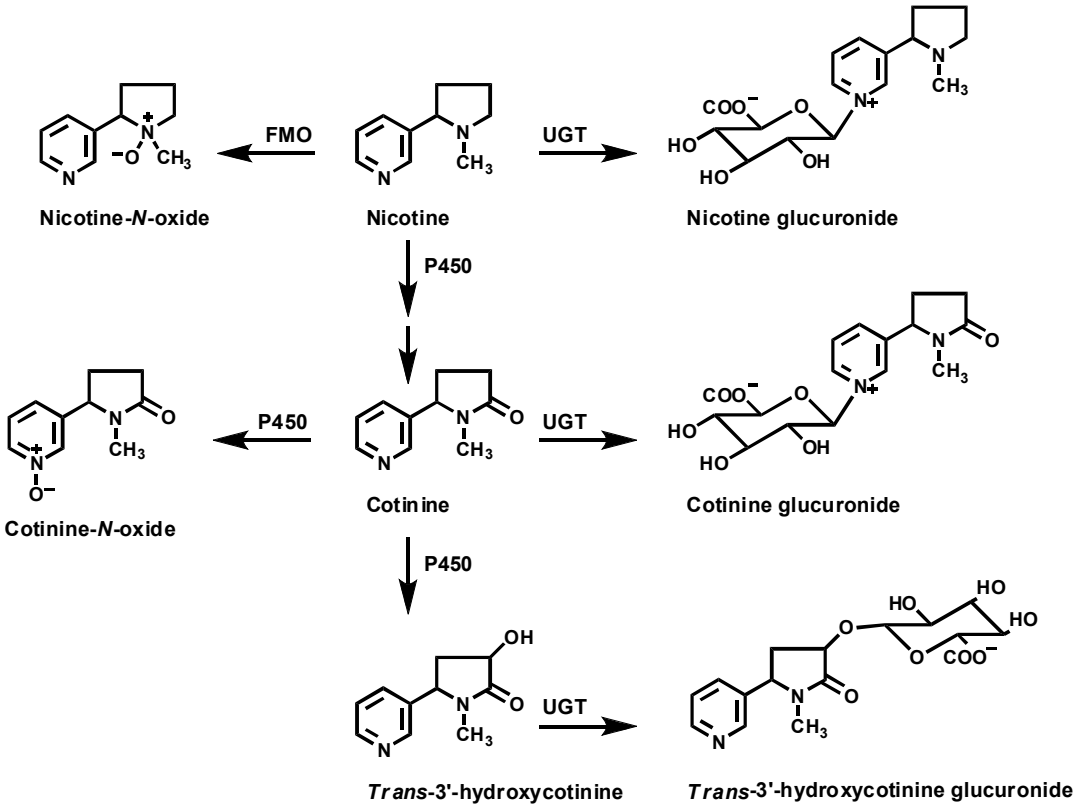

Table 2-1. Distribution of urinary nicotine metabolites

Analytes as molar percentages of ∑ nicotine and its metabolites					
Analyte	**Smoking: 24h urine** Benowitz *et al.* N = 12 [a]	**Smoking: morning urine** Murphy *et al.* N = 46	**Smokeless: 24h urine** Andersson *et al.* N = 54 [b]	**Transdermal: 24h urine** Benowitz *et al.* N= 12 [a]	**Infusion: 8h urine** *Benowitz et al.* N = 215
Nicotine	10.4	9.3	8.3	11.1	21.6
Nicotine glucuronide	4.6	6.2	3	5.3	8
Cotinine	13.3	11.4	7.9	14.9	24.4
Cotinine glucuronide	15.8	21.6	8.9	15.4	8.9
Trans-3'-hydroxycotinine + *O*- glucuronide	46.9	51.6	61.0	44.9	37.1
Nicotine-*N*-oxide [c]	3.7	n/a	8.6	2.7	n/a
Cotinine-*N*-oxide [c]	5.2	n/a	2.5	5.2	n/a

[a] Analytes were quantified in participants while smoking and while abstinent and on the transdermal nicotine patch.
[b] Participants were users of Swedish oral moist snuff (snus) or chewing tobacco
[c] Other studies by Byrd *et al.* and Scherer *et al.* reported mean molar percentages of urinary nicotine-*N*-oxide from 3.7 – 12.2 % and cotinine-*N*-oxide from 3.1 – 4.5 %. * References: (32), (112), (121), (115), (122), (119)

P450s catalyze the 5'-oxidation of nicotine and can subsequently catalyze the metabolism of the iminium ion to cotinine (45;123). The immediate product of nicotine 5'-oxidation is 5'-hydroxynicotine, which is in equilibrium with the nicotine$^{\Delta 1',5'}$ iminium ion (Figure 2-2). Cytosolic aldehyde oxidase also converts the iminium ion to cotinine (124;125). In humans, P450 2A6 is the predominant contributor to 5'-oxidation of nicotine. Individuals with no P450 2A6 due to a genetic deletion have a greater than 85 % reduction in 5'-oxidation (118;126). Also, in human liver microsomes, treatment with anti-P450 2A6 antibody inhibits 90 % of nicotine 5'-oxidation (127). Hepatic P450 2B6 and extrahepatic P450 2A13 may contribute to *in vivo* nicotine metabolism, but P450 2B6 is a poor catalyst relative to P450s 2A6 and 2A13, and P450 2A6 is much more abundant than P450 2A13 (127-129).

Figure 2-2. Nicotine 5'-oxidation to cotinine

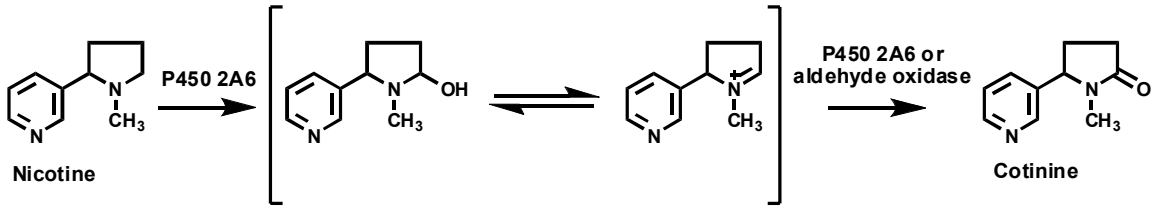

Cotinine is further oxidized to *trans*-3'-hydroxycotinine, which is the most abundant urinary metabolite of nicotine detected in smokers (112;130). The ratio of *trans*-3'-hydroxycotinine to cotinine is being used as a biomarker of C-oxidation phenotype and also as a proxy measure for P450 2A6 activity (108;115;131). In a large

pharmacokinetic study (n = 268) where non-smokers and smokers were co-administered deuterium labeled nicotine (D_2) and cotinine (D_4), the plasma and urine ratio of *trans*-3'-hydroxycotinine to cotinine was correlated with nicotine clearance, r = 0.6 and r = 0.5 respectively (115). While these correlations are moderate, differences in smoking behavior have been observed among individuals with low ratios, particularly among individuals with well-characterized low activity CYP2A6 alleles and Japanese Americans who have a higher prevalence of these alleles (115;132;133). Briefly, groups with low ratios have been reported to have lower urinary nicotine equivalents, smoke slightly fewer cigarettes/day, smoke less intensely on a smoking machine, and Malaiyandi *et al*. reported a higher 6-month success rate for smoking cessation (132;134-137). Other studies have not found any associations with cigarettes/day or indices of addiction (e.g. Fagerstrom index, time to first cigarette) (108;138). A concern is that no study has controlled for a potentially independent effect of nicotine dose on the ratio of *trans*-3'-hydroxycotinine to cotinine.

While there is strong evidence for CYP2A6 as the predominant catalyst of nicotine C-oxidation to cotinine this is not the case for cotinine C-oxidation to *trans*-3'-hydroxycotinine. If CYP2A6 is not the predominant catalyst of the latter reaction then the ratio of of *trans*-3'-hydroxycotinine to cotinine would not be a specific marker for CYP2A6 activity. There is an interesting case report of a pack-a-day smoker who had a CYP2A6 null allele and had 10-fold lower than average plasma cotinine concentrations, but was found to have essentially normal cotinine clearance in a pharmacokinetic study (139). Nakajimi *et al.* demonstrated that P450 2A6 catalyzes cotinine oxidation, and a product eluted at the retention time of *trans*-3'-hydroxycotinine standard (140). Product

inhibition was observed with anti-2A antibody and activity correlated with P450 2A6 content and coumarin 7-hydroxylation, which is catalyzed exclusively by 2A6 in HLMs. Unfortunately, the product peak was not further characterized, and a conflicting report that human liver microsomes formed surprisingly low levels of *trans*-3'-hydroxycotinine from nicotine has been largely ignored (141). It turns out that *trans*-3'-hydroxycotinine is only one of three products generated by P450 2A6 when incubated with cotinine. *N*-(hydroxymethyl)norcotinine, is the major product formed by human liver microsomes or P450 2A6, followed by *trans*-5'-hydroxycotinine and *trans*-3'-hydroxycotinine which are formed at rates less than half of that for methyl hydroxylation (142). However, consistently less than 5 % of metabolites in urine are derived from *N*-(hydroxymethyl)norcotinine (114). Therefore, it is unclear which enzyme is the major catalyst responsible for *trans*-3'-hydroxycotinine formation *in vivo* either from cotinine or directly from nicotine.

Glucuronide conjugates are formed from nicotine, cotinine, and *trans*-3'-hydroxycotinine and are excreted in urine (111). *N*-glucuronidation of nicotine and cotinine occurs at the pyridyl nitrogen. These reactions are catalyzed by UGTs 2B10 and 1A4 *in vitro*; UGT2B10 has the lowest K_m and it is ~10-fold lower than UGT1A4 (87). However, the V_{max} may be higher for UGT1A4, as estimated by Chen *et al*. to be 10-fold and 3- fold higher for nicotine and cotinine glucuronidation respectively (143). Hepatic mRNA levels are comparable between these UGTs, although protein levels have not been compared (87). In an *in vitro* study of eleven UGTs, 2B7 and 1A9 were identified as the strongest candidates for *trans*-3'-hydroxycotinine *O*-glucuronidation (144). Indeed, *trans*-3'-hydroxycotinine *O*-glucuronide is the major glucuronide in

smokers' urine. Cotinine and nicotine *N*-glucuronide concentrations are correlated *in vivo*, and are not correlated with *trans*-3'-hydroxycotinine glucuronides (112). The ratio of cotinine glucuronide:cotinine in urine was used previously to compare glucuronidation phenotypes in a pharmacokinetic study but it has not been used as a biomarker *per se* (115;145).

The fate of nicotine depends on the activity, and presence or absence, of enzymes along the metabolic pathways. Studies on variation in nicotine metabolism have focused primarily on the C-oxidation of nicotine, as it is the major pathway of nicotine metabolism and polymorphisms resulting in inactive protein (CYP2A6*2, CYP2A6*4) were identified in the 1990s (146-148). Indeed, the P450 2A6 (CYP2A6) gene is highly polymorphic, and several variants are associated with altered (increased or decreased) nicotine metabolism, including variants found in African Americans (149-151). Yet even among African Americans who are genotypically considered CYP2A6 wild-type, there is significant variation in phenotype (150). UGT1A4 and UGT2B10 are also polymorphic, though few variants have been evaluated in nicotine metabolism and no variants that have a specific role in the African American population have been identified (143;152;153).

A controlled dose nicotine metabolism study of African Americans and European Americans was conducted to evaluate intraindividual variation and any ethnic differences in nicotine metabolism. Nicotine and its major metabolites were analyzed in urine while participants were abstinent from smoking and at steady state on the nicotine patch, as well as while participants were smoking *ad libitum*. Nicotine

equivalents and the metabolite ratios, *trans*-3'-hydroxycotinine to cotinine and cotinine glucuronide:cotinine, were further explored as biomarkers of nicotinine intake and oxidation and glucuronidation phenotypes.

2.2 Methods

2.2.1 Nicotine patch study

Patch Study Recruitment

The study was approved by the University of Minnesota's Institutional Review Board. Smokers were recruited from the Minneapolis-St. Paul area through newspaper advertisements, flyers, and word of mouth. Potential participants were scheduled by telephone for a screening visit. Inclusion criteria were (1) age 18-74, (2) grandparents who were all either African American or European American, (3) daily smoking > 10 cpd, and (4) in good health. A medical history questionnaire and vital signs were used to assess health. Individuals who used illicit drugs and women who were pregnant were ineligible. A total of 105 individuals enrolled.

Patch Study protocol

The 8-day study included baseline smoking assessment, and a controlled dose period during which the nicotine patch was administered (Figure 2-3). Participants

completed questionnaires about demographics and smoking behavior. Current smoking was verified by exhaled carbon monoxide (CO) and a urine spot check for nicotine (NicCheck). Participants collected 24-hour urine while smoking as usual. Subsequently, participants were instructed to abstain from smoking and to use 21 mg nicotine patches (Nicoderm). On days 5-7 of using the patch, after reaching steady state, participants visited the study center for CO testing, blood pressure and heart rate assessment, and 24-hour urine drop-off. A subset of participants provided plasma (n= 70, 75 %) during days 5-7. Compliance was determined as having a CO < 8 ppm and turning in used nicotine patches. Participants were offered referrals to smoking cessation programs and received compensation ($200).

Figure 2-3. Nicotine patch study design

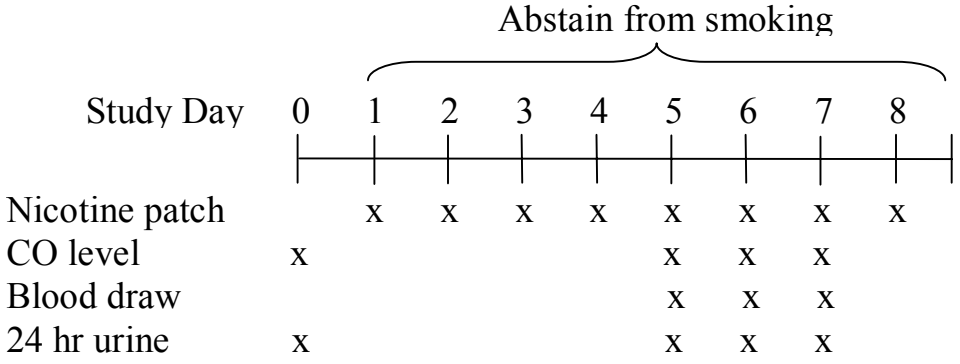

2.2.2 Chemicals and reagents

(S)-[5-^{3}H]Nicotine was purified as previously described (123). Nicotine *N*-βD-glucuronide was purchased from Toronto Research Chemicals (North York, ON, Canada). Other chemicals were purchased from Sigma-Aldrich (St. Louis, MO) unless otherwise noted.

2.2.3 Nicotine and metabolite analysis

Urine was stored at -20˚C until analysis. Four 24-hour urine samples were analyzed (days 1 and 5-7) per participant by gas chromatography/mass spectrometry (GC/MS). A brief description of these published methods is provided here (39;112;154). Base treatment was used to cleave *N*-glucuronide conjugates of nicotine and cotinine; 0.1 N NaOH for 30 min at 80°C. Internal standards, [methyl-D_3]cotinine and [methyl-D_3]nicotine, were added prior to addition of 50 % aqueous K_2CO_3 and extraction with CH_2Cl_2. The CH_2Cl_2 layer was mixed with CH_3OH and concentrated under N_2 (to ~100 µl). GC/MS was performed with selected ion monitoring for the nicotine-derived ions: m/z 84 $[C_4H_7NCH_3]^+$, 87 $[C_4H_7NCD_3]^+$, 162 $[M^+$, nicotine], and 165$[M^+$, $[CD_3]$nicotine]; and cotinine-derived ions m/z 98 $[C_4H_5ONCH_3]^+$, 101 $[C_4H_5ONCD_3]^+$, 176 $[M^+$, cotinine], and 179 $[M^+$, $[CD_3]$cotinine]. Free nicotine, total nicotine (free nicotine + *N*-glucuronide), free cotinine, and total cotinine (free cotinine + *N*-glucuronide) were quantified by comparison to the internal standards (39;112;154). β-glucuronidase was used to cleave *trans*-3'-hydroxycotinine glucuronides for analysis of

total *trans*-3'-hydroxycotinine (*trans*-3'-hydroxycotinine + its glucuronides), and *cis*-3'-hydroxycotinine was added as an internal standard. An extraction with CH_2Cl_2/IPA was performed prior to derivitization with tert-butyldimethylsilyl followed by a second extraction with toluene:butanol (154). Selective ion monitoring was performed for m/z 249, loss of the tert-butyl group. From whole blood, plasma was separated and stored at -20ºC. Nicotine, cotinine and their *N*-glucuronides were quantified by GC/MS as performed for urinary metabolites except that an initial solid phase extraction using a MCX column was performed (Waters Corporation, Milford, MA) (39). Analyses were performed in duplicate and repeated if values differed by > 10 %.

Other analyses

Exhaled CO was determined using a Medical Gas Monitor (Bedfont Scientific Ltd., Kent, United Kingdom). Urine spot checks for nicotine were performed using NicCheck (Mossman Associates, Blackstone, MA).

2.2.4 Statistics

Patch participants were excluded from analyses if they were noncompliant: not using the nicotine patch as directed, smoking during the abstinence period, or incomplete urine collection. Specifically, participants were excluded if on more than one visit they excreted < 20 % or > 120 % of the patch dose or had exhaled CO levels >

8 ppm. Single visits that met noncompliance criteria were excluded from analysis (8 of 279, 3%). Overall, 12 participants (7 African American) were excluded due to: ethnicity was American Indian (n=1), not completing the study (n=2), dose recovery was < 20 % (n=6), dose recovery was > 120 % (n=3). Included in analyses were 93 participants. Baseline urine was available for 59 participants, after exclusion of 4 participants who returned < 400 ml of 24-hour urine at baseline.

Statistical analyses were conducted using SAS (SAS Institute, Cary, NC) and Excel (Microsoft, Redmond, WA). Wilcoxon two-sided t-approximation statistics were calculated to compare means of continuous variables that did not have a normal distribution, and a p-value less than 0.05 was considered significant. Chi-square approximation statistics were analyzed for categorical variables. Spearman nonparametric correlation was used to assess univariate correlations. Multivariate linear regression models were evaluated to assess predictors of cotinine glucuronidation (square-root transformed ratio of cotinine glucuronide to free cotinine) and the C-oxidation ratio (square-root transformed ratio of total *trans*-3'-hydroxycotinine to total cotinine) (133).

2.3 Results

2.3.1 Patch study population

African American and European American participants were not statistically different in age (mean = 38; range 26-56), gender (51 % female), cigarettes per day

(cpd) (mean = 21), or quit attempts (mean = 4). The distribution of time to first cigarette after waking was 48 %, 0-5 min.; 37%, 6-30 min.; 11.5 %, 31-60 min.; 3.5 %, > 60 min, and there was no difference by ethnicity. African American women reported more quit attempts than men (6.1 versus 3.2, p =0.012) or European American women (6.1 vs. 3.3, p = 0.02). Mentholated cigarettes were smoked by 86 % of the African Americans and 24 % of European Americans (p < 0.0001). Fewer African Americans than European Americans reported attending at least some college (43 % vs. 64 %, p = 0.04).

2.3.2 Nicotine metabolism on the patch

Free nicotine and free cotinine were quantified in plasma to assess nicotine dosing achieved with the patch in 70 of 93 (75 %) of participants. At steady-state (day 6), free cotinine concentrations were comparable to levels observed in smokers. Mean free nicotine and free cotinine were 28.1 +/- 30.6 ng/ml and 311 +/- 170 ng/ml for African Americans and 18.3 +/- 11.8 ng/ml and 245 +/- 129 ng/ml for European Americans and were not statistically different by ethnicity. Plasma free cotinine was correlated with 24-hour urinary free cotinine; 0.49, p < 0.0001.

The dose of nicotine obtained from patch use was estimated relative to the amount of nicotine in a patch. Specifically, the molar sum of nicotine and its metabolites in 24-hour urine were expressed as a molar percentage of nicotine in a 21 mg patch (estimated dose recovered). The mean estimated dose recovered on days 5-7 was 61 +/- 20 % for

African Americans and 70 +/- 25 % for European Americans (p = 0.09). The intraindividual variation in the estimated dose recovered was 13 % for both African Americans and European Americans.

Nicotine and nicotine metabolites were quantified in 24-hour urine from each collection day and the values of 3 days for each individual were analyzed. Mean intraindividual variation was less than half of mean interindividual variation. This was assessed by calculating the mean of standard deviations for individuals and comparing this value to the group standard deviation for a given analyte. Free cotinine had the lowest intraindividual variation while free nicotine had the largest intraindividual variation relative to interindividual variation.

There were no significant differences by ethnicity in mean total nicotine or total cotinine (Table 2-2). However, free cotinine was higher among African Americans than European Americans, 12.7 +/- 6.2 nmol/ml versus 9.5 +/- 4.2 nmol/ml, respectively (p = 0.01). While free nicotine was higher among African Americans than European Americans, 12.9 +/- 9.4 nmol/ml versus 9.9 +/- 6.5 nmol/ml, the means were not statistically different (p = 0.17). The observation that African Americans had higher free cotinine but similar total cotinine levels reflects a difference in glucuronidation. Nicotine equivalents, defined as the sum of nicotine, cotinine, *trans*-3'-hydroxycotinine and their respective glucuronides, expressed as nmol/ml or µmol/24-hour urine, were the same for African Americans and European Americans; 81.2 +/- 39.4 nmol/ml and 84.0 +/- 42.7 nmol/ml, respectively (120).

Glucuronide conjugation of both nicotine and cotinine was significantly lower among African Americans compared with European Americans (Table 2-2). The percent of nicotine excreted as a glucuronide conjugate in 24-hour urine was 18.1 +/- 12.7 % for African Americans versus 29.3 +/- 16.9 % for European Americans ($p = 0.002$). The percent of cotinine excreted as a glucuronide conjugate was 41.4 +/- 20.7 % for African Americans versus 61.7 +/- 14.2 % for European Americans ($p < 0.0001$). Nicotine and cotinine glucuronidation were correlated in African Americans and European Americans, 0.73 and 0.53 respectively ($p= 0.11$ for difference in correlation by ethnicity). The distribution of percent cotinine excreted as a glucuronide was distinct for African Americans (Figure 2-4). Few European Americans excreted less than 50 % of cotinine as its glucuronide while this was common among African Americans. We observed large interindividual variation in glucuronidation regardless of ethnicity. The ranges of percent glucuronidation for nicotine and cotinine were 0.4 – 67.5 % and 8.6 – 84.4 % respectively. Intraindividual variation in percent glucuronidation on days 5 – 7 was low with a mean standard deviation of 7.3 % for nicotine (range, 0.1-53 %) and 4.9 % for cotinine (range, 0.1-21.8 %). There was no difference in intraindividual variation by ethnicity.

Table 2-2. Urinary nicotine and nicotine metabolite levels in African Americans (A.A.) and European Americans (E.A.)

	Nicotine Patch [a]			***Baseline Smoking*** [b]		
Metabolite Mean (nmol/ml)	**A.A. (N=51)** Mean (SD; mean intraindividual SD)	**E.A. (N=42)** Mean (SD; mean intraindividual SD)	**(N=93)** Range	**A.A. (N=32)** Mean (SD)	**E.A. (N=27)** Mean (SD)	**(N=59)** Range
Free nicotine	12.9 (9.4; 4.8)	9.9 (6.5; 4.0)	1.6 - 42.0	8.8 * (4.8)	6.0 * (4.9)	0.2 - 22.6
Total nicotine [c]	15.6 (11.2; 5.4)	13.7 (8.1; 4.4)	1.9 - 49.3	19.4 (11.5)	15.1 (12.8)	1.7 - 64.6
Free cotinine	12.7 * (6.2; 2.2)	9.5 * (4.2; 1.9)	2.0 - 32.1	6.1* (2.8)	4.4 * (2.9)	1.1 - 13.1
Total cotinine [c]	24.4 (14.0; 7.7)	28.2 (16.1; 6.8)	2.4 - 79.9	25.3 (12.7)	23.6 (15.1)	4.1 - 59.9
Total *trans*-3'-hydroxycotinine[c]	41.2 (27.7; 11)	42.0 (25.5; 12.7)	1.7 – 124	32.6 (21.8)	22.6 (17.4)	2.2 - 94.2
Nicotine equivalents [d]	81.2 (39.4; 16.8)	84.0 (42.7, 21.0)	14.9 – 216	77.4 (34.9)	61.7 (36.7)	13.4 - 161
Nicotine equivalents, umol/24h	78.7 (25.6)	90.2 (32.8)	31.6 – 144	---	---	---
Percent nicotine glucuronide [e]	18.1 * (12.7)	29.3 * (16.9)	0.4 - 67.5	51.4 (9.1)	57.4 (15.3)	19.6 - 89.4
Percent cotinine glucuronide [e]	41.4 ** (20.7)	61.7 ** (14.2)	8.6 - 84.4	71.2 * (13.9)	79.8 * (11.8)	35.8 - 94.4

[a] Nicotine and metabolites were quantified in 24-hour urine while participants were on the nicotine patch; mean values from 3 days per participant. Note: difference in means, * p-value < 0.05, ** p-value < 0.005

[b] Nicotine and metabolites were quantified in a 24-hour urine sample while participants were smoking *ad libitum*

[c] Total analyte represents the sum of the analyte and its glucuronide conjugate

[d] Sum of urinary total nicotine, total cotinine, and total *trans*-3'-hydroxycotinine

[e] Percent glucuronide = [(total analyte – free analyte)/total analyte *100]

Figure 2-4. Percent cotinine excreted as its glucuronide in 24-hour urine by ethnicity

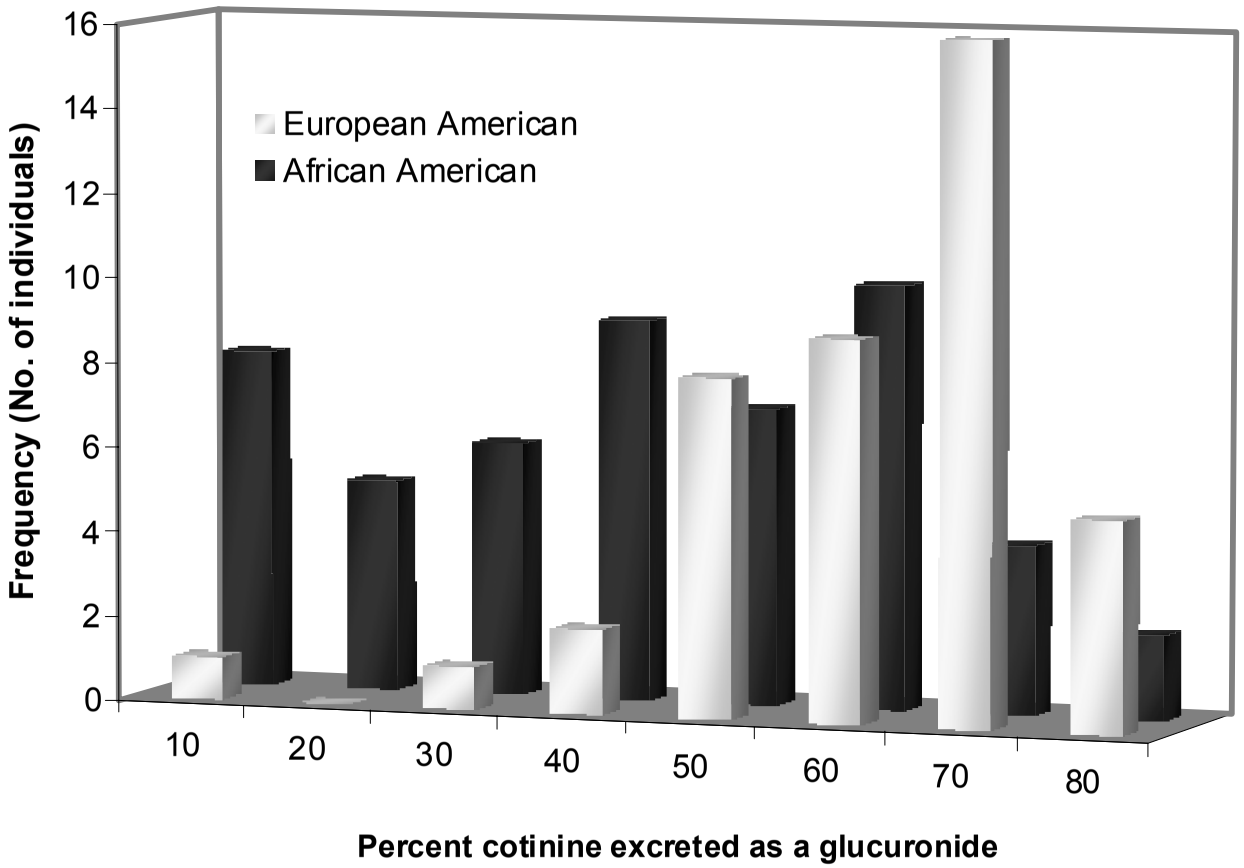

The ratio of *trans*-3'-hydroxycotinine to cotinine has been used and promoted as a marker of nicotine oxidation phenotype (133;135), and we evaluated this ratio in urine as total *trans*-3'-hydroxycotinine to total cotinine. The range of the ratio was 0.10 – 7, plus an outlier of 15.8. The ratio was not statistically different by ethnicity; the mean ratio was 2.28 +/- 2.42 for African Americans and 1.62 +/- 1.12 for European Americans ($p = 0.27$). Total *trans*-3'-hydroxycotinine:total cotinine was highly correlated with the ratio of total *trans*-3'-hydroxycotinine:free cotinine in both ethnic groups, 0.79 ($p < 0.0001$). Notably, both ratios were correlated with percent cotinine glucuronidation.

Predictors of glucuronidation, assessed as the ratio of cotinine glucuronide to cotinine, were evaluated by multivariate linear regression (Table 2-3). The ratio of cotinine glucuronide:cotinine has been used by Benowitz *et al.* to evaluate glucuronidation phenotype (145). This is analogous to using *trans*-3'-hydroxycotinine:cotinine as an estimate of nicotine C-oxidation activity (108;115). In univariate comparisons, a lower glucuronidation ratio was significantly correlated with a number of study variables including African American ethnicity, male gender, older age, lower nicotine equivalents, higher C-oxidation ratio, lower percent of dose excreted as nicotine, and lower percent dose recovered. The glucuronidation ratio was not correlated with baseline cigarettes/day or urine volume. Variables that were correlated with the glucuronidation ratio were entered into a multivariate regression model with stepwise selection. In the final model, a low glucuronidation ratio was associated with African American ethnicity, low nicotine equivalents, high C-oxidation ratio, and older age. Gender was forced back into the model presented in Table 2-3, though it does not

affect the R^2 value. The adjusted R^2 value for the model was 0.41, compared with 0.35 if the C-oxidation ratio was not included.

Predictors of the *trans*-3'-hydroxycotinine:total cotinine ratio were evaluated during use of the nicotine patch (Table 2-4). A higher C-oxidation ratio was correlated with a lower glucuronidation ratio, higher nicotine equivalents, and lower percent of dose excreted as total nicotine in univariate comparisons. In these data, the C-oxidation ratio was not significantly correlated with ethnicity, age, gender, cpd, urine volume, or percent of dose recovered. In multivariate linear regression, 30 % of variation in the C-oxidation ratio was attributable to nicotine equivalents, the glucuronidation ratio, and percent dose excreted as nicotine. Ethnicity, gender, and age were forced back into the model presented in Table 2-4.

Table 2-3. Predictors of the glucuronidation ratio [a]: multivariate linear regression models and univariate spearman correlation coefficients

	Adj. R^2 (%)	*Independent variables[b]*	*p-value*	*Univariate correlation (p-value)*
Patch:				
Glucuronidation ratio	41	African American vs European American	<0.0001	- 0.49 (<0.0001)
		Male vs. female	0.536	- 0.21 (0.04)
		Age	0.138	- 0.22 (0.03)
		Nicotine equivalents [c]	0.0002	0.30 (0.003)
		C-oxidation ratio [d]	0.0031	- 0.37 (0.0003)
Baseline:				
Glucuronidation ratio	50	African American vs. European American	0.032	- 0.35 (0.01)
		Male vs. female	0.103	- 0.36 (0.01)
		Age	0.180	- 0.20 (0.15)
		Nicotine equivalents [c]	0.001	0.27 (0.05)
		C-oxidation ratio[d]	<0.0001	- 0.56 (<0.0001)

[a] Cotinine-*N*-glucuronide / free cotinine; square-root transformed
[b] Stepwise selection was used to select variables included in the models presented, though demographic variables (ethnicity, age, gender) were forced into the model if rejected during selection. Nicotine and its metabolites were measured in 24-hour urine.
[c] Sum of urinary total nicotine, total cotinine, and total *trans*-3'-hydroxycotinine
[d] total *trans*-3'-hydroxycotinine / total cotinine; square-root transformed

Table 2-4. Predictors of the C-oxidation ratio [a]: multivariate linear regression models and univariate spearman correlation coefficients [b]

Dependent variable	*Adj. R^2 (%)*	*Independent variables*	*p-value*	*Univariate correlation (p-value)*
Patch:				
C-oxidation ratio [a]	30	African American vs. European American	0.514	0.12 (0.27)
		Male vs. female	0.531	0.003 (0.98)
		Age	0.378	- 0.004 (0.97)
		Nicotine equivalents [c]	0.0014	0.21 (0.04)
		Glucuronidation ratio [d]	0.0003	- 0.37 (0.0003)
		% dose excreted as nicotine	0.0002	- 0.50 (< 0.0001)
Baseline:				
C-oxidation ratio [a]	0.37	African American vs. European American	0.232	0.19 (0.16)
		Male vs. female	0.936	- 0.02 (0.87)
		Age	0.593	0.10 (0.46)
		Nicotine equivalents [c]	0.215	0.17 (0.20)
		Glucuronidation ratio [d]	<0.0001	- 0.56 (<0.001)
		Urine volume	0.008	- 0.26 (0.05)

[a] Urinary total *trans*-3'-hydroxycotinine / total cotinine; square-root transformed
[b] Stepwise selection was used to select variables included in the models presented, though demographic variables (ethnicity, age, gender) were forced into the model if rejected during selection. Nicotine and its metabolites were measured in 24-hour urine.
[c] Sum of urinary total nicotine, total cotinine, and total *trans*-3'-hydroxycotinine
[d] Cotinine-*N*-glucuronide / free cotinine; square-root transformed

2.3.3 Baseline nicotine metabolism

Nicotine and nicotine metabolites were quantified in 24-hour urine at baseline while participants were smoking *ad libitum* (Table 2-2). Free nicotine and free cotinine were higher in African Americans compared to European Americans, 8.8 versus 6.0 nmol/ml ($p = 0.02$) and 6.1 versus 4.4 nmol/ml ($p = 0.01$), respectively. Between ethnic groups there were no statistically significant differences in total nicotine ($p = 0.07$), total cotinine ($p = 0.54$), or total *trans*-3'-hydroxycotinine ($p = 0.06$). The correlation between total nicotine and total cotinine was 0.70 ($p < 0.0001$). Mean nicotine equivalents were 77.4 nmol/ml and 61.7 nmol/ml among African Americans and European Americans respectively ($p = 0.09$). Notably, mean nicotine equivalents per cigarette were higher for African Americans compared to European Americans, 4.7 nmol/ml versus 3.0 nmol/ml ($p = 0.02$).

The mean percent nicotine or cotinine excreted as a glucuronide at baseline is presented in Table 2-2. The correlation between percent nicotine and cotinine glucuronidation was 0.63 ($p < 0.0001$). The percent nicotine excreted as its glucuronide was 51.4 % and 57.4 % among African Americans and European Americans respectively ($p = 0.05$). The percent cotinine excreted as its glucuronide was lower among African Americans compared to European Americans, 71.2 % versus 79.8 % ($p = 0.01$).

There was no difference in the mean the *trans*-3'-hydroxycotinine : total cotinine ratio by ethnicity at baseline. The ratio had an overall range of 0.1 – 3.7. The mean ratios were 1.5 +/- 1.0 and 1.1 +/- 0.6 among African Americans and European

Americans respectively ($p = 0.17$). There was also no ethnic difference if the ratio was calculated as total *trans*-3'-hydroxycotinine to free cotinine ($p = 0.92$). However, the correlation between total *trans*-3'-hydroxycotinine and total cotinine was lower among African Americans than European Americans; 0.36 versus 0.72 with 95 % confidence intervals, 0.002-0.637 and 0.456-0.864, respectively ($p = 0.06$).

We analyzed predictors of the glucuronidation and oxidation ratios during smoking (Table 2). In univariate comparisons, a low glucuronidation ratio was correlated with male gender, lower nicotine equivalents, and a higher C-oxidation ratio. The strongest correlation was between the glucuronidation ratio and the C-oxidation ratio; - 0.56, $p < 0.0001$). In a multivariate model, African American ethnicity, low nicotine equivalents, and a high oxidation ratio were significant predictors of cotinine glucuronidation with an adjusted R^2 value of 0.50 (Table 3). Predictors of a high C-oxidation ratio were a low glucuronidation ratio and low urine volume, and no associations were observed with ethnicity, gender, age, or nicotine equivalents. A limited linear regression model with the glucuronidation ratio and urine volume had an adjusted R^2 value of 0.39, and this model was not improved by inclusion of other variables.

2.4 Discussion

Higher free cotinine levels have been consistently reported among African Americans compared to European Americans (41;106;108). To the extent that higher cotinine levels reflect higher nicotine exposure and correspondingly exposure to

tobacco carcinogens, higher cotinine could explain a portion of the increased cancer risk observed among African Americans. In our study, African Americans received a higher dose of nicotine per cigarette than European Americans as observed by Benowitz *et al.*, presumably due to a difference in smoking behavior (107;145). However, differences in nicotine metabolism independent of dose per cigarette also contributed to ethnic differences in free cotinine levels. The major finding of this study was that among abstinent smokers on the nicotine patch, African Americans excreted less nicotine and cotinine as their glucuronide conjugates than European Americans. Importantly, higher free cotinine among African Americans was accounted for by lower glucuronide conjugation in the controlled dose setting.

Our study bridges the findings of an elegant pharmacokinetics study published several years ago by Benowitz *et al.* who originally observed that nicotine and cotinine glucuronidation may be lower in African Americans compared to European Americans (145). In this study, smokers were infused with deuterium-labeled nicotine (D_2) and deuterium-labeled cotinine (D_4), and metabolites were quantified in plasma and urine. Among African Americans, the percent glucuronidation of nicotine and cotinine was lower for both labeled and unlabeled (ie. from smoking) analytes in 8-hour urine. Moreover, nonrenal clearance of cotinine was decreased and renal clearance of free cotinine was increased. Ours is the first subsequent study that was designed to quantify any ethnic difference in glucuronidation; it corroborated the previous outcome in a separate population, extended the findings to the nicotine patch, and evaluated short-term intraindividual variation. Also, the observed difference in glucuronidation occurred in the absence of exposure to other constituents in tobacco smoke since

participants had not smoked for 4 days prior to sample collection and this eliminated the possibility that a tobacco constituent for which exposures differ between ethnic groups caused the variation in glucuronidation.

Since the majority of African Americans smoke menthol cigarettes compared to a minority of European Americans, this has been proposed as an explanation for ethnic differences in nicotine metabolism. However, menthol was not a factor in our study since the half-life of menthol is about an hour and our participants were biochemically confirmed to be abstinent from smoking (155). In the study by Benowitz *et al*., menthol could have affected metabolite concentrations only in later plasma samples (6- and 8-hour timepoints) and in the 8-hour urine because participants were abstinent from 10 p.m. the night preceding the study to 1 pm during the procedure day (145).

In multivariate analyses, lower cotinine glucuronidation was associated with African American ethnicity as well as a higher total *trans*-3'-hydroxycotinine to total cotinine (C-oxidation ratio) in urine. However, there was no association between ethnicity and the C-oxidation ratio, either while participants were on the patch or smoking. The C-oxidation ratio in urine is highly correlated with the plasma ratio, which has been used as a biomarker for P450 2A6 activity (135). Yet, Swan *et al.* reported that variation in the urine ratio is greater than in the plasma ratio and it is likely influenced by the contribution of other genes (156). We observed that glucuronidation is associated with the urinary C-oxidation ratio, and contributes to variation in the urinary C-oxidation ratio. Consequently, caution is warranted in comparing the urinary oxidation ratio as a marker of P450 2A6 activity at least between populations with different glucuronidation

phenotypes. This observation is independent of the additional problem that P450 2A6-catalyzes the formation of two other cotinine metabolites and that the *in vivo* catalyst(s) has not been definitively ascertained.

We did not observe evidence for an ethnic difference in C-oxidation of nicotine or cotinine. On the nicotine patch, there were no differences in total cotinine or total *trans*-3'-hydroxycotinine in urine or plasma. Also, there was no difference in the ratio of total *trans*-3'-hydroxycotinine to total cotinine by ethnicity. The higher cotinine concentrations observed for African Americans on the patch were accounted for by a decrease in its glucuronide conjugate.

In contrast, Benowitz *et al.* interpreted their data as indicating that African Americans had lower glucuronidation and lower oxidation (145). The fractional conversion of nicotine to cotinine ($f_{nic->cot}$) was calculated as the AUC-D_2-cotinine/dose-D_2-nicotine * dose-D_4-cotinine/AUC-D_4-cotinine. The first term reflects metabolism of D_2-nicotine to cotinine and the second term is total cotinine clearance based on co-administered D_4-cotinine. Total clearance of D_4-cotinine was definitively lower among African Americans in this pharmacokinetics study, perhaps due solely to decreased glucuronidation. In any case, even if nicotine metabolism to cotinine was identical between ethnic groups the $f_{nic->cot}$ still would have been lower based on the calculation used. Only if total clearance of cotinine had been faster among African Americans, resulting in a decreased AUC-D_4-cotinine, could the calculated $f_{nic->cot}$ have been the same or higher compared to European Americans. Thus, these data are not necessarily

consistent with decreased oxidation and it seems that a decrease in glucuronidation among African Americans could entirely explain the previously published data.

2.5 Conclusion

In conclusion, the major finding of our study was that African Americans had lower nicotine and cotinine glucuronidation than European Americans on the nicotine patch and during baseline smoking. Cotinine is the most commonly used biomarker of nicotine exposure (157;158). However, we have shown that use of cotinine as the sole biomarker would result in overestimation of nicotine exposure among African Americans compared to European Americans. For example, higher cotinine levels due to lower glucuronidation, independent of exposure, could confound ethnic studies of cancer risk. Knowledge of nicotine metabolism in a population can facilitate selection of tobacco biomarkers, and in the situation where tobacco exposure is compared between African Americans and European Americans, total cotinine (cotinine + glucuronides) or nicotine equivalents are better biomarkers than free cotinine. We expect that the higher prevalence of a low glucuronidation phenotype among African Americans, due to genetic or environmental factors, will also proportionally affect the disposition of other drugs and xenobiotics. A low glucuronidation phenotype could increase risk of toxicity from compounds that are detoxified by *N*-glucuronidation.

2.6 Acknowledgements

Many thanks to Elizabeth Thompson, Gregory Blaufuss, and May Wang for their assistance in preparing samples and quantifying nicotine metabolites. I also thank Dr. Jasit Ahluwalia and Office of Clinical Research, Univ. of MN, for generous support.

2.7 Publication of thesis work

The work discussed in Chapter 2 was published: Jeannette Zinggeler Berg, Jesse Mason, Angela J. Boettcher, Dorothy K. Hatsukami, and Sharon E. Murphy. Nicotine metabolism in African Americans and European Americans: variation in glucuronidation by ethnicity and UGT2B10 haplotype. J Pharmacol. Exp. Ther. 2009; available online September 28, 2009.

CHAPTER 3

UGT2B10 genotype and nicotine metabolism

3.1 Introduction

Nicotine and cotinine glucuronidation contribute to overall nicotine metabolism, and there is significant interindividual variation in the formation of these glucuronides. Nicotine and cotinine glucuronides constitute 25 % of the sum of nicotine and its metabolites in smokers' urine on average (159). A similar percentage of nicotine and cotinine glucuronides are excreted in urine following intravenous or transdermal nicotine administration (32). Nicotine glucuronide can account for greater than 40 % of nicotine and its metabolites in individuals with low capacity for nicotine C-oxidation (118). Cotinine glucuronide can also account for up to 40 % of the estimated nicotine dose (112). However, in other individuals, nicotine and cotinine glucuronides are not detected (32;111;112).

It is not known if differences in glucuronidation can explain variation in smoking behavior or addiction to nicotine. However, individuals with substantially decreased nicotine C-oxidation, such as individuals with deleted CYP2A6, do exhibit lower

intensity smoking behavior (e.g. lower nicotine equivalents, a modest decrease in cigarettes/day) (115;132). The pharmacokinetics of nicotine metabolism are altered in individuals who are homozygous or heterozygous for known low activity CYP2A6 alleles, resulting in a longer nicotine $t_{1/2}$ and slower nonrenal nicotine clearance (115). The prevailing view is that these individuals achieve and maintain similar levels of nicotine compared to individuals with average nicotine oxidation while having lower nicotine intake (134;137;160;161). Therefore a decrease in glucuronidation – perhaps in the context of lower nicotine C-oxidation – may also affect smoking behavior. There are no published reports that have evaluated an effect of glucuronidation on smoking.

Identifying the enzymes responsible for nicotine and cotinine glucuronidation has progressed slowly, and has depended on several scientific advances. Around 1990, nicotine and cotinine glucuronides were first identified as nicotine metabolites. The structure of cotinine glucuronide was deduced based on liquid chromatography/mass spectrometry (LC/MS) analysis of cotinine glucuronide in smokers' urine in comparison to NMR-confirmed synthetic standard (162). NMR analysis of nicotine glucuronide standard as well as products from incubations with human liver microsomes (HLMs) and UGT1A4 confirmed the structure of nicotine glucuronide (163). Specifically, conjugation occurs at the nitrogen of the pyridine ring for both molecules (Figure 3-1). These glucuronides were initially quantified in incubations with HLMs using radioactive substrates and radioflow HPLC. However, a ~20-fold lower limit of detection was achieved with LC/MS/MS and this facilitated evaluating the role of individually-expressed UGTs, which have low activity compared to HLMs (87;163). Unfortunately, there are still a limited number of specific antibodies and inhibitors.

Standardized enzyme quantification by adding a his tag to UGT expression constructs and using an anti-His antibody has also aided comparisons between individual enzymes (87). Some UGTs including UGT2B10, were only recently identified to have enzymatic activity after initial screens for activity failed (164).

Figure 3-1. Major glucuronide metabolites of nicotine

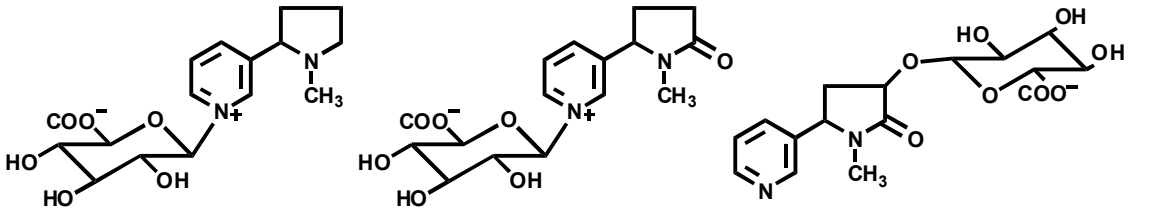

The most promising candidate for the main catalyst of nicotine and cotinine glucuronidation prior to 2007 was UGT1A4 (163). This UGT is expressed in liver at significant levels and catalyzes a host of *N*-linked conjugation reactions broadly encompassing secondary and tertiary aliphatic amines, primary aromatic amines, as well as secondary and tertiary aromatic *N*-hetrocyclic compounds (165-168). UGT1A4 is a better catalyst of *N*-glucuronidation than most other UGTs. However, while the UGTs 1A1, 1A3, 1A7, 1A9, and 2B7 primarily catalyze *O*-glucuronidation they are also capable of catalyzing certain *N*-glucuronidation reactions (165;166;169;170). Kuehl *et al*. demonstrated that UGT1A4 catalyzes *N*-glucuronidation of nicotine and cotinine using baculovirus-expessed UGTs; the rate of product formation was ~30-fold greater than for UGT1A3 and UGT1A9 (171). UGT2B7 has also been reported to have some

nicotine glucuronidation activity, but no cotinine glucuronidation was observed (87). Nicotine glucuronidation by HLMs was inhibited by 30-50 % with imipramine, a UGT1A4 substrate (163). In 2007 the role of UGT1A4 as a catalyst of nicotine and cotinine glucuronidation was again confirmed, but at this time two groups also identified UGT2B10 as a good catalyst of nicotine and cotinine glucuronidation (87;143). UGT2B10 has the lowest K_m for nicotine and cotinine glucuronidation of all UGTs tested *in vitro*.

UGT2B10 was considered an inactive or orphan UGT for years prior to discovery that it is active and metabolizes both endogenous and exogenous molecules. UGT2B10 was cloned in 1993, expressed in COS-7 cells, and screened for activity with >40 compounds, including imipramine, but no glucuronidation activity was detected (172). Subsequently, human embryonic kidney fibroblast (HEK) expressed UGT2B10 was found to catalyze *O*-linked glucuronidation of hydroxyeicosatetraenoic acids and 13-hydroxyoctadecadieneoic acid and *N*-linked glucuronidation of the heterocyclic amine *N*-hydroxy-2-amino-1-methyl-6-phenylimidazo[4,5-*b*]-pyridine (*N*-hydroxy PhIP, a dietary carcinogen)(164;173). It also turns out that UGT2B10 does catalyze impramine glucuronidation. There has been no public discussion on if a difference in DNA sequence or expression system contributed to the discrepancy in observed enzymatic activity or lack thereof. Kaivosaari *et al.* have reported that UGT2B10 loses activity during the preparation of microsomes; UGT2B10 microsomes lost 60 % of activity compared to cell homogenate while no difference was observed for UGT1A4 (87).

UGT2B10 and UGT1A4 likely both contribute to nicotine metabolism. UGT2B10 and UGT1A4 are predicted to be expressed at similar levels in the liver, although the only data available is quantitative RT-PCR of 47 pooled liver samples (87). *In vitro* kinetic parameters published for UGT2B10 and UGT1A4 are presented in Table 3-1. Kaivosaari *et al.* reported K_m values for HEK-expressed UGT2B10 and UGT1A4 where rates were standardized to mg his-tagged protein and products were analyzed by LC/MS (87). K_m values were 10-fold and 1.5-fold lower for UGT2B10 than UGT1A4 for nicotine and cotinine glucuronidation, respectively. However, glucuronidation rates (pmol/min/mg) were 100-fold lower for expressed enzyme than HLMs and therefore V_{max} was not estimated. Chen *et al.* determined K_m and V_{max} values for baculovirus-expressed UGT2B10 and UGT1A4, where products were analyzed by radioflow HPLC (143). This group reported K_m values that were 37-fold and 3-fold lower for UGT2B10 than UGT1A4 for nicotine and cotinine glucuronidation, respectively. Interestingly, Chen *et al.* observed a higher apparent V_{max} for nicotine and cotinine glucuronidation by UGT1A4 than by UGT2B10. However, if UGT2B10 is unstable during the preparation of microsomes then the V_{max} may be underestimated.

Polymorphisms exist in both UGT1A4 and UGT2B10, and some of these polymorphisms cause or are linked to altered metabolism of substrates. UGT1A4 is part of the complex UGT1A locus containing 13 genes, each with a unique exon that is essentially spliced to four common 3′ exons that are shared by members of the locus (75).(174) Throughout the UGT1A locus there are 598 NCBI SNPs, including 12 missense SNPs in the coding region of UGT1A4 and 11 SNPs in the 3'- untranslated region (The Single Nucleotide Polymorphism Database (dbSNP) of Nucleotide

Sequence Variation (2008) NCBI, NIH). The UGT1A4 polymorphisms Leu48Val and Pro24Thr have altered metabolism of several substrates (e.g. imipramine, clozapine, β-naphthylamine, dihydrotestosterone) *in vitro* (153;175). For example, the presence of a Pro24Thr substitution in UGT1A4 correlated with increased *N*-glucuronidation of the tobacco carcinogen 4-(methylnitrosamino)-1-(3-pyridyl)-1-butanol (NNAL) in a series of human liver microsomes (176). The UGT1A4 Leu48Val polymorphism is found in 17 % of the Japanese population in 9 % of Caucasians; Pro24Thr was found in 8 % of Caucasians (153;175). No studies on nicotine or cotinine metabolism by these variants have been published. In the gene region of UGT2B10 there are 139 NCBI SNPs including at least 3 missense SNPs (dbSNP). Identifying haplotypes has facilitated screening for genotype-phenotype associations and has led to the identification of previously undescribed SNPs that affect enzyme function or stability (152;177). A variant of UGT2B10, described in detail below, decreases but does not abolish nicotine and cotinine glucuronidation by HLMs.

A haplotype of UGT2B10 was found that was associated with significantly decreased NNAL glucuronidation by human liver microsomes. DNA sequencing identified only one nonsynonymous SNP in the coding region. This SNP was present in 2 liver samples that were homozygous for the haplotype associated with low glucuronidation and was absent in 5 liver samples with other haplotypes and average glucuronidation (177). *In vitro*, HEK cells transfected with UGT2B10 67Tyr results in mRNA levels that are similar to wild type, but microsomes prepared from these cells had almost now NNAL glucuronidation activity (177).

Table 3-1. Nicotine and cotinine glucuronidation by expressed UGTs

UGT1A4 and UGT2B10: K_m (mM) for nicotine and cotinine glucuronidation				
			UGT1A4	**UGT2B10**
Study	*Expression system*	*Preparation*	K_m	K_m
Nicotine-*N*-glucuronidation:				
Kaivosaari *et al*. 2007	Baculovirus	Cell lysate	2.4	0.29
Lazarus *et al.* 2007	HEK293	Microsomes	17.5	0.5
Cotinine-*N*-glucuronidation:				
Kaivosaari *et al*. 2007	Baculovirus	Cell lysate	1.5	1
Lazarus *et al.* 2007	HEK293	Microsomes	10.3	3.5
References: (87), (143)				

Nicotine and cotinine glucuronidation activities were decreased by 20 % and 30 % among HLMs that were heterozygous for the Asp67Tyr allele compared to wild-type HLMs. Two HLMs that were homozygous for Asp67Tyr had dramatically decreased glucuronidation activity, although in reactions with 5 mM nicotine a rate of greater than 100 pmoles nicotine glucuronide/min/mg protein still occurred (Chen 2007). Chen *et al.* reported that heterologously expressed UGT2B10 Asp67Tyr had no NNAL or cotinine glucuronidation activity, and "barely detectable" activity for nicotine glucuronidation. However, while Chen *et al*. assessed mRNA expression and observed no significant difference by genotype, they did not evaluate protein expression and

different protein levels for the Asp67Tyr construct or a difference in enzyamtic activity may explain the results.

A potential deletion of UGT2B10 may also exist, based on publically available data from copy number variation (CNV) discovery projects. Putative insertion/deletion regions overlap with UGT2B10. PCR analysis could positively identify the presence of a deletion if primers are designed for sequences 5' and 3' to the break point regardless of the size of the deletion. However, this approach is dependent on accurate assessment of breakpoints which in turn depends on the coverage of comparative genome hybridization arrays.

To determine if UGT2B10 influences nicotine and cotinine glucuronidaiton *in vivo* we genotyped smokers for the UGT2B10 Asp67Tyr allele and evaluated the association of genotype with nicotine metabolism phenotype. We hypothesized that individuals with the Asp67Tyr variant would excrete less nicotine and cotinine as glucuronides in urine. In addition, we investigated if the Asp67Tyr variant was present among African Americans and if the frequency of the variant was increased relative to European Americans, as a potential explanation for the decreased glucuronidation observed among African Americans in Chapter 2. We analyzed *in vitro* nicotine glucuronidation by HLMs from African American and European American donors and genotyped these samples. Also, DNA samples available from a subset of participants in the ethnic metabolism study were genotyped.

3.2 Methods

3.2.1 TRIP Study

UGT2B10 genotype-phenotype analyses involved samples from a prior study of nicotine metabolism among European American smokers. Tobacco Reduction Intervention Program (TRIP) participants were smokers aged 18 – 70 who smoked > 14 cpd (112;178). While smoking as usual, participants provided first morning urine; 2 – 4 samples were collected at least one week apart.

3.2.2 Human liver tissue source

Frozen normal liver tissues from African American (n=14) or European American (n=14) donors were obtained through the Liver Tissue Cell Distribution System from the University of Pittsburgh repository (NIH Contract # N01-DK-7-0004/HHSN26700700004C). Donor characteristics were average age (49 years), gender (50 % female), BMI (26.6 kg/m^2), and smoker (36 %).

3.2.3 Chemicals and reagents

(S)-[5-^{3}H]-Nicotine was purified as previously described (123). Nicotine *N*-βD-glucuronide was purchased from Toronto Research Chemicals (North York, ON,

Canada). Other chemicals were purchased from Sigma-Aldrich (St. Louis, MO) unless otherwise noted.

3.2.4 Nicotine and metabolite analysis

All urine samples were stored at -20°C prior to analysis. Urinary nicotine and nicotine metabolite concentrations were analyzed by GC/MS and were previously reported (112). Free nicotine, total nicotine (free nicotine + *N*-glucuronide), free cotinine, and total cotinine (free cotinine + *N*-glucuronide) and total *trans*-3'-hydroxycotinine (*trans*-3'-hydroxycotinine + its glucuronides) were quantified. Analyses were performed in duplicate for each urine sample and repeated if values differed by > 10 %. An overview of the analytic method is provided in Chapter 2.

3.2.5 UGT2B10 haplotyping

DNA was isolated from blood (Ethnic nicotine patch study, n=32; TRIP study, n=84) with the GFX DNA purification kit (Amersham Biosciences, Piscataway, NJ) or from frozen human liver tissue (n=28) using the DNeasy kit (Qiagen, Valencia, CA). PCR-restriction fragment length polymorphism (RFLP) analysis was performed as previously described on the UGT2B10 SNP rs7657958 that is linked with Asp67Tyr in Caucasians (haplotype C) (177). DNA samples that tested positive for the rs7657958 variant and an equal number of samples that were called wild-type were subjected to a

second RFLP targeting the codon 67 position with HinfI digestion (177). DNA from all African Americans and from all European Americans in the ethnic study was genotyped at the codon 67 position. The Asp67Tyr substitution was confirmed by DNA sequencing in 8 individuals (2 African Americans and 6 European Americans) and its absence was confirmed in 2 wild-type individuals.

3.2.6 Nicotine glucuronidation by human liver microsomes (HLMs)

Microsomes from human liver samples were prepared by the method of Fowler *et al.* and aliquots were stored at -80°C (179). Total protein concentrations were determined by the Bradford assay with Coomassie Plus (Pierce, Rockford, IL). Microsome quality was evaluated by *p*-nitrophenol *O*-glucuronidation activity. Product formation was quantified by UV-HPLC after incubation with 500 μM p-nitrophenol and 5 mM UDPGA (163). These HLMs had p-nitrophenol glucuronidation activity ranging from 10-55 nmol/min/mg protein.

HLMs (2mg/ml) were incubated with 0.5 or 5 mM (S)-[5-^{3}H]nicotine (specific activity, 25nCi/nmol or 2.5 nCi/nmol respectively) and 5 mM UDPGA essentially as described by Kuehl *et al*. (163). Metabolites were quantified by radioflow HPLC using a Gemini C18 5 μM 250 x 4.60 mm column (Phenomenex, Torrance, CA), SPD-10Avp UV-VIS detector (Shimadzu, Kyoto, Japan), and β-RAM radioflow detector (IN/US Systems, Tampa, FL). The mobile phase was 20 mM ammonium bicarbonate (pH 9.2) in water (A) and acetonitrile (B) and the gradient was 2.5%B for 0-12 min., to 25% B in

15 min., hold at 25 % B for 5 min. The eluant flow was 0.8 ml/min and the scintillant flow was 2.4 ml/min using Monoflow 5 (National Diagnostics, Atlanta, GA). Nicotine glucuronide was retained longer on this HPLC system than when an acidic TFA aqueous phase was used. No significant cleavage of nicotine *N*-glucuronide was observed during HPLC analysis. We observed good separation between nicotine *N*-glucuronide (11 min.) and nicotine (41 min.). The tritiated reaction product co-eluted with nicotine *N*-glucuronide standard, and formed nicotine following β-glucuronidase treatment. No other products were observed. Activity assays were performed with microsomes that underwent a single freeze-thaw since repeated freeze-thaw resulted in significantly decreased p-nitrophenol and nicotine glucuronidation activity; however, this did not appear to vary by donor ethnicity or UGT2B10 haplotype.

3.2.7 Statistics

Statistical analyses were conducted using SAS (SAS Institute, Cary, NC) and Excel (Microsoft, Redmond, WA). Wilcoxon two-sided t-approximation statistics were calculated to compare means of continuous variables that did not have a normal distribution, and a p-value less than 0.05 was considered significant. Since 2-4 urine samples were available per participant, repeated measures analysis of variance was used to compare the percent of analytes excreted as glucuronides and nicotine equivalents by genotype. Spearman nonparametric correlation was used to assess univariate correlations. Multivariate linear regression models were evaluated to assess predictors of cotinine glucuronidation (square-root transformed ratio of cotinine glucuronide to

free cotinine) and the nicotine C-oxidation ratio (square-root transformed ratio of total *trans*-3'-hydroxycotinine to total cotinine) (133).

3.3 Results

3.3.1 In vitro nicotine glucuronidation by human liver microsomes

Nicotine glucuronidation was characterized *in vitro* for 28 liver samples (14 from African American donors) that were genotyped for UGT2B10 Asp67Tyr. A 50-fold variation was observed in glucuronidation activity when liver microsomes were incubated with either 0.5 mM or 5 mM nicotine; range, 1.1 to 51 and not quantifiable to 112.4 pmol/min/mg protein, respectively. Mean nicotine glucuronidation activity was not different between samples obtained from African American and European American donors, 15.1 +/- 12 versus 14.3 +/- 13 pmol/min/mg protein, respectively ($p = 0.90$). Unlike ethnicity, UGT2B10 genotype did predict nicotine glucuronidation (Figure 3-2). The UGT2B10 Asp67Tyr variant was present in 2 African American and 6 European American samples. The mean rate of nicotine glucuronidation was 46-50 % lower for Asp67Tyr samples compared to wild-type, 8.1 pmol/min/mg protein compared to 17.5 pmol/min/mg protein ($p = 0.07$).

Figure 3-2. *In vitro* nicotine glucuronide conjugation by UGT2B10 haplotype [a]

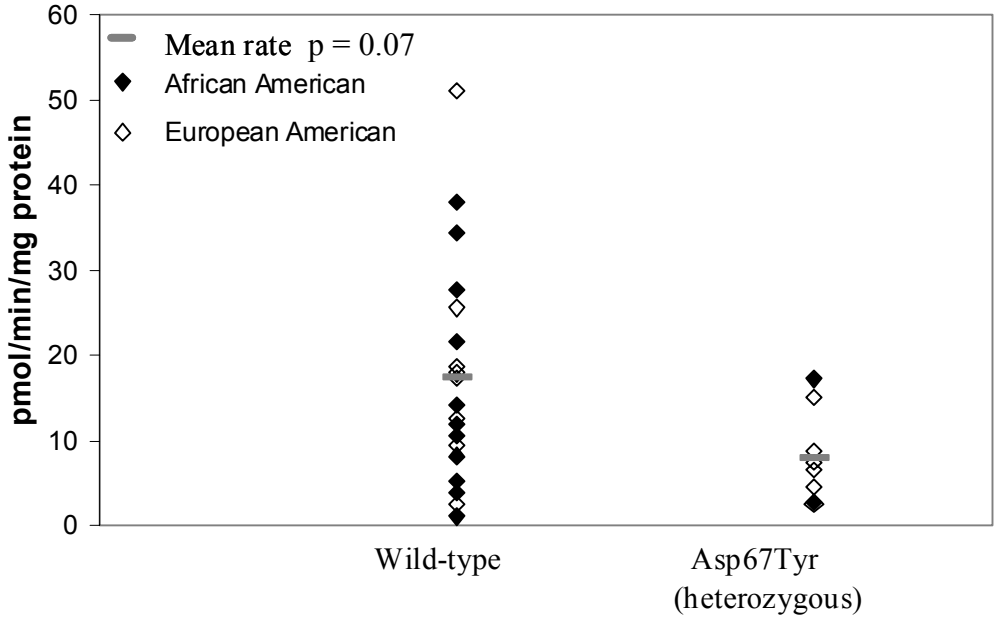

[a] HLMs incubated with 0.5 mM ^{3}H-nicotine (S.A. = 25 nCi/nmol) and 5 mM UDPGA

3.3.2 In vivo glucuronidation and UGT2B10 haplotype – ethnic nicotine patch study

DNA was available from 32 subjects in the patch study (18 African Americans and 14 European Americans). These subjects were genotyped for the UGT2B10 Asp67Tyr allele (177). In this small number of subjects there was no evidence that the Asp67Tyr allele was more common in African American than European American individuals. Five participants, 3 African Americans and 2 European Americans, were heterozygous and one African American was homozygous for the Asp67Tyr allele. No statistical differences were observed in nicotine metabolites by genotype. Interestingly, the percent nicotine and cotinine glucuronidation in the single homozygous Asp67Tyr variant, was low, 7.5 % and 11.9 %, respectively.

3.3.3 In vivo glucuronidation and UGT2B10 haplotype – TRIP study

In a population of smokers (TRIP study) for which both urinary nicotine metabolites and DNA was available, we further investigated the relationship of the UGT2B10 Asp67Tyr variant to nicotine and cotinine metabolism. Nicotine metabolite data on this population had been previously published (112;178). For the current study, participants were genotyped for the UGT2B10 haplotype that is tagged by the rs7657968 SNP and linked to Asp67Tyr (haplotype C) (177). Genotyping results were concordant in the subset of samples, including all the heterozygous individuals, which were analyzed by two RFLP analyses and a subset (n = 8) that were sequenced. Asp67Tyr was detected as a G>T substitution at nucleotide +199, and this co-occurred with a synonymous SNP at nucleotide 111 (T>C) as reported by Lazarus *et al.* (177). The allele frequency was 0.11 and was in Hardy-Weinberg equilibrium.

The mean percent glucuronidation of urinary metabolites in these smokers was determined for each haplotype (Table 3-2). The percent of cotinine and nicotine excreted in urine as glucuronide conjugates was 20 % lower among smokers who were heterozygous for UGT2B10 Asp67Tyr relative to smokers with no Asp67Tyr alleles (p-values; 0.006 and 0.03, respectively). The distribution of percent cotinine excreted as a glucuronide was related to UGT2B10 genotype (Figure 3-3). However, there were wild-type individuals who excreted less than 10 % of cotinine as its glucuronide conjugate and heterozygotes who excreted as much as 80 % of cotinine as a glucuronide conjugate. Interestingly, nicotine equivalents were significantly lower among

individuals with a UGT2B10 Asp67Tyr allele (Table 3-1); the mean was 35 % lower than wild-type.

Table 3-2. Urinary nicotine metabolites in smokers by UGT2B10 haplotype [a]

UGT2B10	*N*	*Nicotine equivalents Mean (SD.)[b,c]*	*Percent cotinine glucuronidation Mean (SD)[d,e]*	*Percent nicotine glucuronidation Mean (SD)[d,f]*
Wild-type	66	101.3 (58.1)	65.4 (13.5)	42.5 (18.9)
Asp67Tyr	18	69.2 (42.0)	52.7 (11.4)	34.0 (15.6)

[a] Metabolites were quantified in morning (1st void) urine, 2-4 baseline visits per participant and the effect of haplotype was tested by repeated measures analysis of variance.
[b] Sum of total nicotine, total cotinine, and total *trans*-3'-hydroxycotinine; [c] $p = 0.01$
[d] Percent of analyte excreted as a glucuronide; [e] $p = 0.003$, [f] $p = 0.02$

The effect of glucuronidation phenotype, independent of genotype, on nicotine equivalents and the ratio of total *trans*-3'-hydroxycotinine:cotinine (C-oxidation ratio) was also assessed. As for the ethnic patch study (Chapter 2), there was a negative correlation between glucuronidation, cotinine glucuronide:cotinine, and the oxidation ratio albeit it was weak, $r = -0.23$, $p = 0.01$. A positive correlation was observed between the glucuronidation ratio and nicotine equivalents; 0.38, $p < 0.0001$. In a linear regression model, a portion of the variability in the C-oxidation ratio was explained by nicotine equivalents (18 %) and the glucuronidation ratio (5 %).

Figure 3-3. Percent cotinine excreted as its glucuronide in 24-hour urine by UGT2B10 genotype

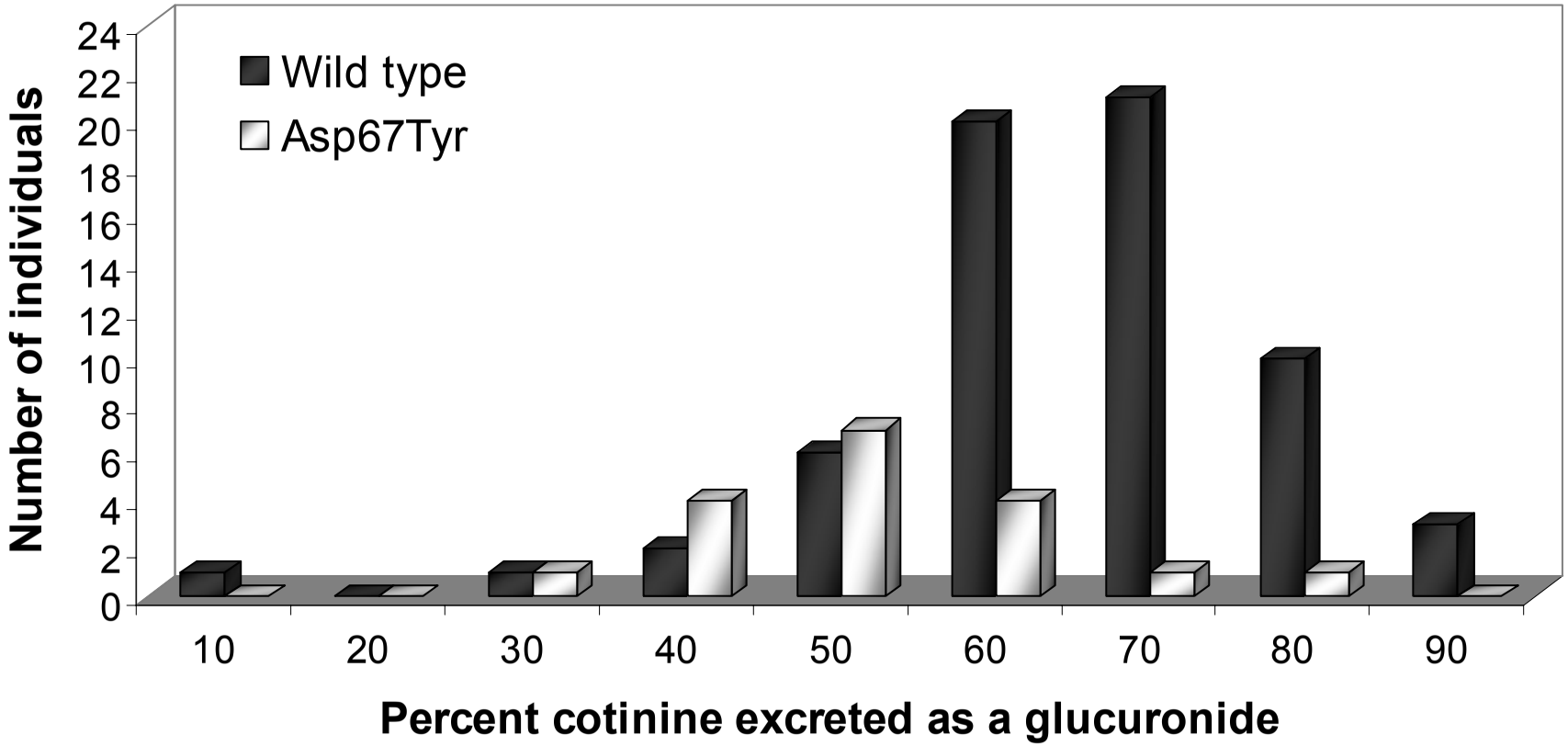

Discussion

Previously we observed lower glucuronidation of nicotine and cotinine among African Americans compared to European Americans. Here we investigated the role of the only UGT polymorphism that has been demonstrated to affect nicotine and cotinine glucuronidation *in vitro* as a possible explanation for the decreased glucuronidation observed in African Americans. While we demonstrated that the UGT2B10 Asp67Tyr is present among African Americans, the frequency of this allele was not higher among African Americans compared to European Americans in the 59 samples tested (N=31 participants from the ethnic patch study and 28 human liver samples). *In vitro* we observed that UGT2B10 Asp67Tyr was a better predictor of low nicotine glucuronidation than ethnicity. In fact, there was no difference in nicotine glucuronidation by ethnicity in this small *in vitro* study. Regretfully, the availability of liver tissue from African American donors was limited, in particular since we preferred tissues from the same procurement source. In conclusion, we expect that the UGT2B10 Asp67Tyr allele is unlikely to explain the observed decreased levels of glucuronidation in African Americans compared to European Americans. However, an uncharacterized variant in UGT2B10 may well contribute.

UGT2B10 is predicted to be the major enzyme responsible for nicotine and cotinine glucuronidation in smokers based on *in vitro* studies (87;143). This is the first report of *in vivo* nicotine and cotinine glucuronidation by UGT2B10 genotype, and our finding that smokers with a variant Asp67Tyr allele had decreased excretion of glucuronide conjugates provides convincing evidence that UGT2B10 significantly contributes to

nicotine metabolism *in vivo*. However, as illustrated in Figure 4, the Asp67Tyr UGT2B10 variant is clearly only one contributor to variation in nicotine and cotinine glucuronidation. The relatively high percentage of cotinine glucuronidation in some individuals who were heterozygous for this variant could be due to either variation in UGT2B10 expression or the contribution of UGT1A4, as a second catalyst of cotinine glucuronidation.

Biomarkers of glucuronidation that do not require knowledge of genotype would have utility in comparing nicotine metabolism, particularly among diverse populations. However, in this study and the ethnic patch study we observed that the urinary cotinine glucuronide:cotinine and *trans*-3'-hydroxycotinine:cotinine ratios were both positively correlated with nicotine equivalents. Therefore the possibility that these ratios vary as a function of nicotine dose must be considered. Clearly, the tradeoff between ease of measurement and more comprehensive profiling of phenotype or genotype depends on the particular goals of a study. However, we assert that the use of metabolite ratios as biomarkers of oxidation or glucuronidation in smokers requires further study, preferably prior to application in large epidemiological studies of tobacco-associated cancers.

Interestingly, individuals with the UGT2B10 Asp67Tyr variant had lower nicotine equivalents than individuals without this allele. Is it possible that these individuals smoke less? We have accounted for the major metabolites of nicotine metabolism, and no increases were observed in total C-oxidation. If a shift occurs in nicotine metabolism to other minor pathways of nicotine metabolism, such as N-oxide formation, we would have underestimated nicotine equivalents. For instance, nicotine

N-oxide represented 40 % of nicotine and its metabolites in the urine of an individual who had very low C-oxidation activity and deleted CYP2A6 (118). Also, Benowitz *et al*. observed that a higher amount of unchanged nicotine and nicotine glucuronide were excreted in urine of individuals with a low activity CYP2A6 allele and decreased nicotine C-oxidation compared to wild-type individuals. Yet, the percent of nicotine excreted as a glucuronide was not different, and thus the increase in nicotine glucuronide was due to an increase in free nicotine availability and not upregulation of glucuronidation. If low glucuronidation results in elevated blood nicotine concentrations, perhaps in the context of relatively low nicotine C-oxidation, an individual may smoke less intensely as is observed for individuals with low nicotine oxidation. The potential role of UGT2B10 on smoking behavior merits further investigation based on the intriguing finding that individuals who were heterozygous for Asp67Tyr had lower nicotine equivalents than wild-type.

We expect that differences in UGT2B10 activity, due to genetic or environmental factors, will affect the disposition of other drugs and xenobiotics. For instance, UGT2B10 was reported to catalyze the metabolism of the analgesic, medetomidine, and its role in the metabolism of other drugs that undergo *N*-glucuronidation is being investigated (180). UGT2B10 catalyzes *N*-glucuronidation of the tobacco carcinogen 4-(methylnitrosamino)-1-(3-pyridyl)-1-butanol (NNAL) *in vitro* and is predicted to contribute to its detoxification *in vivo* (177;181). UGT2B10 may modulate cancer risk through an effect on smoking behavior or carcinogen metabolism. In brief, low UGT2B10 activity may have important health consequences.

3.5 Conclusions

UGT2B10 contributes to *in vivo* nicotine and cotinine glucuronidation. The role for UGT2B10 was demonstrated by the effect of a variant genotype on glucuronidation phenotype. Smokers who were heterozygous for the variant UGT2B10 Asp67Tyr allele had decreased excretion of nicotine and cotinine as their glucuronide conjugates. UGT2B10 haplotype was a better predictor of glucuronidation phenotype than ethnicity (African American versus European American). Also, the UGT2B10 Asp67Tyr allele does not explain the ethnic variation in glucuronidation that was presented in Chapter 2. When the study population was sorted by UGT2B10 genotype, nicotine equivalents were lower among individuals with the variant allele. This observation could reflect a gene-mediated effect on smoking behavior which would be a substantial finding. We conclude that these genotype-phenotype analyses should be verified in another study population.

3.6 Acknowledgements

Many thanks to Elizabeth Thompson and Jodi Blustin for their assistance with UGT2B10 genotyping.

3.7 Publication of thesis work

Published in combination with Chapter 2 content; see page 50.

CHAPTER 4

Nicotine metabolite profiling including nicotine-*N*-oxide and UGT2B10 genotype

4.1 Introduction

Cancer etiology and epidemiology studies frequently require assessment of tobacco exposure due to tobacco's role in the development of several cancers (14;182-184). Error in estimating tobacco exposure can obscure important observations, while accuracy in exposure assessment is useful to identify it as either a causal or confounding factor. Many approaches have been used to evaluate tobacco exposure broadly including: self-report of smoking history (cigarettes/day, pack-years of smoking, time spent around a smoker, etc.), collection of used products (cigarette butts, discarded chew), topography measures (puff volume, frequency), and biomarkers (exhaled carbon monoxide, nicotine metabolites, tobacco specific nitrosamines) (112;120;122;185-187). Selecting a measure to assess exposure is not a trivial choice and depends on the goals of a particular study.

Quantifying one or more nicotine metabolites is an objective measure of current exposure from smoking, smokeless tobacco use, or environmental/secondhand smoke.

Plasma or urinary cotinine are the most frequently utilized biomarker of tobacco exposure, other than exhaled carbon monoxide (157;158;158). The only significant source of cotinine is metabolism from nicotine, and it is highly correlated with nicotine intake (32;117). However, interindividual differences in nicotine metabolism also influence cotinine levels (33;188). A potentially more robust biomarker of nicotine exposure is nicotine equivalents, defined as the sum of nicotine and its major metabolites in urine (120). Total nicotine (nicotine + nicotine glucuronide), total cotinine (cotinine + cotinine glucuronide) and *trans*-3'-hydroxycotinine (*trans*-3'-hydroxycotinine + its glucuronides) can be assessed with minimal sample preparation (e.g. a single solid phase extraction) by liquid chromatography/mass spectrometry with high throughput capacity (LC/MS) (119). Therefore, assessing nicotine equivalents is feasible in the time typically used to quantify a single nicotine metabolite. Nicotine equivalents directly account for over 80 % of nicotine intake, and since it is a sum of metabolites the effect of interindividual differences in any of the major metabolites is minimized (32;117;119).

Polymorphisms are common in nicotine metabolism genes and their regulatory regions, although only a minority of the known variants have been fully characterized (189). Enzyme amount and relative activity affect the metabolic fate of nicotine. Several polymorphisms in CYP2A6, the hepatic enzyme responsible for oxidation of nicotine to cotinine and a major catalyst of cotinine oxidation to trans-3'-hydroxycotinine, are associated with lower intensity smoking (115;136;190). For example, CYP2A6 polymorphisms that influence smoking behavior include CYP2A6*4, a deletion allele, CYP2A6*2, an inactivating point mutation, and

CYP2A6*9 which alters the TATA box promoter region (115;191;192). Furthermore, low nicotine C-oxidation and low concentrations of the tobacco carcinogen NNAL have been observed among Japanese Americans, a population with a high prevalence of deletion alleles, compared to European Americans (133). UGT2B10 and UGT1A4 catalyze the *N*-glucuronidation pathways of nicotine metabolism *in vitro* and the genes encoding these enzymes are also polymorphic (87;143;153;177).. Recently, we reported that the UGT2B10 polymorphism Asp67Tyr was associated with a 20 % decrease in the excretion of cotinine and nicotine as their glucuronide conjugates in urine of 84 smokers (188). This UGT2B10 variant was characterized *in vitro* by Chen *et al.* as having decreased nicotine and cotinine glucuronidation activity (188).

The main goals of the current study were to evaluate if the relationship between Asp67Tyr and lower glucuronidation could be confirmed, to assess if glucuronidation was associated with a shift in nicotine metabolism through other pathways including to nicotine-*N*-oxide, and to explore nicotine equivalents as a pathway-independent measure of tobacco exposure. In this population, where a defined genetic variant influenced phenotype, we could probe the strengths and weaknesses of different nicotine metabolites as biomarkers of exposure.

4.2 Methods

4.2.1 Study population and protocol

This research was approved by the University of Minnesota's Institutional Review Board. A total of 327 adult smokers who were recruited from the Twin Cities metropolitan area and who participated in one of three tobacco research studies conducted at the University of Minnesota were included in this genotype-phenotype investigation. Participants were recruited through advertisements on campus and local media, were screened by telephone, and were willing to participate in a smoking reduction or cessation study similarly for these studies. Participants were in good physical and psychiatric health, had no contraindications to nicotine replacement therapy, were not pregnant or nursing, and were not using barbituates or anti-convulsants.

For each study, participants were asked to provide a first void morning urine sample while they were smoking as usual, and this sample was collected at least two weeks prior to any study intervention (and before randomization to an intervention group). A blood sample was also collected from participants. Study 1 included 110 participants aged 18-65 who smoked > 15 cigarettes per day and who subsequently participated in a cessation trial of traditional nicotine replacement or smokeless tobacco. Study 2 included 145 participants aged 18 – 70 who were smokers of 10 – 40 ''light'' cigarettes (0.7–1.0 mg nicotine/cigarette) per day and who then participated in a study of low and no nicotine cigarettes (132). Study 3 included 84 smokers aged 18 – 70 years who smoked 15 – 45 cigarettes/day and subsequently participated in a smoking reduction trial (112;188). Initial genotype-phenotype analyses of UGT2B10 Asp67Tyr genotype and the percent of nicotine and cotinine excreted as glucuronide conjugates were recently conducted on study 3 samples (188).

4.2.2 Nicotine and metabolite analysis

Urinary nicotine and nicotine metabolite concentrations were analyzed by GC/MS and were previously reported (112). Free nicotine, total nicotine (free nicotine + *N*-glucuronide), free cotinine, and total cotinine (free cotinine + *N*-glucuronide) and total *trans*-3'-hydroxycotinine (*trans*-3'-hydroxycotinine + its glucuronides) were quantified. Analyses were performed in duplicate for each urine sample and repeated if values differed by > 10 %, and average error was 3 %. An overview of the analytic method is provided in Chapter 2.

Nicotine-*N*-oxide was analyzed in urine of study 1 samples by LC/MS. In brief, urine (20 μl) with added D3-nicotine *N*-oxide internal standard was processed by solid phase extraction with an Oasis MCX column. LC/MS/MS was performed using a Finnigan Discovery triple quadrupole mass spectrometer (Thermo Electron, San Jose, CA) with an ESI source in positive ion mode. Selective reaction monitoring was performed of the mass transitions for D0-nicotine *N*-oxide (*m/z* 179→130 and *m/z* 179→117).

Plasma was separated from blood and stored at -20ºC for study 1 samples. Plasma free cotinine, total cotinine (free + *N*-glucuronide), and total *trans*-3'-hydroxycotinine were quantified by GC/MS as performed for urinary metabolites except for an initial solid phase extraction using an Oasis MCX column (Waters Corporation, Milford, MA) (39). Analyses were performed in duplicate and repeated if values differed by > 10 %.

4.2.3 UGT2B10 Genotyping

DNA was isolated from blood using the DNeasy kit (Qiagen, Valencia, CA). PCR-restriction fragment length polymorphism (RFLP) analysis was performed targeting UGT2B10 at the codon 67 position with Hinf*I* digestion as previously described (Chen et al 2008). A second RFLP for the SNP rs7657958 that is linked with UGT2B10 Asp67Tyr in Caucasians (haplotype C) was performed in a subset of samples (N = 107 of 327, 32 %) (177). Genotyping results were concordant between the two assays, as well as with DNA sequencing for 10 samples.

4.2.4 Statistical analysis

Statistical analyses were conducted using SAS (SAS Institute, Cary, NC) and Excel (Microsoft, Redmond, WA). Wilcoxon two-sided t-approximation statistics were calculated to compare means of continuous variables that did not have a normal distribution, and a p-value less than 0.05 was considered significant. Spearman nonparametric correlation was used to assess univariate correlations. A general linear model was used to compare phenotypes by UGT2B10 genotype, and to adjust for nicotine equivalents. Individuals with the highest and lowest 1 % of urinary nicotine equivalents were excluded from analyses, < 9 nmol/ml or > 236 nmol/ml. Nicotine and cotinine glucuronidation were assessed as the percent of the analyte that was present as its *N*-glucuronide and as the square-root transformed ratio of glucuronide conjugate to

free analyte. The square-root transformed ratio of total *trans*-3'-hydroxycotinine to free cotinine in plasma or total *trans*-3'-hydroxycotinine to free cotinine in urine was used as an estimate of C-oxidation. K-median cluster analysis was performed using Cluster 3.0 and Java Treeview which is available at http://rana.lbl.gov/EisenSoftware.htm.

4.3 Results

4.3.1 Study population

A total of 327 participants were included in the genotype-phenotype analyses, which included samples collected at baseline while participants were smoking as usual from 3 studies. Study participants were predominantly European American. The mean ages +/- SD by study were 1) 43 +/- 11.6 years; 2) 41 +/- 14 years; and 3) 46 +/- 10.6 years. Diary recorded cigarettes per day at baseline were mean +/ SD: 1) 21 +/- 6.5; 2) 21 +/- 8.8; 3) 24 +/- 5.8. Total allele frequency of the UGT2B10 Asp67Tyr variant was 10.6 %, and this was consistent with Hardy-Weinberg equilibrium. Correspondingly individuals who were heterozygous for the Asp67Tyr allele represented 20 % of participants: study 1, 17.4 %; study 2, 18.3 %; and study 3, 22.2%. The percent of cotinine excreted as a glucuronide conjugate in first morning urine was significantly decreased among individuals who were heterozygous for the Asp67Tyr allele compared to individuals without this allele in each of the three studies. Subsequently, analyses were conducted on the combined data unless indicated.

4.3.2 Urinary nicotine and its metabolites

The distribution of urinary nicotine and its metabolites by UGT2B10 Asp67Tyr genotype is presented in Table 4-1. Analytes are presented as molar percentages of the sum of nicotine and its metabolites in urine, and reflect the relative contribution of different pathways to the fate of nicotine. The molar percentages of nicotine and cotinine *N*-glucuronides in urine were 30 % lower for Asp67Tyr heterozygous individuals than for wild-type, 4.2 % versus 6.1 % ($p = 0.003$) and 17.6 % versus 24.2 % ($p < 0.0001$) respectively. Similarly, the fractions of nicotine and cotinine excreted as their glucuronide conjugates, ie. percent glucuronidation, were lower among Asp67Tyr heterozygotes than wild-type; 29.5 % versus 38.2 % ($p = 0.007$) and 51.3 % versus 62 % ($p < 0.0001$).

As might be expected, a decrease in the molar percent of cotinine glucuronide was accompanied by an increase in excretion of free cotinine, 16 % versus 13.4 % ($p = 0.003$) for Asp67Tyr heterozygotes compared to wild-type. Moreover, a significant increase was observed in the molar percent of total *trans*-3'-hydroxycotinine in urine of Asp67Tyr heterozygotes compared to wild-type, 51.1 % versus 44.3 %, $p = 0.001$. In summary, the Asp67Tyr allele was associated with relatively lower urinary abundance of nicotine and cotinine *N*-glucuronides, higher free cotinine, and higher total *trans*-3'-hydroxycotinine.

There were 3 individuals whose DNA yielded a restriction digest pattern that would be consistent with homozygosity for UGT2B10 Asp67Tyr. No urine samples were available for one individual who appeared homozygous, another individual excreted a

low percentage of cotinine as its glucuronide conjugate (7.1 %) and had undetectable nicotine glucuronidation, and the third individual had a normal-to-high glucuronidation phenotype (73 % cotinine glucuronidation, 67 % nicotine glucuronidation). DNA sequence analysis of UGT2B10 is planned for these samples, and at this time they were excluded from the analyses which were focused on characterizing heterozygous carriers of UGT2B10 Asp67Tyr.

Table 4-1. Distribution of urinary metabolites by genotype as a molar percentage of nicotine and its metabolites [*]

Analyte	Wild-type Mean percent (SD) (n = 263)	UGT2B10 Asp67Tyr[†] Mean percent (SD) (n = 62)	p-value
Nicotine	11.8 (9.5)	11.8 (8.5)	0.75
Nicotine glucuronide	6.1 (5.1)	4.2 (3.3)	0.003
Cotinine	13.4 (6.8)	16.0 (7.4)	0.003
Cotinine glucuronide	24.2 (10.7)	17.6 (8.0)	< 0.0001
Trans-3'-hydroxycotinine	44.3 (16.7)	51.1 (14.6)	0.001
Percent nicotine glucuronidation[‡]	38.2 (23.6)	29.5 (18.8)	0.007
Percent cotinine glucuronidation[‡]	62.8 (18.2)	51.3 (18.5)	< 0.0001

[*] Molar percentage = (analyte / ∑ nicotine + cotinine + *trans*-3'-hydroxycotinine + glucuronides)* 100.

[†] UGT2B10 Asp67Tyr heterozygous individuals

[‡] Percent of analyte excreted as its glucuronide conjugate

4.3.3 Urinary excretion of nicotine-N-oxide

Nicotine-*N*-oxide is a minor nicotine metabolite but it may be increased in individuals with decreased metabolism through other pathways. Therefore, we evaluated the effect of glucuronidation and C-oxidation phenotype on nicotine-*N*-oxide abundance in urine (Figure 4-1) (118). Nicotine-*N*-oxide was quantified in study 1 participants (N = 108) and phenotype was assessed using metabolite ratios. The phenotype biomarkers were urinary cotinine glucuronide:free cotinine ratio for glucuronidation and plasma *trans*-3'-hydroxycotinine:free cotinine ratio for C-oxidation. Phenotypes were categorized as low, high, or average, based on the lowest and highest quartiles of the metabolite ratio distribution and the interquartile range. Nicotine-*N*-oxide was assessed as a molar percent of nicotine and its metabolites in urine and comparisons were performed by phenotype group.

The abundance of nicotine-*N*-oxide increased for each group with successively lower *trans*-3'-hydroxycotinine:free cotinine ratios, means (95 % CI): 4.3 % (3.3 – 5.3), 6.1 % (5.4 – 6.8), and 8.7 (7.7 – 9.7) for high, average, and low C-oxidation phenotype respectively ($p < 0.005$ between each group). No significant differences were observed in mean nicotine-*N*-oxide abundance by glucuronidation phenotype, means (95 % CI): 5.5 % (4.4 – 6.6), 6.1 % (5.4 – 6.9), and 6.8 % (5.7 – 7.9) for high, average, and low glucuronidation phenotype, respectively; and Chi-square test for trend, $p = 0.055$.

Figure 4-1. Excretion of *N*-oxide in urine by (A) C-oxidation or (B) glucuronidation phenotype *

* Phenotype was assessed by metabolite ratios: low = lowest quartile, average = interquartile range, high = highest quartile.

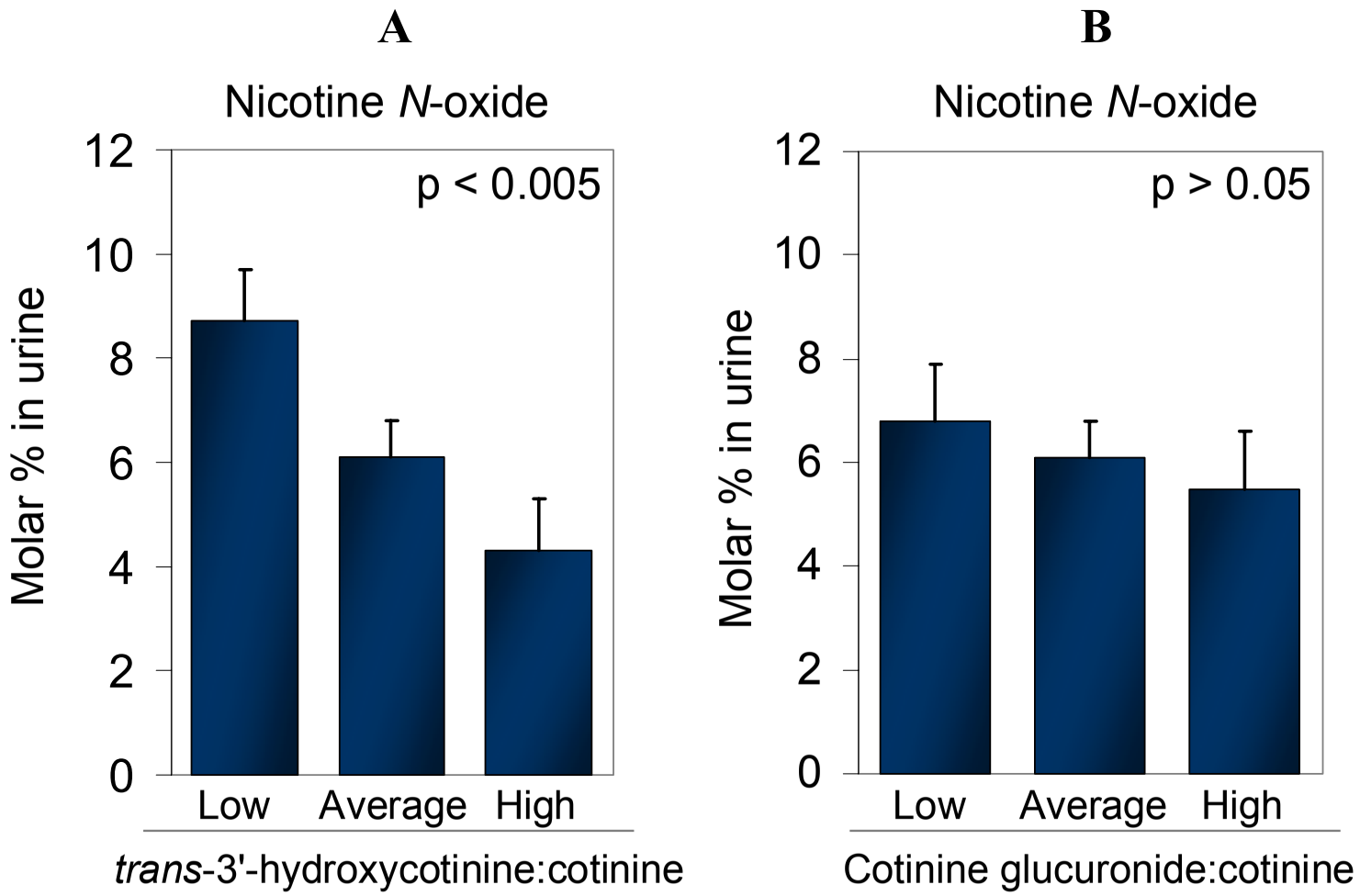

4.3.4 Plasma nicotine and metabolites

The effect of the UGT2B10 Asp67Tyr allele on plasma concentrations of nicotine metabolites was evaluated in study 1 participants (Table 4-2). Free plasma cotinine was higher among Asp67Tyr heterozygotes than wild-type individuals, 1.31 nmol/ml (231 ng/ml) versus 1.09 nmol/ml (192 ng/ml), p = 0.03. No difference in cotinine glucuronide concentration was detected, 0.13 nnmol/ml versus 0.15 nmol/ml, for Asp67Tyr heterozygotes and for wild-type individuals respectively. Since the percent of cotinine that is conjugated in plasma is low with an overall mean of 10 % it is difficult to quantify relatively small differences in cotinine glucuronidation in plasma. Total *trans*-3'-hydroxycotinine was higher in the plasma of Asp67Tyr heterozygotes compared to wild-type, 0.46 nmol/ml versus 0.39 nmol/ml, p = 0.04. Therefore, the effect of the Asp67Tyr allele on free cotinine and total *trans*-3'-hydroxycotinine was consistent in urine and plasma, both were higher among heterozygotes than wild-type.

4.3.5 Cluster analysis of urinary nicotine and metabolites

Urinary metabolite profiles were explored using cluster analysis and an example array is depicted in Figure 4-2 that includes free nicotine, free cotinine, cotinine glucuronide, and total *trans*-3'-hydroxycotinine. To account for the effect of variation in nicotine exposure, analytes were expressed as a molar fraction of nicotine and its metabolites in urine and were then normalized to the median value. The array serves as a tool for thinking about several metabolites from over a hundred participants at a

glance. Foremost, it is clear that different distributions of nicotine metabolites are common. An evident pattern is that when *trans*-3'-hydroxycotinine is high then cotinine glucuronide is frequently low and vice versa. Typically low nicotine occurs when either *trans*-3'-hydroxycotinine or cotinine glucuronide are high and the reverse is also observed.

4.3.6 Nicotine equivalents as a pathway independent biomarker

Since nicotine equivalents is a sum of metabolites, it is insensitive to variation in metabolite distribution and this can improve accuracy in tobacco exposure assessment, as illustrated in Table 4-3. The first pair of observations in Table 4-3 depicts two individuals with identical plasma free cotinine concentrations, but their exposure to nicotine is different. In this case, the individual with lower nicotine equivalents has relatively high plasma free cotinine as a consequence of decreased total clearance of cotinine which was indicated by the very low urinary and plasma *trans*-3'-hydroxycotinine concentrations. In the second example, two individuals have identical free cotinine in urine due to a difference in glucuronidation phenotype, and this could obscure the relatively high nicotine exposure of the individual who excreted 85 % of cotinine as its glucuronide conjugate if free cotinine is the biomarker of exposure. In the final example, nicotine equivalents were identical but use of free urinary cotinine as the biomarker would result in classifying the individual with higher free cotinine as being more exposed, when in fact the difference in free cotinine is attributable to a difference in the distribution of urinary metabolites.

Table 4-2. Plasma nicotine metabolites by UGT2B10 genotype (Study 1)

Analytes	Wild-type (n = 95) Mean (SD)	Asp67Tyr* (n = 20) Mean (SD)	Range
Free cotinine (nmol/ml)	1.09 (0.49)	1.31 (0.40) †	0.19 – 2.75
Cotinine glucuronide (nmol/ml)	0.15 (0.14)	0.13 (0.14)	0.00 – 0.54
Percent cotinine glucuronide	11.3 (9.7)	8.72 (9.0)	0.0 – 36.4
Total *Trans*-3'-hydroxycotinine (nmol/ml)	0.39 (0.32)	0.46 (0.24)	0.04 – 1.92
Total *Trans*-3'-hydroxycotinine: free cotinine	0.38 (0.28)	0.37 (0.18) ‡	0.07 – 1.29

* UGT2B10 heterozygous individuals

† p = 0.03

‡ p = 0.04

Figure 4-2. Cluster analysis of urinary nicotine and its metabolites

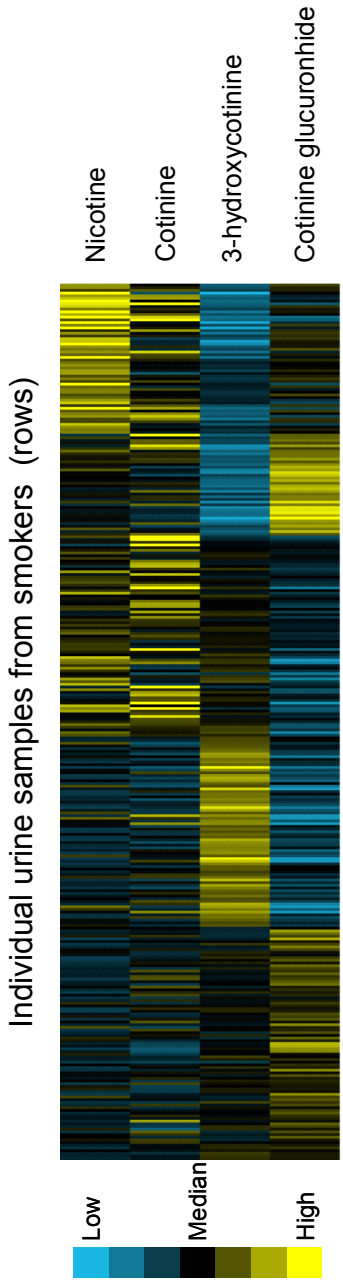

Table 4-3. Examples of discrepancies in assessing tobacco exposure by nicotine equivalents or free cotinine in urine or plasma

Comparisons between selected individuals [a]		***Distribution of urinary analytes (nmol/ml)***			
Traditional biomarker (nmol/ml)	Nicotine equiv.	Total nicotine	Free cotinine	Total cotinine	Total 3'OH cotinine
Plasma free cotinine :					
0.68	69	13.0	8.1	29.4	21.1
0.68	24	12.9	3.1	7.1	1.4 [b]
Urine free cotinine:					
6.4	104	2.5	6.4	10.9	10.1
6.4	25	11.6	6.4	44.7	46.0
18.0	**80**	11.4	18.0	30.4	28.5
7.4	**80**	11.1	7.4	14.7	53.3

[a] Pairs of individuals selected for comparison are indicated in bold
[b] Plasma *trans*-3'-hydroxycotinine was also low at 0.05 nmol/ml (9 ng/ml)

4.3.7 Effect of nicotine equivalents on metabolite ratios (Study 2)

To investigate the stability of the urinary glucuronide ratio and the effect of nicotine dose, we evaluated the ratio among individuals who decreased their smoking (Table 4-4). The ratio of cotinine glucuronide:cotinine was assessed in a group of individuals at baseline and after 12 weeks at which point they had reduced their nicotine intake by 60 %, as assessed using nicotine equivalents. The ratio of cotinine glucronide:cotinine decreased by 40 % as they decreased their nicotine intake, mean (95 % CI): 2.59 (2.05 – 3.24) at baseline versus 1.51 (1.04 – 2.10) at week 12, $p = 0.008$. However, when the ratio was adjusted for nicotine equivalents this difference disappeared, mean (95 % CI): 1.99 (1.49 – 2.52) and 2.07 (1.58 – 2.63) for baseline and week 12 respectively, $p = 0.81$. A decrease of similar magnitude was observed in the urinary ratio of total trans-3'-hydroxycotinine:free cotinine as individuals decreased their nicotine intake, and adjusting for nicotine equivalents eliminated this difference.

Table 4-4. Stability of urinary metabolite ratios (Study 2)

Visit [*]	N	Nicotine equivalents [†] Mean (SD)	Cotinine glucuronide: cotinine [‡]		Total *Trans*-3'-hydroxycotinine: free cotinine [‡]	
			Unadjusted	*Adjusted*	*Unadjusted*	*Adjusted*
Baseline	27	124.5 (78.1)	2.59 (2.05 – 3.24)	1.99 (1.49 – 2.52)	6.97 (5.15 – 9)	5.67 (4.30 – 7.24)
Week 12	27	47.5 (36.3)	1.51 (1.04 – 2.10)	2.07 (1.58 – 2.63)	4.41 (3.24 – 5.76)	5.55 (4.19 – 7.10)
			p = 0.008	p = 0.81	p = 0.02	p = 0.91

[*] Smokers were smoking as usual at baseline and had achieved > 40 % decrease in urinary nicotine equivalents by week 12
[†] Sum of nicotine, cotinine, *trans*-3'-hydroxycotinine, and their respective glucuronides in nmol/ml, quantified in first morning urine
[‡] Geometric mean (95 % CI), adjusted values were adjusted for nicotine equivalents in a general linear model

4.3.8 Metabolite ratios by UGT2B10 genotype

The relationship between Asp67Tyr genotype and phenotype assessed as metabolite ratios is presented in Table 4-5. The urinary ratio of cotinine glucuronide to cotinine, adjusted or unadjusted for nicotine equivalents, was significantly lower among Asp67Tyr heterozygotes than wild-type individuals, mean (95 % CI): 1.26 (1.00 – 1.56) versus 2.03 (1.86 – 2.20), $p < 0.0001$. The ratio of urinary nicotine glucuronide to nicotine was also significantly lower among Asp67Tyr heterozygotes than wild-type individuals (p 0.005). In summary, UGT2B10 Asp67Tyr genotype and glucuronidation ratios, as a biomarker of phenotype, were strongly associated. No statistical difference was observed in the urinary ratio of total *trans*-3'-hydroxycotinine:free cotinine, although a higher ratio of total *trans*-3'-hydroxycotinine:total cotinine was observed for Asp67Tyr heterozygotes compared to wild-type, mean (95 % CI): 1.73 (1.46 – 2.03) versus 1.29 (1.18 – 1.41), $p = 0.048$.

4.3.9 Nicotine equivalents by UGT2B10 genotype

During the evaluation of urinary nicotine metabolite concentrations, we suspected that nicotine equivalents were lower among Asp67Tyr individuals than for wild-type. Nicotine equivalents accounts for greater than 80 % of nicotine intake and therefore this biomarker is useful to estimate nicotine intake during *ad libitum* smoking. Moreover, we demonstrated in study 2 that there is no substantial shift to nicotine-*N*-oxidation among Asp67Tyr heterozygotes (Figure 4-1). Nicotine equivalents were 15 % lower

for Asp67Tyr heterozygotes relative to wild-type, mean (95 % CI): 58.2 nmol/ml (48.9 – 68.2) versus 69.2 nmol/ml (64.3 – 74.5) respectively, p = 0.048 (Table 4-6).

Table 4-5. Metabolite ratios by UGT2B10 genotype: geometric means and 95 % confidence intervals

UGT2B10 Genotype	Cotinine glucuronidation ratio *	Nicotine glucuronidation ratio *	Total *trans*-3'-hydroxycotinine:free cotinine †
Wild-type (N = 264)	2.03 (1.86 – 2.20)	0.77 (0.64 – 0.89)	3.80 (3.96 – 4.15)
Asp67Tyr δ (N = 63)	1.26 (1.00 – 1.56)	0.41 (0.25 – 0.62)	3.96 (3.35 – 4.64)
	p < 0.0001 §	p = 0.005 §	p = 0.715 §

* Glucuronide conjugate / unconjugated analyte

† Total *trans*-3'-hydroxycotinine / total cotinine was higher among Asp67Tyr heterozygotes compared to wild-type: 1.73 (1.46 – 2.03) versus 1.29 (1.18 – 1.41), p = 0.003, adjusted for nicotine equivalents

δ UGT2B10 Asp67Tyr heterozygous individuals

§ Adjusted for nicotine equivalents.

Table 4-6. Urinary nicotine equivalents and metabolite ratios by UGT2B10 genotype: geometric means and 95 % confidence intervals

UGT2B10 Genotype	Nicotine equivalents
Wild-type (N = 264)	69.2 (64.3 – 74.5)
Asp67Tyr * (N = 63)	58.2 (48.9 – 68.2)
	p = 0.048

* UGT2B10 Asp67Tyr heterozygous individuals

4.4 Discussion

Interindividual variation in glucuronidation of nicotine and cotinine is substantial and the contribution of glucuronidation to total nicotine metabolism ranges from < 1 – 40 % based on nicotine and its metabolites recovered in smokers' urine (112). On average, an estimated 25 % of nicotine is metabolized to *N*-glucuronide conjugates of nicotine or cotinine in individuals (159). Variation in glucuronidation influences the distribution of nicotine metabolites and therefore may affect nicotine exposure assessment using nicotine metabolite biomarkers. We observed that smokers who are heterozygous for the Asp67Tyr allele have a unique distribution of nicotine metabolites and that nicotine equivalents, a robust biomarker of nicotine intake, were lower among Asp67Tyr heterozygotes compared to individuals without this allele. Therefore, variation in nicotine glucuronidation, as with C-oxidation (115), may influence nicotine consumption by smokers.

UGT2B10 is the most efficient catalyst of nicotine and cotinine *N*-glucuronidation *in vitro* followed by UGT1A4 (87;163). Chen *et al.* identified the Asp67Tyr polymorphism in UGT2B10 because it was linked to a haplotype that was associated with decreased glucuronidation of the tobacco carcinogen 4-(methylnitrosamino)-1-(3-pyridyl)-1-butanal (NNAL) by human liver microsomes (177). Subsequently, a 20 – 30 % decrease in nicotine and cotinine glucuonidation was observed among human liver microsomes that were heterozygous for the Asp67Tyr allele compared to wild-type (143).

Recently, we reported that the UGT2B10 Asp67Tyr allele is associated with a decrease in the percent of cotinine and nicotine excreted as their glucuronide conjugates in smokers' urine (188). The allele frequency of this polymorphism is about 10 % in European Americans and we demonstrated that it is also present in African Americans, at an allele frequency that is likely similar to or lower than for European Americans (177;188). To further investigate the effect of the Asp67Tyr polymorphism on nicotine metabolism, beyond a direct effect on percent conjugation, we now have evaluated a larger number of subjects while they were smoking as usual (n = 327; 263 wild-type individuals and 63 heterozygotes).

In this study we corroborated our prior finding that UGT2B10 Asp67Tyr is associated with decreased nicotine and cotinine *N*-glucuronidation. Significantly less nicotine and cotinine were excreted as their glucuronide conjugates by individuals who were heterozygous for the Asp67Tyr allele compared to wild-type; the mean values were 22 % and 17 % lower for the Asp67Tyr group. The distribution of urinary metabolites was distinct for individuals with the Asp67Tyr allele compared to wild-type as these individuals had a lower fraction of nicotine and cotinine *N*-glucuronides, but higher free cotinine and *trans*-3'-hydroxycotinine. Higher plasma concentrations of free cotinine and *trans*-3'-hydroxycotinine were also observed in Asp67Tyr heterozygotes. Overall, we observed that the Asp67Tyr allele affects concentrations of both plasma and urinary nicotine metabolites and that the effect is consistent with a decrease in glucuronidation.

UGT2B10 genotype clearly differentiated glucuronidation phenotypes, assessed as the ratio of urinary cotinine glucuronide:cotinine or nicotine glucuronide:nicotine. The glucuronide ratio for cotinine was 63 % lower and for nicotine was 53 % lower for Asp67Tyr heterozygotes compared to wild-type (Table 4). Adjusting for variation in nicotine equivalents did not diminish the difference in glucuronidation phenotype observed by UGT2B10 Asp67Tyr genotype. We did not observe a significant increase in nicotine-N-oxide excretion by glucuronidation genotype or phenotype. In comparison, individuals with low glucuronidation genotype or phenotype had an increase in the excretion of *trans*-3-hydroxycotinine. Perhaps low glucuronidation phenotype is compensated by an increase in the clearance of cotinine through C-oxidation to *trans*-3'-hydroxycotinine in some individuals. Shifts in the distribution of metabolites that occur as a consequence of decreased metabolism through one pathway are an indication that the relationships between metabolic pathways are dynamic. Total nicotine metabolism is a function of the efficiency and capacity of all the major pathways of nicotine metabolism.

Variation in metabolism is a source of error in estimating nicotine exposure. Though free cotinine has been instrumental as a tobacco biomarker it can fail to differentiate nicotine exposure between individuals in which the contribution of glucuronidation and oxidation to total metabolism is different. Examples where misclassification might occur, based on individuals in this study, were presented in Table 4-3. Cluster analysis and generation of a metabolic heatmap was also used to better visualize variation in the distribution of urinary nicotine metabolites. When comparing groups in a study, misclassification error could be similar between the two

groups and may not be problematic. However, particularly in multi-ethnic study populations where the frequency of polymorphisms in nicotine metabolizing genes is different, nicotine exposure may be over- or under- estimated in one group relative to another. Nicotine equivalents are better suited to estimate nicotine intake independent of variation in the major pathways of nicotine metabolism.

We observed that urinary ratios of nicotine metabolites, including the ratio of cotinine glucuronide:cotinine and *trans*-3'-hydroxycotinine:cotinine (total:total or total:free), are influenced by nicotine equivalents and that this represents a dose effect. Among individuals who were assessed both at baseline and after reducing nicotine intake by 60 %, urinary metabolite ratios were significantly lower when the individuals were smoking less, but this difference disappeared after adjusting for nicotine equivalents. In contrast, adjusting for nicotine equivalents had no effect or actually increased the strength of the reported associations between UGT2B10 genotype and nicotine metabolite ratios (Table 4-4).

The most important finding of this study was that individuals who were heterozygous for the Asp67Tyr allele had lower nicotine equivalents, which is a robust measure of nicotine intake. When stratified by UGT2B10 genotype, nicotine equivalents were 58.2 among heterozygotes compared to 69.2 nmol/ml for individuals who did not have an Asp67Tyr allele ($p < 0.05$). Since the study participants were smoking *ad libitum* this difference likely represents a moderate but significant decrease in nicotine consumption that is attributable to the Asp67Tyr polymorphism in UGT2B10. Nicotine equivalents were 84 % of that for wild-type. The effect of

CYP2A6 low activity alleles on nicotine equivalents specifically has not been reported. However, nicotine equivalents are 34 % lower among Japanese Americans who have a 10-15 % higher allelic prevalence of the CYP2A6 deletion than European Americans (133). Interestingly, we noticed that individuals with the lowest and highest plasma trans-3'-hydroxycotinine to cotinine ratios had lower nicotine equivalents than individuals with an average ratio. Then, individuals with incomplete metabolic compensation for either low glucuronidation or low C-oxidation would represent groups more likely to be low intensity smokers. Even a modest decrease in smoking intensity could have a significant impact on risk of smoking attributable disease over a lifetime. This is the first report demonstrating that a polymorphism in UGT2B10 may influence smoking behavior. In different populations, the frequency of polymorphisms in CYP2A6 and in UGT2B10 may influence the relative contribution of these alleles to variation in nicotine metabolism and smoking behavior.

The extent to which variation in nicotine metabolism affects smoking behavior, relative to other factors that influence smoking, is unknown. Ho *et al.* reported that light smokers (<10 cigarettes/day) with low activity CYP2A6 alleles or a low oxidation phenotype did not show behavioral compensation for slow metabolism based on having higher plasma nicotine levels than other light smokers (150). Other genes that are not involved with nicotine clearance also affect smoking behavior. The nicotinic CHRNA3 and CHRNA5 that encode subunits of the nicotinic acetylcholine receptor A was recently reported by Derby *et al.* to influence smoking behavior (132). Polymorphisms in CHRNA3 and CHRNA5 were associated with an increased risk of lung cancer, and it was not until nicotine equivalents were measured that the increased cancer risk could be

attributed to increased smoking. Namely, polymorphisms in CHRNA3 and CHRNA5 are associated with increased nicotine equivalents and increased intake of tobacco.

4.5 Conclusions

The main finding was that UGT2B10 Asp67Tyr was associated with lower glucuronidation phenotype and decreased nicotine intake, which supports the outcome described in Chapter 3. Individuals who were heterozygous for the Asp67Tyr allele excreted less nicotine or cotinine as their glucuronide conjugates than wild-type, resulting in a 60% lower ratio of cotinine glucuronide:cotinine, a 50% lower ratio of nicotine glucuronide: nicotine, and an increase in urinary and plasma cotinine and *trans*-3'-hydroxycotinine. Moreover, nicotine equivalents, a robust biomarker of nicotine intake, were lower among Asp67Tyr heterozygotes compared to individuals without this allele. The distribution of metabolites in urine was affected by glucuronidation or oxidation phenotype. Nicotine equivalents were useful to quantify nicotine intake regardless of the relative contribution of the metabolic pathways.

4.6 Acknowledgements

Many thanks to Cassie Retzlaff, Nicole Thomson, and Aleks Knezevich for their assistance in preparing samples and quantifying nicotine metabolites.

4.7 Publication of thesis work

The research discussed in Chapter 4 was submitted to Cancer Epidemiology Biomarkers and Prevention in September 2009: Jeannette Zinggeler Berg, Linda von Weymarn, Elizabeth A. Thompson, Katherine M. Wickham, Natalie A. Weisensel, Dorothy K. Hatsukami, Sharon E. Murphy. UGT2B10 genotype influences nicotine glucuronidation, oxidation and consumption.

CHAPTER 5

Cytochrome P450 2A7

5.1 Introduction

In the U.S. lung cancer is the most common fatal cancer and 90 % of lung cancers are attributable to tobacco exposure (15). US adults and adolescents recognize smoking as a risk of lung cancer, and in polls since 1990, over 90 % would agree that smoking is a cause of lung cancer (18). Smokers interested in cessation also cite risk of lung cancer as a motivating factor to quit. Nevertheless quitting and sustained cessation of tobacco use are often difficult to achieve and thus tobacco use is likely to remain a public health problem for some time to come. A common misperception is that nicotine is carcinogenic, which it is not. There are 60 recognized carcinogens in tobacco smoking, and among these polyaromatic hydrocarbons (i.e. benzo[a]pyrene) and 4-(methylnitrosamino)-1-(3-pyridyl)-1-butanone (NNK) are potent lung carcinogens in a number of animal models (34;193). The primary mechanism of NNK-mediated carcinogenesis is metabolic activation by cytochrome P450 enzymes (P450s) and generation of unstable metabolites that react with DNA and result in appreciable genotoxicity (35;127;194;195). NNK metabolites have been quantified in plasma, urine, and tissues including toe nails of smokers and individuals who are passively exposed to smoke (37;38;196;197). The cumulative dose of NNK as well as variation

in the activation and detoxification of NNK is predicted to influence individual lung cancer risk (132;193;198).

Metabolic activation is due to hydroxylation at the methylene and methyl carbons adjacent to the N-nitroso group and these reactions result in the formation of reactive electrophiles (Figure 5-1). Methyl α-hydroxylation generates 4-(3-pyridyl)-4-oxo-butyldiazohydroxide which can form pyridyloxobutyl adducts with DNA or protein and it reacts with water to form 4-hydroxy-4-(3-pyridyl)butanol (HPB) (199;200). Methylene hydroxylation results in decomposition to methane diazohydroxide and 4-oxo-4-(3-pyridyl) butanal (OPB). Methane diazohydroxide is a DNA and protein methylating species; it also reacts with water and forms methanol (201). OPB can be further oxidized to the carboxylic acid, denoted OPBA. In animal carcinogenicity studies, NNK-derived adducts include O^6-methylguanine, 7-methylguanine, O^4-methylguanine and pyridyloxobutyl-adducted nucleotides (202;203). Recently α-hydroxylation metabolites were quantified in the urine of smokers who smoked low nitrosamine cigarettes that were spiked with [pyridine-D_4] NNK in place of their usual cigarettes, which would contain a similar amount of unlabeled NNK (198). The excretion of α-hydroxylation products represented 86 % of total NNK metabolites in urine. In comparison, the percent of α-hydroxylation products previously reported in the urine of laboratory animals was 58 %, 54 %, and 68 % for mice, rats, and primates (198).

Figure 5-1. NNK α-hydroxylation

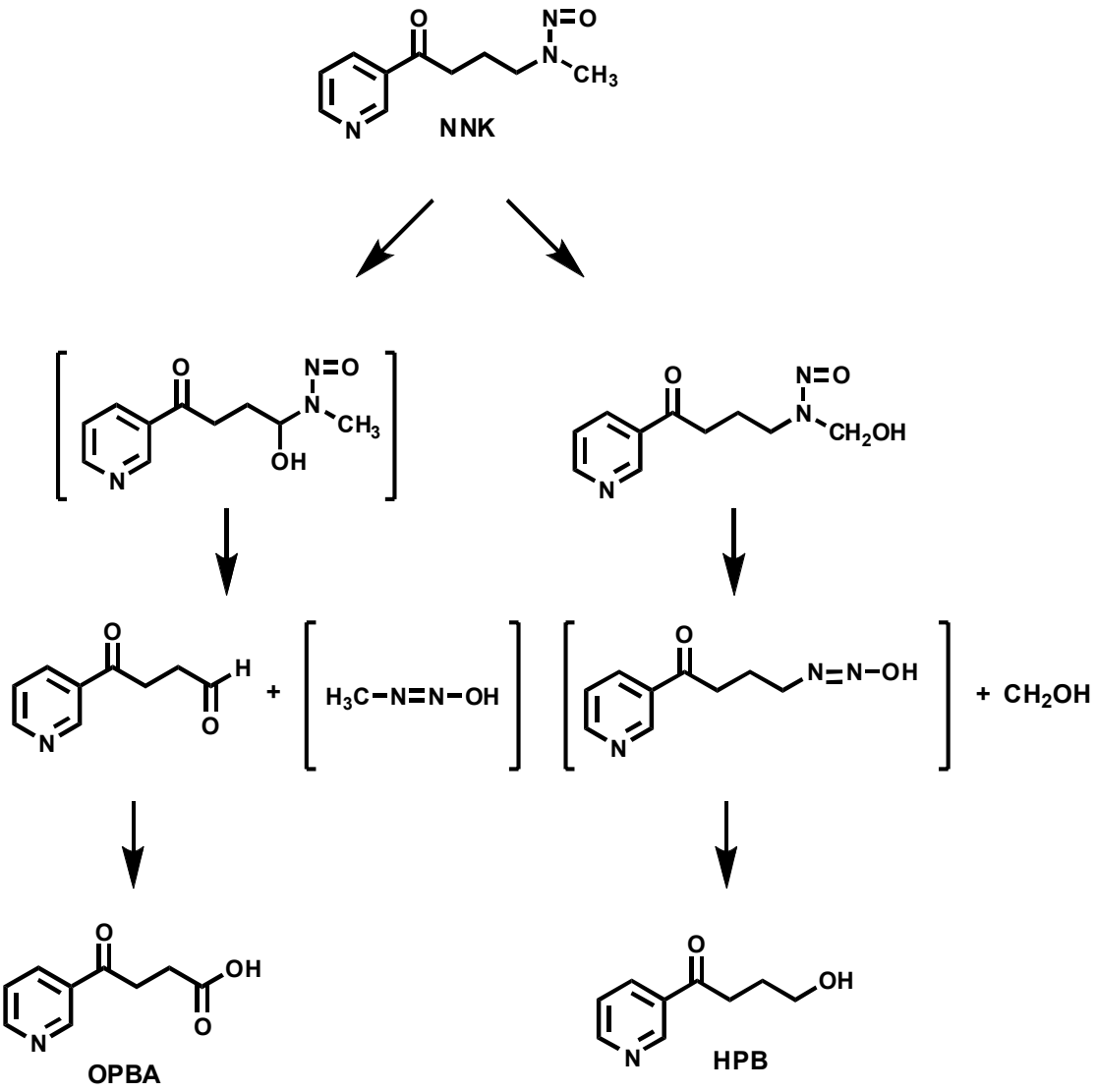

Since the half-life of reactive NNK metabolites is in the order of seconds, tissue specific activation by cytochrome P450s is predicted to influence the site of tumorgenicity in humans (200;204). NNK is not exclusively a lung carcinogen and also causes cancers in the nasal cavity, liver, and pancreas of laboratory animals (35). Ding *et al*. elegantly demonstrated that tissue-specific knock out of cytochrome P450 reductase in the lung or the liver of mice affects the distribution of tumors, with a decrease in tumors in the lung when the reductase is absent in the lung but not when reductase was absent in the liver. This demonstrated that NNK α-hydroxylation in the lung is critical (204). The most efficient human catalyst of NNK α-hydroxylation is P450 2A13 and this enzyme is an extrahepatic P450 that is expressed in the respiratory tract (128;129). A more abundant hepatic enzyme, P450 2A6, is 93.5 % identical to P450 2A13 but it is 300-fold less efficient at catalyzing α-hydroxylation (34). Crystal structures of P450 2A13 and P450 2A6 have been solved, and docking of NNK into the active site predicts that the volume and shape of the P450 2A13 active site is slightly larger and can better accommodate NNK in a position that favors α-hydroxylation (205;206).

Other human enzymes that likely contribute to hepatic NNK α-hydroxylation are P450s 2B6 and 1A2. These enzymes are also poor catalysts compared to P450 2A13. In human liver microsomes, 30 – 67 % of NNK hydroxylation is inhibited by anti-2A6 and anti-2B6 antibodies (127). Also co-incubation with phenacetin, a substrate of P450 1A2, results in up to 70 % inhibition of NNK metabolism (127). In Dr. Murphy's

laboratory it was previously found that the total NNK hydroxylation attributable to P450 2A enzyme in human liver microsomes is greater than expected for 2A6 alone (unpublished). There is one other P450 2A in liver, P450 2A7, for which enzymatic activity has not been demonstrated.

P450 2A7 is recognized as one of ~ 13 human P450s that have no known substrate and unconfirmed function (207). The P450 2A7 proximal promoter appears to be intact as individuals who are homozygous for a naturally-occurring 2A7/2A6 hybrid, where the 5' regulatory region and exons 1–2 are of CYP2A7 origin and exons 3–9 are of CYP2A6 origin, have significant 7-hydroxylation of the 2A6 probe substrate coumarin (208). In liver, P450 2A7 mRNA is expressed at levels ranging from 1:10 to 10:1 relative to P450 2A6 mRNA (209). Ironically, P450 2A13 was predicted to be inactive based on its similarity to P450 2A7, until it was successfully expressed in *Spodoptera frugiperda* (SF9) insect cells and found to be an efficient catalyst of coumarin, NNK, and nicotine oxidation (128).

A comparison of P450 2A7 to P450s 2A6 and 2A13 is presented in Table 5-1. The National Center for Biotechnology Information (NCBI) reference amino acid sequence is 94 % identical to P450 2A6 and 92 % identical to P450 2A13. P450 2A7 does not have any unique residues in its predicted active site: 6 residues are identical to both 2A13 and 2A6, 3 residues are identical to 2A6 only, and 2 residues are identical only to 2A13 (Table 5-2). The conserved cysteine residue that forms a heme-thiolate ligand is present in P450 2A7. However, in 2A6 and 2A13 residue 128 is an arginine that forms

a hydrogen bond with the heme propionate and this residue is a leucine in the P450 2A7 reference sequence.

Table 5-1. Comparison of human P450 2A enzymes

Protein	Amino acid identity with 2A7 [a]	Expression site	Specificity toward NNK (K_m) [b]
P450 2A13	92 %	Respiratory tract	3.4 μM [c]
P450 2A6	94 %	Liver	371 μM [d]
P450 2A7	n/a	Liver	

[a] NCBI composite reference amino acid sequence
[b] Kinetics performed with enzyme expressed in a baculovirus expression system
[c] Su et al. (2000) Cancer Res.; 60: 5074. (210)
[d] Patten et al. (1996) Arch. Biochem. Biophys.; 333: 127. (211)

Table 5.2 Active site residues in human P450 2A protein [a]

Residue	P450 2A7	P450 2A6	P450 2A13
107	F	F	F
111	F	F	F
117	A	V	A
118	F	F	F
209	F	F	F
297	N	N	N
300	I	I	F
301	A	G	A
305	T	T	T
365	V	V	M
366	I	I	L
370	L	L	L
480	F	F	F

[a] Residues that are not identical between proteins are highlighted

Two other groups have cloned P450 2A7 and screened for coumarin 7-hydroxylation activity. Notably, mouse P450 2A4 that is >80 % identical to the human P450 2A enzymes does not catalyze coumarin 7-hydroxylation, and therefore it can not be assumed that 2A7 will catalyze this reaction if it is functional (212). Ding *et al.* cloned P450s 2A6, 2A7, and a spice variant of 2A7 that lacks exon 2 from human liver and subsequently transfected Simian-virus-40-transformed monkey kidney fibroblasts (COS-7) to evaluate expression (213). By Western blotting with anti-P450 2A antibody, 49 kD immunoreactive bands were observed for both full-length P450s 2A6 and 2A7. A 44 kD and a 42 kD band were observed for the 2A7 splice variant (214). No reduced P450 spectra were obtained. This group detected 7-hydroxycoumarin in

media from 2A6-transfected cells that were incubated with coumarin but not 2A7-transfected cells. The methodology lacked sensitivity and low levels of product would not have been detected. Yamono *et al.* also cloned P450s 2A6 and 2A7 from a human liver and used recombinant vaccinia virus to express protein in HepG2 cells (146). Significant protein expression was achieved for P450 2A6 but not for P450 2A7.

P450 2A7 does not appear to contribute significantly to *in vivo* coumarin 7-hydroxylation or nicotine-5'-oxidation. A number of genetic crossover events have occurred between CYP2A7 and CYP2A6 and have resulted in deletion and duplication alleles that provide some insights about P450 2A7. Figure 5-2 illustrates the wild-type chromosomal orientation of CYP2A6 and CYP2A7 and four allelic polymorphisms. For instance, *1B represents a cross-over event in which a portion of the 3'-untranslated region of CYP2A7 has replaced the analogous region in CYP2A6 (215). The *1B allele is associated with increased nicotine oxidation (216). The *2 allele lacks CYP2A6 activity due to an inactivating point mutation, L160H, but has intact CYP2A7 (146). Individuals who are homozygous for the *2 allele or the *4 deletion alleles exhibit very low levels of coumarin 7-hydroxylation *in vivo*, and have 10-30 % of wild-type levels of cotinine, the 5'-oxidation product of nicotine, in urine (115;217). In regards to P450 2A7 this could mean that the enzyme is (a) inactive; (b) poorly expressed; or (c) not efficient at catalyzing nicotine C-oxidation or coumarin 7-hydroxylation compared to P450 2A6. Alternatively, the *2 and *4 alleles may be exist as a haplotype that is linked with a low activity allele of P450 2A7.

Figure 5-2. Examples of polymorphic alleles affecting CYP2A6 or CYP2A7

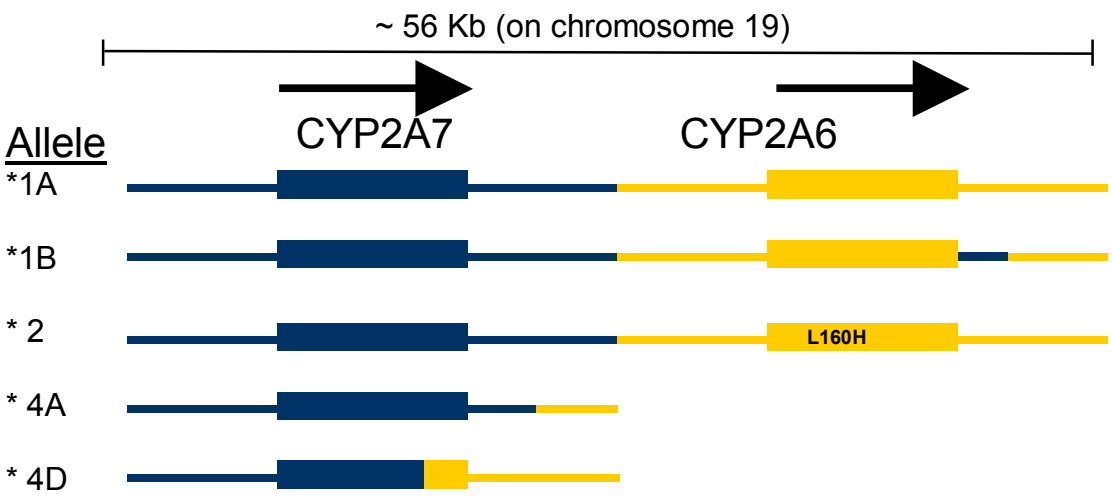

To determine if P450 2A7 might contribute to systemic NNK metabolism, we first cloned this gene from human liver tissues and used heterologous expression in *E. Coli* and human embryonic kidney fibroblasts (HEK293) to evaluate P450 2A7 function. Western blotting and reduced CO difference spectra were used to evaluate protein expression. Enzyme activity was evaluated with coumarin, chlorzoxazone, p-nitrophenol, and NNK.

5.2 Methods

5.2.1 Source of liver tissue and preparation of cDNA

Frozen histologically normal human liver tissues (n = 5) were obtained from the Masonic Cancer Center Tissue Procurement facility, University of Minnesota. The frozen tissue, ~2 x 2 mm, was pulverized, homogenized using QIAshreader, and RNA was extracted with RNeasy according to the manufacturer's instructions (Qiagen, Valencia, CA). First strand cDNA synthesis was performed with Superscript (Stratagene, La Jolla, CA). Polymerase chain reaction was performed immediately after first strand synthesis, to amplify CYP2A6 or CYP2A7 sequence.

5.2.2 PCR to detect CYP2A7 – partial sequence amplification

To assess if CYP2A7 mRNA was present, primers were designed to amplify exons 1-3 of CYP2A7 in a region where there were several nucleotide differences between the CYP2A6 and CYP2A7 DNA sequence (Table 5-3). Pfx polymerase was used (Invitrogen, Carlsbad, CA) and 35 amplification cycles of 94 ˚C for 45 sec., 60 ˚C for 45 sec., 68 ˚C for 90 sec were performed. The 350 bp products were visualized on 1 % agarose gels. This assay would also amplify the uncommon CYP2A6*12 hybrid allele.

5.2.3 PCR amplification of full-length 2A7 and blunt-end cloning

Primers designed from the start to stop codons resulted in co-amplified CYP2A6 and CYP2A7. To more efficiently isolate CYP2A7 clones, a primer was designed to anneal to the 3'-untranslated sequence of CYP2A7. Primer sequences are presented in

Table 5-3. Pfx polymerase was used (Invitrogen, Carlsbad, CA) and 35 amplification cycles of 94 ˚C for 45 sec., 56 ˚C for 45 sec., 68 ˚C for 90 sec were performed. The ~1.6 kb products were visualized on 1 % agarose gels.

Table 5-3. Primer sequences for cloning and detecting CYP2A7

Name	Primer Sequence
CYP2A7 exon 1 Forward [a]	5'- CCAGCTGAACACAGAGCACATATGTG -3'
CYP2A7 exon 3 Reverse [a]	5'- TGCGTGCTCCGGATGGCC -3'
2A7 EcoRI Forward	5'- GCGGCGAATTCATGCTGGCCTCAGGGCTGC TTCTGGTGGCCTTGCTGGC -3'
2A7 NotI utr Reverse	5'- GATGATGCGGCCGCTCTTCCCCCCATTCTTATACC -3'

[a] Nucleotides unique to the CYP2A7 sequence are underlined for these primers.

5.2.4 Cloning into expression vectors

PCR products were cloned into pSC-B with Cre-assisted blunt end cloning (Stratagene, La Jolla, CA) and were subsequently transferred into expression vectors. After changing the second codon to an alanine to facilitate expression in *E.Coli*, CYPs 2A7, 2A6, and 2A13 were inserted into the NdeI and SalI restriction sites of pCW. CYP2A7 or CYP2A13 were inserted into the NotI and XhoI restriction sites

downstream of the EF-1α promoter in the mammalian expression vector pBUDCE4.1 with or without a 6X His tag at the C-terminus (Invitrogen, Carlsbad, CA). The constructs were confirmed by restriction enzyme digestions and by DNA sequence analysis of the inserted gene.

5.2.5 Expression in E. Coli

Various expression conditions were tested. Expression constructs were transformed into DH5α cells or Topp3 cells. Overnight cultures grown in Luria broth with 100 μg/ml ampicillin were used to seed 0.1 or 1L cultures (1:100). Expression media was TB peptone containing 100 μg/ml carbenicillin, 1 mM thiamine, and trace elements (218). The cells were grown at 32 ˚C or 37 ˚C until the OD at 600 nm was 0.6 at which time δ-aminolevulinic acid (0.5 mM) was added. The cells were induced with freshly prepared 1 mM isopropyl-b-D-thiogalactoside when the OD at 600 nm was 1.2; induction at 0.7-1.5 was tested. The cells were incubated further for 24, 36, 48, or 72 hours at 32, 30, or 28 ˚C with 190-200 rpm shaking. A trial of co-expression +/- the chaperone proteins pG-KJE8, pGro7, pKJE7, pG-Tf2, pTf16, was also performed (Takara, Japan). Expression controls included simultaneously expressing CYP2A6 or CYP2A13 as a positive control and untransformed *E.Coli* as a negative control.

5.2.6 Truncated CYP2A7 mutant

Dr. Emily Scott and Natasha DeVore generously provided truncated P450 2A7-transfected *E. Coli* membrane fraction prepared from the full-length clone we isolated. The truncated construct, 2A7dH, did not contain the N-terminal 30 residues. The residues MAKKTSSK preceded amino acid 31, and a tetra-His tag was present at the C-terminus.

5.2.7 Expression in human embryonic kidney fibroblasts (293T cells)

HEK293T cells were transfected using calcium phosphate, 20 µg plasmid per T-75 flask when cells were ~60 % confluent (219). Media was replaced with complete DMEM after 6 hours and cells were incubated at 37 ˚C, 5 % CO_2 for 48 hours.

5.2.8 Protein expression evaluation

SDS-page gel electrophoresis followed by gelcode blue staining (Pierce, Rockford, IL) and Western blotting with anti-2A6 antibody (BD biosciences) was performed as previously described (127). Heme-binding was assessed by dithionite-reduced CO difference spectra obtained using an Olis DW- 2000 UV-Vis spectrophotometer (Olis Inc., Bogard, GA) (61).

5.2.9 Activity assessment

Activity was assessed by incubating whole cells, cell lysate, or microsomes with coumarin or ^{14}C-coumarin (50 – 200 μM), chlorzoxazone (50, 150 μM), and p-nitrophenol (50, 150 μM). HEK-expressed 2A7 was also incubated with ^{3}H-NNK (80 μM). CYP2A7 or CYP2A7dH *E.Coli* preparations were pre-incubated with oxidoreductase (1:2 – 1:6) and dilauroyl-L-α-phosphatidylcholine (0.2 μg/pmol P450) for 15-45 min at 4°C just prior to use (206). Coumarin 7-hydroxylase activity was determined as previously described (220). Detection of metabolites was performed using UV-HPLC or radioflow HPLC analysis as described previously (206). Chlorzoxazone 6-hydroxylation and 4-nitrocatechol formation were monitored by UV-HPLC as previously reported (221;222).

5.3 Results

5.3.1 CYP2A7 cloning and isolation of wild-type and variant sequences

CYP2A7 was amplified successfully from 4 of 5 human livers. Initially, exons 1 to 3 were amplified to screen for the presence of CYP2A7 (Figure 5-3A), and DNA sequencing confirmed the presence of CYP2A7. Full-length amplification generated the expected 1.6 kB product, which was not affected by repeated digestion with a CYP2A6-specific restriction enzyme (Figure 5-3B). Also, a 1.4 kB product was observed for two samples. Several clones were isolated and sequenced from each

individual. Despite repeated attempts, no CYP2A7 was cloned from one liver from which CYP2A6 was isolated.

Wild-type CYP2A7, a polymorphic variant, and a splice variant were cloned from 4 livers. Clones from two livers were identical to the NCBI reference sequence for CYP2A7. However, a full-length variant that differed from the reference sequence of CYP2A7 was detected in three different individuals. Since this variant was present in multiple clones from different individuals it was not due to a cloning artifact or sequencing error. The CYP2A7 variant (CYP2A7.1) shared 9 of 13 residues with CYP2A7 that are not found in CYP2A6 or CYP2A13. These differences span the coding region and therefore are unlikely to have arisen from a recent cross-over event.. Also the variant had two residues that differ from the reference CYP2A7 sequence and are also not present in CYP2A6 or CYP2A13: Asp169Glu and Arg311Cys substitutions. The splice variant was detected in all of the livers and was identical to the previously published in-frame splice variant that results in replacement of a 163 bp section of exon 2 with 10 bp. Splicing occurs at a G/gcagg alternative splice site. A DNA sequence comparison of the CYP2A7 clones to wild-type 2A7 and 2A6 is presented in Figure 5-4.

Figure 5-3. CYP2A7 amplification products

A.

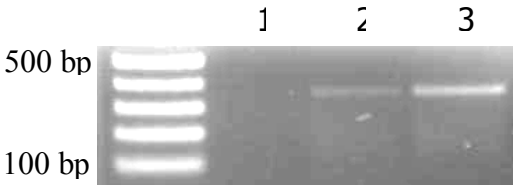

Exons 1-3 of CYP2A7 from two human liver cDNA samples: lanes 2-3. Lane 1: negative control.

B.

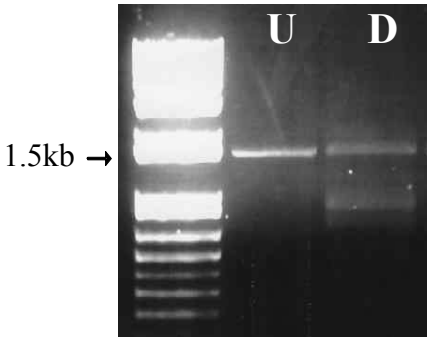

U: Undigested PCR product
D: Specific digestion of 2A6, serial digest

Figure 5-4. CYP2A7 and its variants in comparison to CYP2A6 and CYP2A13

The amino acid sequence of CYP2A6 is presented, and only the residues that differ from CYP2A6 are shown for CYP2A7 and CYP2A13. The conserved cysteine residue at 439 that ligates the heme iron is bolded and underlined.

```
                                                                                                                  Amino acid
2A13          L    T       A             R      R
2A6   MLASGMLLVA  LLVCLTMVL MSVWQQRKSK GKLPPGPTPL PFIGNYLQLN TEQMYNSLMK ISERYGPVFT IHLGPRRVVV       80
2A7           L            A                    R                          H I CD I      F    C
2A7.1         L            A                    R                          H I CD I

2A13           K                                L          A                        G
2A6   LCGHDAVREA LVDQAEEFSG RGEQATFDWV FKGYGVVFSN GERAKQLRRF SIATLRDFGV GKRGIEERIQ EEAGFLIDAL      160
2A7                                                    A              L    A                                S      E  I
2A7.1                                                                                                          E  I

2A13       H                                       E                  S       A                                  KE
2A6   RGTGGANIDP TFFLSRTVSN VISSIVFGDR FDYKDKEFLS LLRMMLGTFQ FTSTSTGQLY EMFSSVMKHL PGPQQQAFQL      240
2A7    S  H                                       E            S                                                K
2A7.1  S  H      E                                 E            S                                                K

2A13                                                                                          F  A
2A6   LQGLEDFIAK KVEHNQRTLD PNSPRDFIDS FLIRMQEEEK NPNTEFYLKN LVMTTLNLFT GGTETVSTTL RYGFLLLMKH       320
2A7                                      Q          H                          M  S          A
2A7.1                                    Q                                     M  S          A              C

2A13                                               T                 ML   G    H
2A6   PEVEAKVHEE IDRVIGKNRQ PKFEDRAKMP YMEAVIHEIQ RFGDVTPMSL ARRVKKDTKF RDFFLPKGTE VFPMLGSVLR       400
2A7                                      T
2A7.1                                    T

2A13                          DK                           Y                          T         F
2A6   DPSFFSNPQD FNPQHFLNEK GQFKKSDAFV PFSIGKRNCF GEGLARMELF LFFTTVMQNF RLKSSQSPKD DVSPKHVGF       480
2A7                           DD                                                                              V
2A7.1                         DD

2A13
2A6   ATTIPRNYTMS FLPR          494
2A7
2A7.1
```

5.3.2 CYP2A7 expression

P450 expression with full-length CYP2A7 was achieved inconsistently and at low levels of expression compared to either CYP2A6 or CYP2A13. Wild-type CYP2A7, CYP2A7.1, and CYP2A7 with a portion of the 3'-untranslated region were transfected into *E. Coli* or HEK293 cells for heterologous expression. Varying time of induction, temperature of incubation, shaking speed, total incubation time, host *E.Coli* strain, and a limited trial of co-expression with chaperone proteins did not improve expression of CYP2A7. CYP2A6 or CYP2A13 transfections were conducted at the same time and under the same conditions as for CYP2A7, and these constructs typically expressed without difficulty. Western blotting with anti-2A6 antibody and reactions with coumarin were used to evaluate expression, and reduced CO-difference spectra was performed on a subset of expression trials.

A Western blot of full-length CYP2A7-transfected HEK cells with an immunoreactive band at the expected size of 49 kD is presented in Figure 5-5. In later experiments, new anti-body from BD biosciences had significantly lower sensitivity and specificity compared to the prior lots. After adjusting blotting conditions, the new antibody still performed poorly and was only marginally more better than Gel-code blue staining at detecting purified P450 2A6 or purified P450 2A13. Therefore, the limit of detection was ~ 0.5 pmol protein. Figure 5-6 illustrates non-specific banding on the anti-CYP2A6 western blot in CYP2A7-transfected and untransfected HEK cells. Also, Figure 5-6 depicts immunoreactive bands from *E.Coli* microsomes that were transformed with truncated CYP2A7 (a gift from Natasha DeVore in the laboratory of

Dr. Emily Scott); a strong band at ~37 kD is present but this size is smaller than expected for the construct, as it is only 22 amino acids shorter than full-length.

Figure 5-5. Western blot of CYP2A7-HEK transfected cells

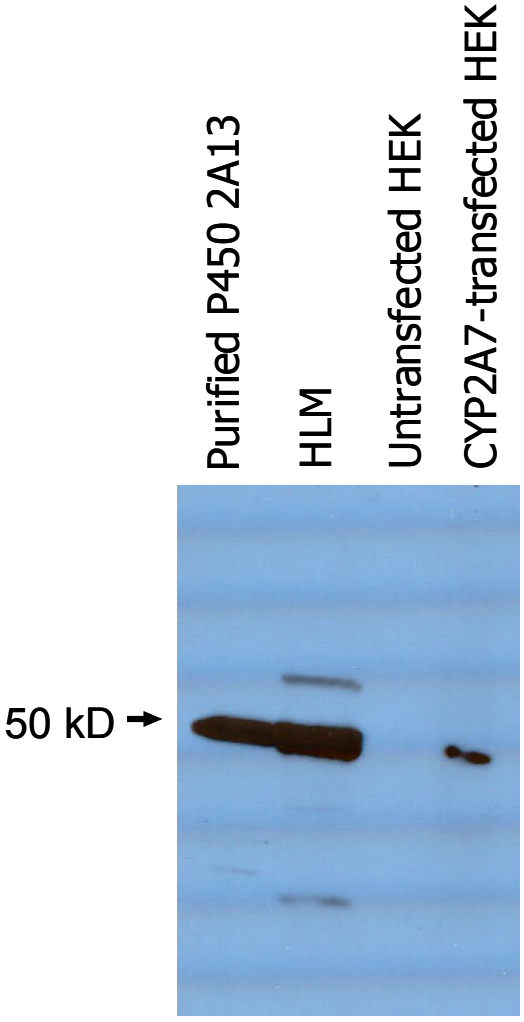

Figure 5-6. Western blot of CYP2A7-HEK transfected cells and *E.Coli* transformed with truncated CYP2A7

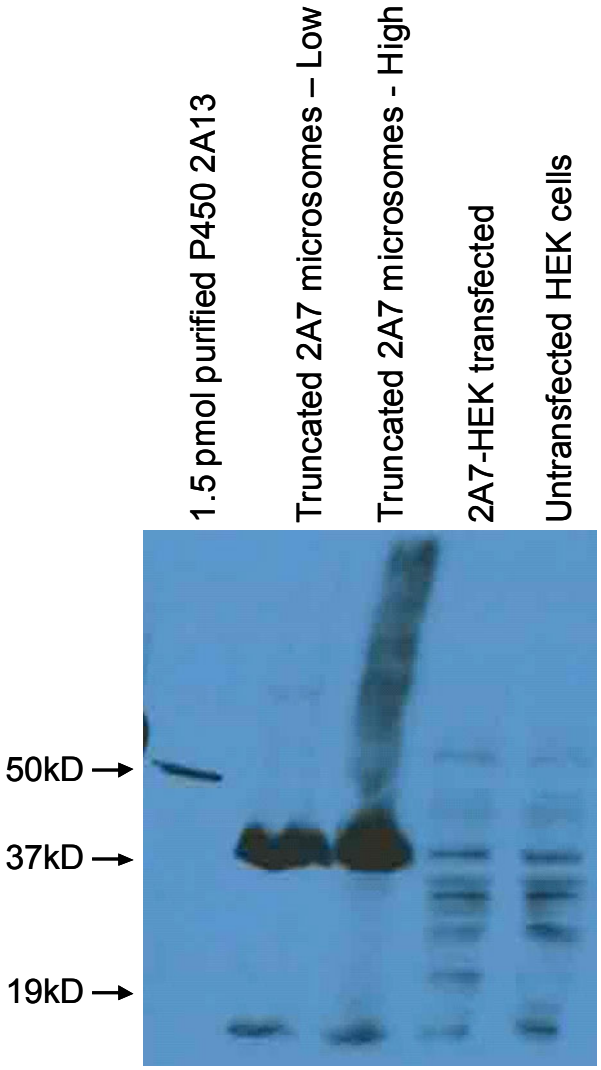

Truncated 2A7 microsomes were prepared from E.Coli, the observed band is smaller than expected. Non-specific bands were observed for 2A7-HEK and untransfected HEK cells from this experiment.

5.3.3 Reduced CO-difference spectra

Full-length and truncated P450 2A7 preparations exhibited a peak at 420 nm when reduced-CO difference spectra were obtained. Spectra of truncated P450 2A7 microsomes was performed by Natasha DeVore in the laboratory of Dr. Emily Scott, University of Kansas. A distinct peak at 450 nm was never observed.

5.3.4 Activity assays

Total coumarin metabolism and coumarin 7-hydroxylation by P450 2A7 preparations were compared to untransfected preparations and either P450 2A6 or P450 2A13. No coumarin 7-hydroxylation was observed for P450 2A7 preparations. In a preliminary experiment, a peak that co-eluted with 8-hydroxycoumarin was observed after incubating CYP2A7-transfected HEK microsomes with ^{14}C-coumarin (Figure 5-6); however this result was not reproduced subsequently. Incubation of the same preparation with NNK did not show α-hydroxylation.

Full-length and truncated P450 preparations were evaluated for chlorzoxazone 6-hydroxylation and p-nitrophenol oxidation to 4-nitrocatechol. No products were observed for any P450 2A7 preparation, while P450 2A13 expressed under the same conditions exhibited detectable activity even when Western blotting was inconclusive. The addition of b_5 and increasing the amount of oxidoreductase also did not have an effect on P450 2A7 activity.

5.4 Discussion

We had predicted that P450 2A7 might be an active enzyme and that it would be a good candidate to evaluate for NNK metabolism. We had no difficulty isolating CYP2A7 mRNA, albeit co-amplification of CYP2A6 was a problem initially. However, we failed to achieve robust levels of full-length CYP2A7 expression in HEK or *E.Coli* cultures. Enzyme activity is detectable even when expression is low (< 1 pmol P450 per reaction volume) if the enzyme is an efficient catalyst of the screening reaction. We observed no product formation upon incubating CYP2A7 preparations with substrates that are metabolized by other P450 2A enzymes.

Also, no activity was observed with a truncated version of wild-type (identical to reference sequence) CYP2A7 with coumarin, p-nitrophenol, or chlorzoxazone in our laboratory or in the laboratory of Dr. Emily Scott. In the absence of a P450 peak, indicating that there was no evidence of properly incorporated heme, we did not screen additional substrates. The CYP2A7.1 variant has not been studied in its truncated form.

CYP2A7 is polymorphic and it is likely that some of these variants or the wild-type have low or no activity. In the NCBI database, there are 114 single nucleotide polymorphisms in CYP2A7, which is similar to the number documented for CYP2A6. Interestingly, wild-type CYP2A7 has a leucine at position 128 and this would interfere with an arginine-mediated interaction between the P450 enzyme and the heme propionate. However, the variant CYP2A7.1 had a conserved arginine in this position and still did not have characteristics of an active P450. A mutagenesis study between

CYP2A7 and CYP2A6 or CYP2A13 could be interesting from a structure-function perspective.

5.5 Conclusion

To date, at least 4 laboratories have evaluated the expression and function of CYP2A7 and none have observed a P450 spectra or enzymatic activity. However, we lack structural information on why this protein might be inactive and therefore can not conclude that CYPA7 protein is entirely inactive at this time. It is improbable that we missed detecting a stable and efficient catalyst, and from a practical standpoint we can assume that P450 2A7 is unlikely to contribute significantly to total NNK metabolism.

5.6 Acknowledgements

Many thanks to Katie Lee for her contribution to cloning CYP2A7 and to expression trials.

CHAPTER 6

CYP2A13 active site mutation Asn297Ala and metabolism of coumarin and tobacco-specific nitrosamines

6.1 Forward

This study was published in Drug Metabolism & Disposition with shared co-first authorship between Dr. Kari Schlicht, a former graduate student in Dr. Murphy's laboratory, and myself. Dr. Schlicht described a significant portion of the research in her PhD thesis and while I will discuss her findings related to NNN and NNK metabolism, I will focus on my contribution which was coumarin metabolism by the P450 Asn297Ala mutant.

6.2 Introduction

The tobacco-specific nitrosamines, (*S*)-*N*′-nitrosonornicotine ((*S*)-NNN) and 4-(methylnitrosamino)-1-(3-pyridyl)-1-butanone (NNK) are carcinogens found in unburned tobacco and cigarette smoke. Both NNN and NNK are classified as human carcinogens (13;223). NNN induces esophageal and nasal tumors in rodents and NNK is a potent lung carcinogen in rodents (35). Both NNN and NNK require P450-catalyzed metabolism to exert their carcinogenic effects. Metabolic activation occurs by hydroxylation of the carbons alpha to the nitroso moiety. For NNN, hydroxylation occurs at the 2′- and 5′-carbon positions to ultimately form 4-oxo-4-(3-pyridyl)-1-butanone (keto alcohol), 5-(3-pyridyl)-2-hydroxytetrahydrofuran (lactol), and reactive diazohydroxide intermediates (Figure 6-1) (34). Hydroxylation of NNK occurs at the α-methyl and α-methylene carbon positions, forming keto alcohol (HPB), 4-oxo-1-(3-pyridyl)-1-butanone (keto aldehyde, OPB), and two diazohydroxides that are capable of pyridyloxobutylating or methylating DNA (Figure 6-1) (34).

In humans, CYP2A13 is an important catalyst of NNN and NNK α-hydroxylation (128;129). The high efficiency of CYP2A13 for NNK metabolic activation combined with its expression in respiratory tissues including nasal mucosa, lung, and trachea suggest that CYP2A13 plays a critical role in tobacco-specific nitrosoamine-induced carcinogenesis (34;128;224)

Figure 6-1 NNN and NNK α-hydroxylation

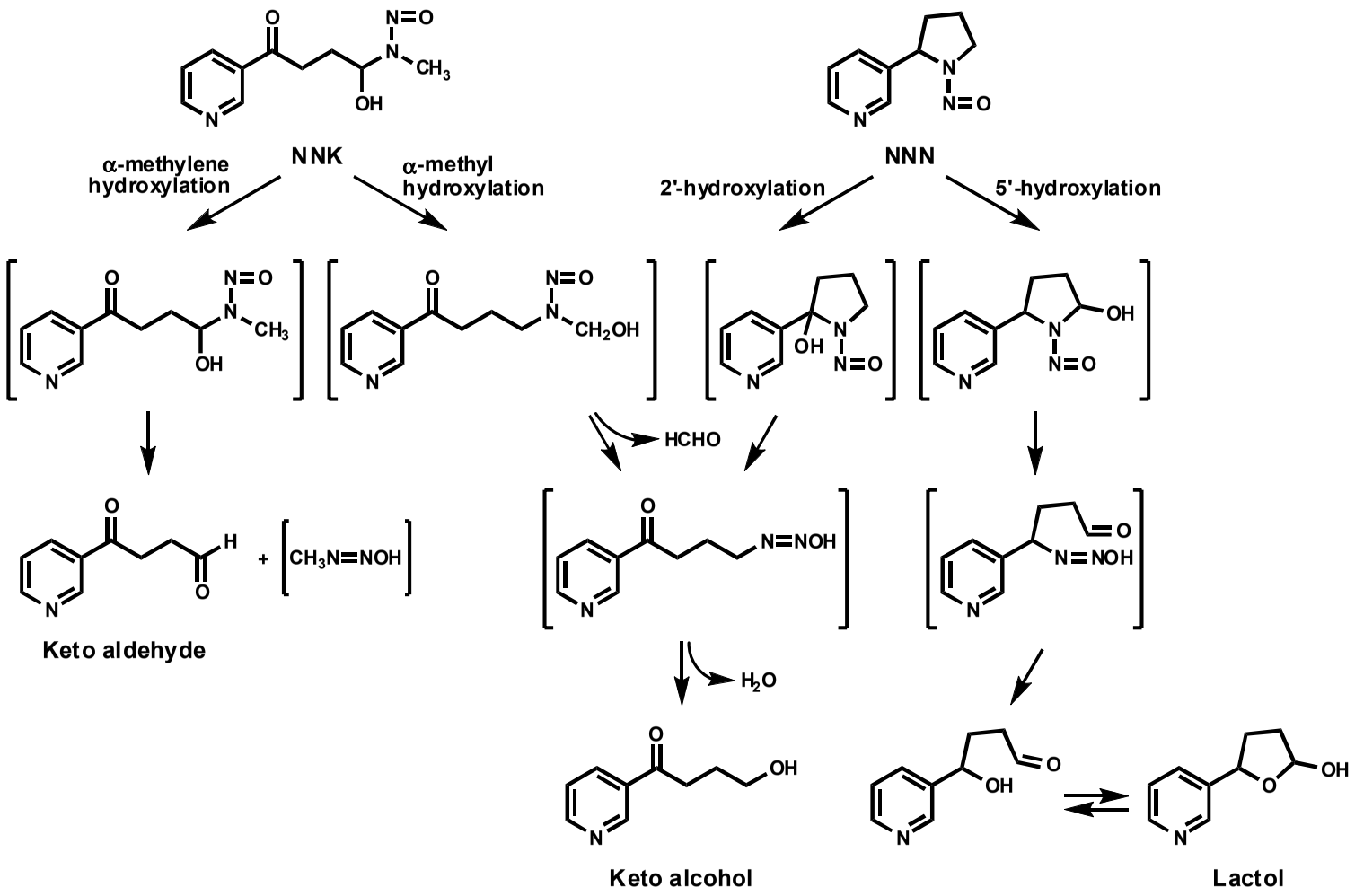

The x-ray crystal structure for CYP2A13 has been reported (205;225). Features of the active site include a cluster of phenylalanine residues that form the "roof" of the active site and two polar residues at opposide sides of the active site, Asn297 and Thr305. Docking NNK into the crystal structures predicts that the active site volume and shape can accommodate NNK in a position that is favorable for α-hydroxylation (205). A hydrogen bond between the pyridine nitrogen of NNK and Asn297 may facilitate an orientation that is compatible with α-hydroxylation. Therefore this amino acid was targeted for mutagenesis to evaluate its effect on enzyme activity and metabolism of NNK and NNN.

Metabolism of (*S*)-NNN by CYP2A13 and the CYP2A13 Asn297Ala resulted in generation of lactol, the product of NNN 5'-hydroxylation (206). The product of 2'-hydroxylation, keto alcohol, was not detected for either enzyme. The K_m value for the mutant was ~3-fold greater than that of the wild type, while the V_{max} was not significantly different. Computational modeling by docking (*S*)-NNN into the active site predicted 5'-hydroxylation and not 2'-hydroxylation for both enzymes. Specifically, positioning of the pyridine nitrogen towards residue 297 was favored regardless of residue type or presence of the hydrogen bond interaction. In brief, while the Asn297Ala mutant had a modest effect on (*S*)-NNN metabolism, the Asn297-substrate interaction was not critical for substrate orientation in the active site.

The Asn297Ala mutation had a greater effect on the efficiency of CYP2A13-catalyzed NNK α-hydroxylation but did not affect product distribution (206). Both CYP2A13 enzymes (wild-type and Asn297Ala) generated products of α-methyl and α-

methylene hydroxylation in a ratio of 1:3 respectively. The K_m for total NNK α-hydroxylation by CYP2A13 Asn297Ala was 6-fold higher than for the wild type enzyme, V_{max} was unchanged. When NNK was modeled in the active site, the pyridine nitrogen consistently positioned towards Asn297 but this did not occur with Ala297. Furthermore the pyridine nitrogen was twisted away from residue 297 in many poses with the α-methyl carbon curled in metabolically unfavorable positions (Figure 6-2).

Figure 6-2. A model of NNK docked in the active site of (A) CYP2A13 and (B) CYP2A13 Asn297Ala

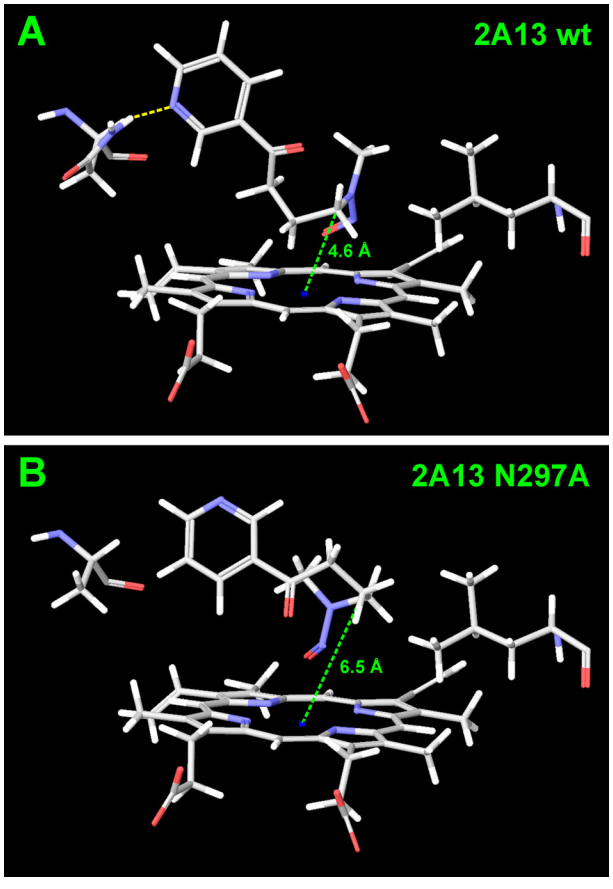

CYP2A13 is an efficient catalyst of coumarin metabolism (212;212;226). CYP2A13 catalyzes both the 7-hydroxylation and 3,4-epoxidation of coumarin with similar efficiency (Figure 6-3). In contrast, CYP2A6, which is 93.5 % identical to CYP2A13 at the amino acid level, exclusively catalyzes coumarin 7-hydroxylation. The crystal structure of CYP2A6 was solved with coumarin in the active site, and a hydrogen bond interaction between Asn297 and the carbonyl oxygen of coumarin contributes to the orientation of coumarin for 7-hydroxylation (225). The 7-hydroxycoumarin product is very stable and is easily quantified by fluorescence detection. However, the 3,4-epoxide is unstable and can react with other components in the incubation. The 3,4 epoxidation of coumarin has been quantified as the formation of o-HPA, which is generated non-enzymatically from coumarin 3,4-epoxide (Figure 6-3) (227;228). The effect of an Asn297Ala mutation on the specificity of CYP2A13-catalyzed coumarin metabolism is reported here.

Figure 6-3. Coumarin 7-hydroxylation and 3,4-epoxidation pathways

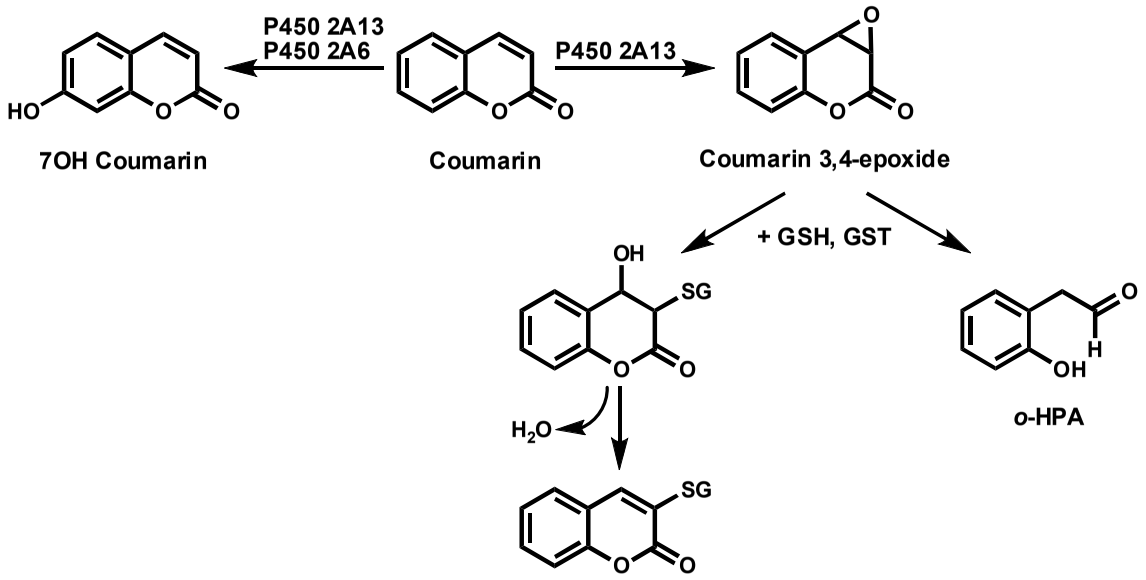

6.3 Materials and Methods

6.3.1 Chemicals and Reagents

[U-^{14}C-benzyl]coumarin (31 mCi mmol^{-1}, 99.5% purity) was purchased from Amersham Pharmacia Biotech (Piscataway, NJ). *o*-Hydroxyphenylacetaldehyde (*o*-HPA) was a gift from Dr. Louis Lehman-McKeeman of Procter & Gamble (Cincinnati, OH). All other chemicals and reagents were purchased from Sigma-Aldrich (St. Louis, MO).

6.3.2 Site-Directed Mutagenesis

Full-length CYP2A13 (with the second codon changed from leucine to alanine and four histidine residues added to the N terminus) in the pKK233-2 plasmid (Pharmacia, Uppsala, Sweden) was a gift from Dr. Emily Scott (University of Kansas, Lawrence, KS). The QuikChange® (Stratagene, La Jolla, CA) method was used to introduce the single nucleotide mutation. Primers used for site-directed mutagenesis were the following: 5′-gtgatgaccaccctggccctcttctttgcgggc-3′ (forward primer, mutated bases are underlined) and 5′-cccgcaaagaagagggccagggtggtcatcacc-3′ (reverse primer, mutated bases are underlined). The single Asn297Ala mutation was confirmed by DNA sequencing.

6.3.3 Protein Expression and Purification

Rat NADPH-P450 oxidoreductase was expressed in *Escherichia coli* and purified as previously described (Hanna et al., 1998). Wild type CYP2A13 and CYP2A13 Asn297Ala were expressed in TOPP-3 *E. coli* cells (Stratagene, La Jolla, CA) at 30˚C with 190 rpm shaking and an with an induction time of 72 hours using the protocol previously described (229). Cells were harvested and purified using a previously published protocol (230).

6.3.4 Protein Characterization and Enzyme Reconstitution

Enzyme expression and purity was visualized by SDS-Page with Gel Code Blue staining (Pierce Biotechnology, Rockford IL). Expression of CYP2A13 and CYP2A13 Asn297Ala was confirmed by Western blot using anti-CYP2A6 antibody (BD Biosciences, San Jose, CA) that also detects CYP2A13 (Wong et al., 2005b). Cytochrome P450 content was determined for each enzyme preparation by dithionite-reduced CO difference spectra obtained using an Olis DW-2000 UV-Vis spectrophotometer (Olis Inc., Bogard, GA) (61). Enzymes were reconstituted with 1:4 P450:oxidoreductase and dilauroyl-L-α-phosphatidylcholine (0.2 μg/pmol P450) for 45 min at 4°C just prior to use.

6.3.5 Coumarin Metabolism

Total coumarin metabolism was determined using [U-^{14}C-benzyl]coumarin and radioflow HPLC analysis. The method used was a modification of a previously described HPLC system (212). Reconstituted CYP2A13 or CYP2A13 Asn297Ala (40 pmol) were each incubated with 65 μM of [U-^{14}C-benzyl]coumarin (31 mCi mmol^{-1}), 100 mM Tris buffer, pH 7.4, an NADPH-generating system (0.4 mM $NADP^+$, 100 mM glucose-6-phosphate, and 0.4 units ml^{-1} glucose-6-dehydrogenase) in a final volume of 150 μL for 10-60 min at 37 °C. Reactions were terminated by addition of 15 μL 15% tricholoroacetic acid. All analyses were conducted in triplicate. Products were analyzed by radioflow HPLC with a Phenomenex Gemini C18 (5 μm, 250 × 4.60 mm) column. A flow rate of 0.8 ml min^{-1} was used. An isocratic system of 72 % A [1% acetic acid in water] and 28 % B [1% acetic acid in methanol] was used. As the column aged, B was decreased to 25 %. Radioactive detection was accomplished using a β-RAM radioflow detector (IN/US Systems, Tampa, FL) with a scintillant flow rate of 2.4 ml min^{-1} [Monoflow 5, National Diagnostics, Atlanta, GA]. ^{14}C-labeled products were co-injected with *o*-HPA, 8-hydroxycoumarin, 7-hydroxycoumarin, and 3-hydroxycoumarin standards detected by absorbance at 270 nm. Initially, 4-hydroxycoumarin, 5-hydroxycoumarin, and 6-hydroxycoumarin were also evaluated as potential products based on retention times.

Coumarin 3,4-epoxidation was quantified by trapping the epoxide as a GSH conjugate. The method used is analogous to that used previously to quantify naphthalene epoxidation (231). Reactions were carried out as above with the addition

of 1 to 5 mM GSH and 2.5 to 20 units GST (from equine liver, Sigma:Aldrich). Using ^{14}C-coumarin, conditions were determined under which the 3,4-epoxide was trapped by the addition of GSH (1.5 mM) and glutathione-S-transferase (GST) (5 units), as determined by the decrease in detection of o-HPA and no further increase in the GSH conjugate peak with increasing amounts of GST. With CYP2A13 Asn297Ala, 87% of the 3,4-epoxide was trapped, while with CYP2A13 *o*-HPA was no longer detectable when GSH and GST were added to the reaction mix. To determine the kinetic parameters of coumarin 7-hydroxylation and 3,4-epoxidation, reconstituted CYP2A13 (7.5 pmol) or CYP2A13 Asn297Ala (2-5 pmol) enzyme was incubated in the presence of GST and GSH with 1 to 500 μM coumarin under the conditions described above. Metabolites were analyzed by HPLC with UV detection at 310mn (λ_{max} for coumarin). By comparing absorbance at 310 nm to radioactivity in reactions carried out with ^{14}C-coumarin, the ratio of the absorbance of 7-hydroxycoumarin relative to the coumarin GSH conjugate was determined to be 1.2. A standard curve of peak area versus 7-hydroxycoumarin was used to determine metabolite concentrations. HPLC conditions were those described above.

6.3.6 LC/MS/MS analysis of coumarin metabolites

Products of coumarin metabolism were collected from the HPLC system described above and concentrated under N_2. Reaction products and hydroxycoumarin standards were analyzed using a Finnigan TSQ Quantum Ultra AM triple quadrupole mass spectrometer operated with electrospray ionization (ESI) (Thermo Electron, San Jose,

CA). Sample (4-8μL) was loaded onto a Zorbax SB-C18 (5 μm, 0.5 x 150 mm) column with a flow rate of 10μL min^{-1} of 70% A [1% acetic acid in water] and 30% B [1% acetic acid in methanol] using a Waters nanoAcquity UPLC solvent delivery module (Waters, Milford, MA). The hydroxycoumarins were analyzed by ESI-MS-MS with selection for the protonated molecular ion at *m/z* 163. The ESI source was set in positive ion mode, voltage 3.3 kV; capillary tube, 250 °C. The Ar collision gas pressure was 1.0 mTorr, collison energy, 20-25 V; scan time, 0.5 sec.; peak width of Q1 and Q3, 0.7. A full scan was performed for detection of a coumarin GSH conjugate with *m/z* 452 $[M + H]^+$ and product spectra were also generated. Additionally, the coumarin GSH conjugate was analyzed in negative ESI mode and the full product scan of the parent ion *m/z* 450 $[M - H]^-$ was evaluated. The ESI source parameters were voltage 3.5 kV; capillary tube, 250 °C. The Ar collision gas pressure was 1.0 mTorr, collison energy, 30 V; scan time, 0.55 sec.; peak width of Q1 and Q3, 0.7.

6.3.7 Statistics

Kinetic parameters, K_m and V_{max} for coumarin 7-hydroxylation, coumarin 3-hydroxylation, coumarin 3,4-epoxidation were determined using the EZ-fit 5 kinetics software from Perrella Scientific (Amherst, NH). Statistical differences between mean K_m or V_{max} values were determined using a Chi square test.

6.3.8 Computer Modeling and Docking

Coordinates from the X-ray crystal structure for CYP2A13 (PDB 2P85) (Smith, 2007), were obtained from the Protein Data Bank (http://www.rcsb.org) and used to model CYP2A13 and CYP2A13 Asn297Ala in MAESTRO (version 3.5, Schrodinger, LLC, New York, NY). Coumarin was generated and minimized in MAESTRO prior to docking. Docking studies were conducted using the program GLIDE within MAESTRO to view the top twenty-five possible binding orientations (out of 10,000 dockings) for the substrates within active sites of CYP2A13 and CYP2A13 Asn297Ala. Substrates were allowed to dock flexibly within the active sites.

6.4 Results

6.4.1 CYP2A13 Asn297Ala expression

CYP2A13 and the single-residue mutant enzyme CYP2A13 Asn297Ala were expressed and purified. Protein expression levels were not hindered by the introduction of the Ala297 site-mutation as confirmed by Western blotting. Proper incorporation of heme was verified with CO-difference spectra and P450 content was quantified.

6.4.2 ^{14}C-coumarin metabolism

The relative metabolism of ^{14}C-coumarin by wild type CYP2A13 and the Asn297Ala mutant were analyzed by radioflow HPLC (Figure 6-4). The major metabolites generated by the wild type enzyme were o-HPA, a product of coumarin 3,4-epoxidation and 7-hydroxycoumarin (Figure 6-4A). These two metabolites were present in approximately equal amounts. In contrast, o-HPA was a 3-fold more abundant metabolite of CYP2A13 Asn297Ala-catalyzed coumarin metabolism than was 7-hydroxycoumarin (Figure 6-4C). In addition, other radioactive products, eluting prior to 10 min and at 48 min, accounted for a significant percentage of the radioactivity. The later eluting metabolite co-eluted with 3-hydroxycoumarin. Its identity as 3-hydroxycoumarin was confirmed by LS/MS/MS analysis of the collected peak. None of the early eluting peaks co-eluted with available standards, including *o*-hydroxyphenyl acetic acid, 6,7-dihydroxycoumarin and all hydroxycoumarin metabolites. We hypothesized these peaks may be secondary metabolites of the coumarin 3,4-epoxide or products of the conjugation of the 3,4-epoxide with a nucleophile or nucleophiles present in the enzyme reaction mixture. A minor product of both CYP2A13- and CYP2A13 Asn297Ala- catalyzed metabolism co-eluted with 8-hydroxycoumarin.

6.4.3 Trapping coumarin 3,4-epoxide as its GSH conjugate

To confirm that the early eluting metabolite(s) are product(s) of coumarin 3,4 epoxidation, and to more accurately quantify the 3,4-epoxidation of coumarin a method was developed which trapped coumarin 3,4-epoxide as its GSH conjugate. Conditions were established under which 87% or greater of the o-HPA formed was no longer detected as a product (Figure 6-4B, 6-4D). Efficient trapping of coumarin 3,4-epoxide required GSH concentrations of at least 1 mM and excess GST, as the reaction was sensitive to the amount of GST available.

Under these conditions, not only did little o-HPA remain but in addition the majority of the radioactivity eluting prior to 12 min was no longer detected. In the presence of GSH and GST the size of the early eluting radioactive peak was the same with either wild type or mutant enzyme. The addition of GSH and GST to the enzyme reactions resulted in the appearance of a new metabolite peak eluting 2 min later than 7-hydroxycoumarin. This peak was presumed to be a GSH conjugate of coumarin 3,4-epoxide (Figure 6-3). The ratio of this peak to 7-hydroxycoumarin was 1.3:1 for CYP2A13 and 9:1 for CYP2A13 Asn297Ala (Figure 6-4B and 6-4D). These values are significantly greater than the ratio of o-HPA to 7-hydroxycoumarin obtained in the absence of GSH and GST (Figure 6-4A and 6-4C); consistent with our hypothesis that quantifying o-HPA alone did not accurately reflect the extent of coumarin 3,4-epoxidation.

Figure 6-4. Radioflow HPLC analysis of ^{14}C-coumarin metabolites

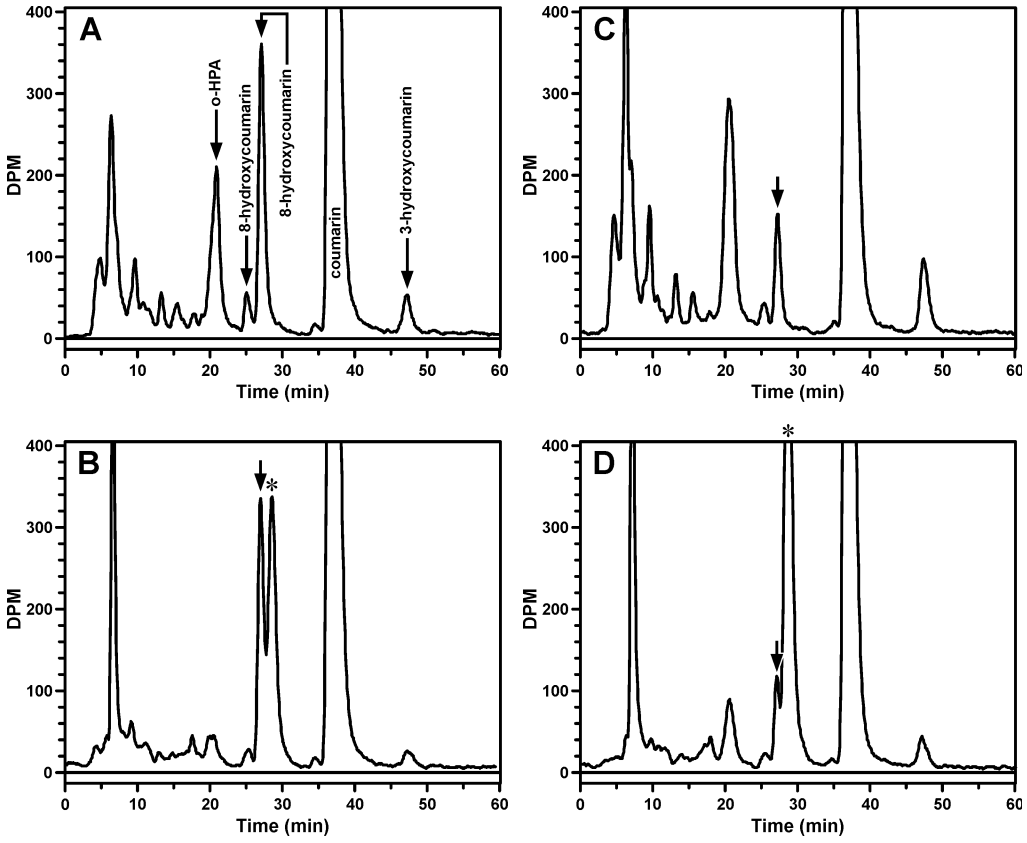

Figure 6-4. Radioflow HPLC analysis of 65 μM [^{14}C]coumarin metabolism by CYP2A13 (10 pmol; 30 min) (A and B) or CYP2A13 Asn297Ala (5 pmol; 20 min) (C and D). Reactions were carried out in the absence (A and C) or presence (B and D) of GSH and GST. Arrows in A indicate retention times of metabolite standards. The arrow in B to D indicate the retention time of 7-hydroxycoumarin. The asterisk (*) is the GSH/GSTdependent peak.

6.4.4 Coumarin metabolism by UV-HPLC and LC/MS

Using the conditions established with ^{14}C-coumarin and radioflow HPLC analysis a UV HPLC method was developed for the detection of 7-hydroxycoumarin and the coumarin GSH conjugate. To determine the rate of coumarin 3,4-epoxidation, the coumarin GSH conjugate was quantified by HPLC with UV detection at 310 nm. Note that the absorbance of 7-hydroxycoumarin at 310nm is 1.2-fold greater than the coumarin GSH conjugate. Sample chromatograms for the UV-HPLC analysis of coumarin 7-hydroxylation and 3,4-epoxidation by CYP2A13 and CYP2A13 Asn297Ala are illustrated in Figure 6-5.

The presumed GSH conjugate, 7-hydroxycoumarin, and the metabolite that co-eluted with 3-hydroxycoumarin were collected and analyzed by LC/MS/MS. Both negative and positive ion tandem mass spectrometry were used to identify the GSH conjugate. The product ion spectra from *m/z* 450 $[M - H]^-$ contained *m/z* 128, 143, 177, 179, 210, 254, and 272. The *m/z* 177 is γ-glutamyl-S-(3-coumarin)cysteinyl glycine, and the other fragments are generated from the glutathione moiety (232). Mass spectral analysis with ESI in the positive mode detected a molecular ion of *m/z* 452 $[M + H]^+$. The major ions in the product spectrum from *m/z* 452 were *m/z* 220; the 1-aminothioether of coumarin, *m/z* 323, (3-coumarin)cysteinyl glycine, and m/z, 305/306, (3-coumarin)cysteinyl glycine, minus NH_3 . (Figure 6-6). The identities of the 7-hydroxycoumarin and 3-hydroxycoumarin metabolites were confirmed by comparison of product spectra from *m/z* 163 $[M + H]^+$ to authentic standards. The major product ion was *m/z* 107 (Figure 6-6).

Figure 6-5. UV HPLC analysis of coumarin metabolism

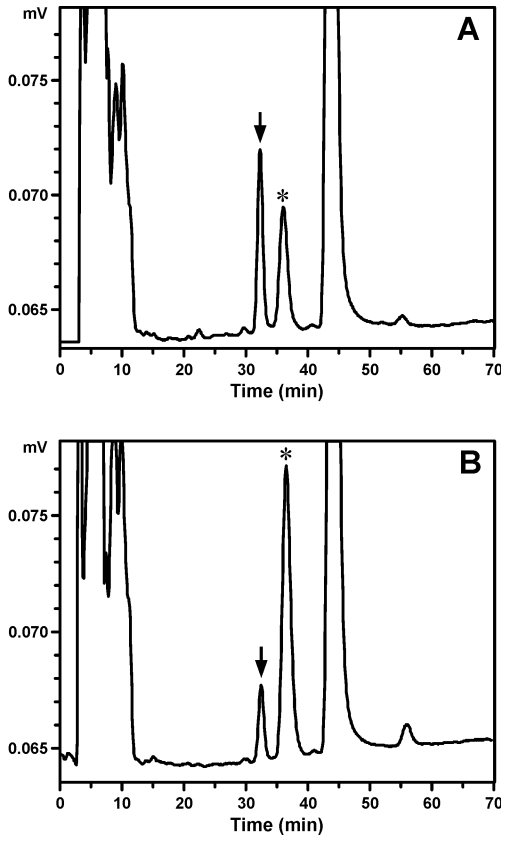

Figure 6-5. UV HPLC analysis of 20 µM coumarin metabolism by (A) CYP2A13 (7.5 pmol, 20 min) or (B) CYP2A13 Asn297Ala (2 pmol, 20 min) in the presence of 1.5 mM GSH and 4 units GST. The arrow indicates the retention time of 7-hydroxycoumarin and the * is the GSH/GST dependent peak.

Figure 6-6. ESI-MS-MS positive ion product spectra

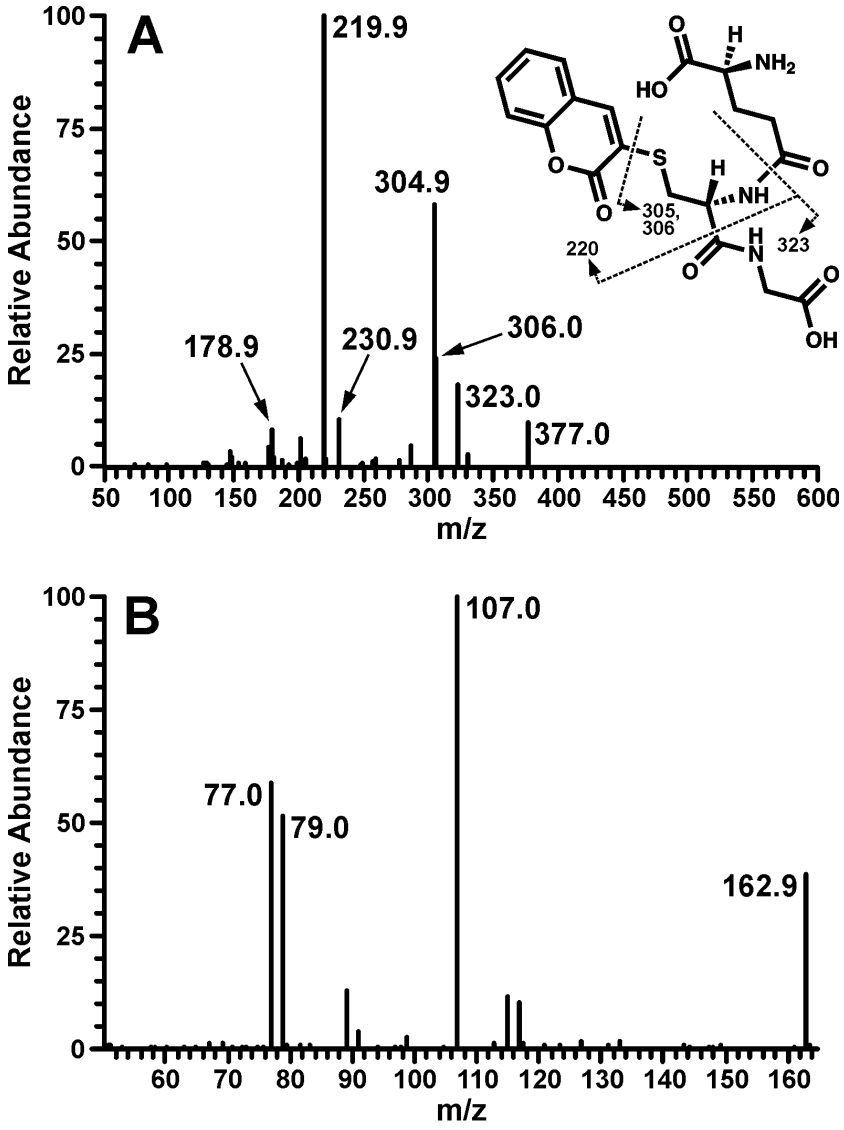

Figure 6-6. ESI-MS-MS positive ion spectra of (A) the collected coumarin-GSH conjugate $[M + H]^+$, *m/z* 452 and (B) the late-eluting coumarin metabolite, 3-hydroxycoumarin *m/z* 163. Spectra are identical to authentic standards.

6.4.5 Kinetic parameters for Asn297A and wild-type P450 2A13

The kinetic parameters of coumarin 7-hydroxylation, 3,4-epoxidation and 3-hydroxycoumarin were determined for CYP2A13 Asn297Ala and CYP2A13 (Table 6-1). Kinetic parameters were determined in the presence of GSH and GST to better quantify 3,4-epoxidation. The K_m values for these reactions were approximately 4-fold greater for the mutant enzyme. However, the v_{max} values increased 3-fold for coumarin 7-hydroxylation, 19-fold for 3-hydroxylation and 40-fold for 3-4 epoxidation. The catalytic efficiency of coumarin 3,4-epoxidation increased 10-fold while coumarin 7-hydroxylation decreased by 25%. Interestingly, 3-hydroxycoumarin was still detected in the presence of GSH and GST, which would be expected if coumarin 3-hydroxylation occurs independently from the 3,4-epoxication pathway. The catalytic efficiency of coumarin 3-hydroxylation was 6-fold greater for the mutant enzyme. Coumarin 7-hydroxylation by wild-type CYP2A13 accounted for about 35% of coumarin metabolism by the 3 pathways, but only 9% of that by the mutant enzyme. Coumarin 8-hydroxylation was catalyzed by wild type and the mutant enzyme, but accounted for less than 3 % of the total coumarin metabolism.

6.4.6 Modeling coumarin orientation in the active site

To further investigate the role of Asn297 on substrate orientation, coumarin, (*S*)-NNN, and NNK were computationally docked into the active site of CYP2A13 and CYP2A13 Asn297Ala. Docking studies generally complemented the enzyme kinetic

analyses. When coumarin was docked in wild-type CYP2A13, it equally favored orientations for 7-hydroxylation and 3,4-epoxidation. Approximately 40 % of the poses predicted a hydrogen bond forming between Asn297 and the carbonyl oxygen of coumarin, positioning the 7'-carbon over the heme iron, as close as 3.9 Å (Figure 6-7). In the other major poses (40 %) the coumarin molecule was flipped so that the double bound was positioned for 3,4-epoxidation by CYP2A13. In contrast, when coumarin was docked into the CYP2A13 Asn297Ala mutant, only 3,4-epoxidation was predicted (Figure 6-7B).

Table 6-1. Kinetic parameters for CYP2A13 and CYP2A13 Asn297Ala reactions [a]

	CYP2A13 wt		**CYP2A13 Asn297Ala**	
Reaction[b]	K_m (μM)[c]	V_{max} (*pmol/min/pmol P450*)	K_m (μM)[c]	V_{max} (*pmol/min/pmol P450*)
Coumarin 7-hydroxylation	3.7 ± 0.39	0.59 ± 0.01	16.6 ± 0.9	1.94 ± 0.03
Coumarin 3,4-epoxidation	3.8 ± 0.43	0.25 ± 0.006	14.8 ± 1.1	9.25 ± 0.09
Couamarin 3- hydroxylation	6.3 ± 1.5	0.06 ± 0.003	18.9 ± 0.3	1.12 ± 0.03
NNK α-hydroxylation[d]	11.9 ± 3.2	0.85 ± 0.07	66.7 ± 8.1	0.87 ± 0.09
(*S*)-NNN 5'-hydroxylation	30.7 ± 10.1	1.28 ± 0.11	108 ± 22.1	1.12 ± 0.12

[a] Values for K_m and V_{max} represent mean ± standard error of 2-5 independent experiments.

[b] Coumarin concentrations were 1, 2, 5, 10, 20, 40, 100, 200, 500 µM, NNK concentrations were 0.5, 2, 5, 10, 25, 50, 75, 100, 200, 300 µm, (*S*)-NNN concentrations were 10, 25, 50, 100, 250, 500, 750,1000 µM. Products were detected by UV-HPLC (coumarin) or radioflow-HPLC (NNK and NNN), details are described in the Materials and Methods.

[c] K_m values for all substrates were significantly different for CYP2A13 Asn297Ala compared to CYP2A13 ($p<0.03$)

[d] α-Hydroxylation was quantified as the sum of methyl and methylene hydroxylation which occurred in a ratio of 1 to 3 at all NNK concentrations.

Figure 6-7. A model of coumarin docked in the active site of (A) CYP2A13 and (B) CYP2A13 Asn297Ala

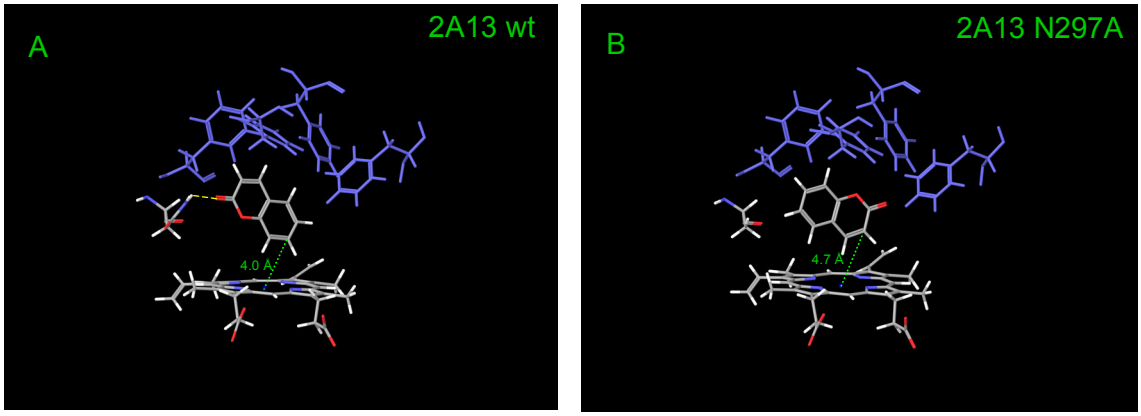

6.5 Discussion

Residue Asn297 has been implicated as an important residue for substrate orientation in CYP2A6. In this study, a single site mutation Asn297Ala was used to investigate the importance of the active site residue Asn297 on CYP2A13-catalyzed coumarin metabolism. The Asn297Ala substitution resulted in an increase in K_m for α-hydroxylation of (*S*)-NNN and NNK relative to wild-type, but there was little effect on V_{max} and no effect on product distribution. To further characterize the Asn297Ala mutant, the metabolism of coumarin was investigated. We hypothesized that coumarin might serve as a structural probe of substrate positioning, and that depending on favored orientations in the active site different hydroxylation products would be formed.

We previously reported that CYP2A13 efficiently catalyzed the 3,4-epoxidation of coumarin as measured by the formation of o-HPA (212). However, it became obvious

in carrying out the studies reported here that o-HPA formation did not accurately reflect the rate of coumarin 3,4-epoxidation. Therefore, to quantitively measure coumarin 3,4 epoxidation, GSH and GST were included in the reaction and the rate of coumarin GSH conjugate formation was determined. Using this methodology, the ratio of coumarin 7-hydroxylation to 3,4-epoxidation by wild-type CYP2A13 was 1.0 to 1.3 compared to a ratio of 1.0 to 0.7 we reported previously (212).

The Asn297Ala mutation had a striking impact on coumarin metabolism, significantly altering the product distribution. The CYP2A13 Asn297Ala mutant catalyzed coumarin 3,4-epoxidation with 10-fold greater efficiency than wild type enzyme. This shift to 3,4-epoxidation is consistent with the preferred substrate orientation predicted by docking coumarin in the active site of the Asn297Ala model. With wild type CYP2A13 coumarin may form a hydrogen bond with the carbonyl oxygen positioning the molecule for 7-hydroxylation. However, a second orientation stabilized by a cluster of phenylalanines in the active site positions coumarin for 3,4-epoxidation. In the mutant enzyme this orientation predominates thereby favoring the 3,4-epoxidation of coumarin.

In contrast to the increase in total coumarin metabolism that was observed with CYP2A13 Asn297Ala compared to CYP2A13, both NNN and NNK metabolism by CYP2A13 Asn297Ala were significantly decreased. The catalytic efficiency of (*S*)-NNN α-hydroxylation decreased 4-fold, due to an increase in the K_m. While the hydrogen bond to Asn 297 was not critical to NNN metabolism by CYP2A13, it does appear to improve enzyme affinity for NNN. The impact of the Asn297Ala mutation on

NNK α-hydroxylation was greater. Catalytic efficiency was decreased 6-fold relative to wild-type CYP2A13. Also, changing the 297 residue from an Asn to Ala in a model of CYP2A13 caused NNK to dock in poses that are unfavorable for α-methyl and α-methylene hydroxylation.

In CYP2A6, mutation of residue Asn297 has been shown to influence substrate binding and metabolism. As observed in CYP2A13, mutation of Asn297 in CYP2A6 resulted in altered coumarin 7-hydroxylation. An Asn297Ser mutant was determined to have ~ 4-fold decreased catalytic efficiency for coumarin 7-hydroxylation (Kim et al., 2005). This mutation also decreased binding affinity for coumarin by nearly 30-fold. The rate of coumarin 3,4-epoxidation was not measured in this study, however, given the dramatically decreased binding affinity of coumarin it is unlikely the Asn297Ser CYP2A6 mutant catalyzed this reaction. Two additional mutants, Asn297His and Asn297Gln have also been shown to have decreased catalytic efficiency for coumarin 7-hydroxylation compared to wild type CYP2A6 (233). Recently, the crystal structure for the CYP2A6 Asn297Gln mutant was reported (234). Although the glutamine substitution had little effect on the overall size of the active site, it did cause altered protein folding interactions between the B′-C helix region and helix I. In addition, no hydrogen bond interactions were able to form between Gln297 and substrates like coumarin.

The ability of Asn297 to hydrogen bond with substrates has been demonstrated in both CYP2A6 and CYP2A13 crystal structures. This interaction was shown to orientate

indole in the active site of CYP2A13 and to position coumarin for 7-hydroxylation in CYP2A6.

6.6 Conclusions

The importance of Asn297 for CYP2A13 substrate orientation and catalysis was confirmed by the present study. The polar amino acid residue Asp297 in the active site contributes to substrate orientation through a hydrogen bonding interaction. An Asn297Ala mutation substantially altered coumarin metabolism. In particular, a shift from 7-hydroxylation to 3,4-epoxidation was observed and this would be consistent with disruption of a hydrogen bond between the carbonyl oxygen of coumarin and Asn297. Product distribution was not altered for NNK or NNN, but the Asn297Ala mutant had decreased product formation. The Asn297Ala had a greater effect on NNK than NNN metabolism, and Asn 297 likely contributes to orientation of NNK in a position that is favorable for α-hydroxylation.

6.7 Acknowledgements

We thank Jessica van Lengerich for her assistance in carrying out the coumarin 3,4-epoxidation assays, Linda von Weymarn for providing LC/MS/MS expertise, and Yuk Sham for his guidance with P450 docking experiments, carried out in the Minnesota Supercomputing Institute. Mass spectrometry was carried out in the Analytical

Biochemistry core supported in part by grant CA-77598 from the National Cancer Institute.

6.8 Publication of thesis work

The work discussed in Chapter 6 was pubished in Drug Metabolism and Disposition: Schlicht KE [*], Zinggeler-Berg J [*], Murphy SE. Effect of CYP2A13 Active Site Mutation Asn297Ala on Metabolism of Coumarin and Tobacco-specific Nitrosamines. Drug Metab Dispos, 2008; 37:665-671. [*]Contributed equally to this work.

CHAPTER 7

Glucuronide conjugation of NNK metabolites

7.1 Introduction

Carcinogenesis by the tobacco specific nitrosamine, 4-(methylnitrosamino)-1-(3-pyridyl)-1-butanone (NNK) occurs as a result of metabolic activation by cytochrome P450-catalyzed α-hydroxylation (34;235). UDP-glucuronsyltransferases (UGTs) partially mitigate carcinogenesis by facilitating the detoxification of NNK metabolites (200). NNK undergoes carbonyl reduction to NNAL and two glucuronide conjugates are formed, an *O*-linked and an *N*-linked glucuronide (236;237). Also, a glucuronide of the unstable hydroxylation metabolite, α-hydroxymethyl NNK, was previously detected in hepatocyte incubations and in urine of phenobarbital-treated rats (200). In rats, the formation of α-hydroxymethyl NNK glucuronide correlated with a decrease in hemoglobin adducts (200). The glucuronidation of unstable product(s) of P450-catalyzed NNK hydroxylation represents an intriguing functional relationship between P450s and UGTs in xenobiotic metabolism wherein a reactive species with DNA-adducting potential is captured by glucuronidation. The conjugation of unstable α-

hydroxymethyl or α-hydroxymethylene NNK metabolites by UGTs may represent an uncharacterized detoxification pathway in humans.

The goals of this preliminary study were to investigate the formation of α-hydroxymethyl NNK glucuronide *in vitro* by primary human hepatocytes; by co-incubation with P450 2A13 and human liver microsomes; and by mixed or co-expressed P450 2A13 and the UGTs 1A9, 2B7, and 2B17.

Figure 7-1. NNK metabolism and formation of glucuronide metabolites

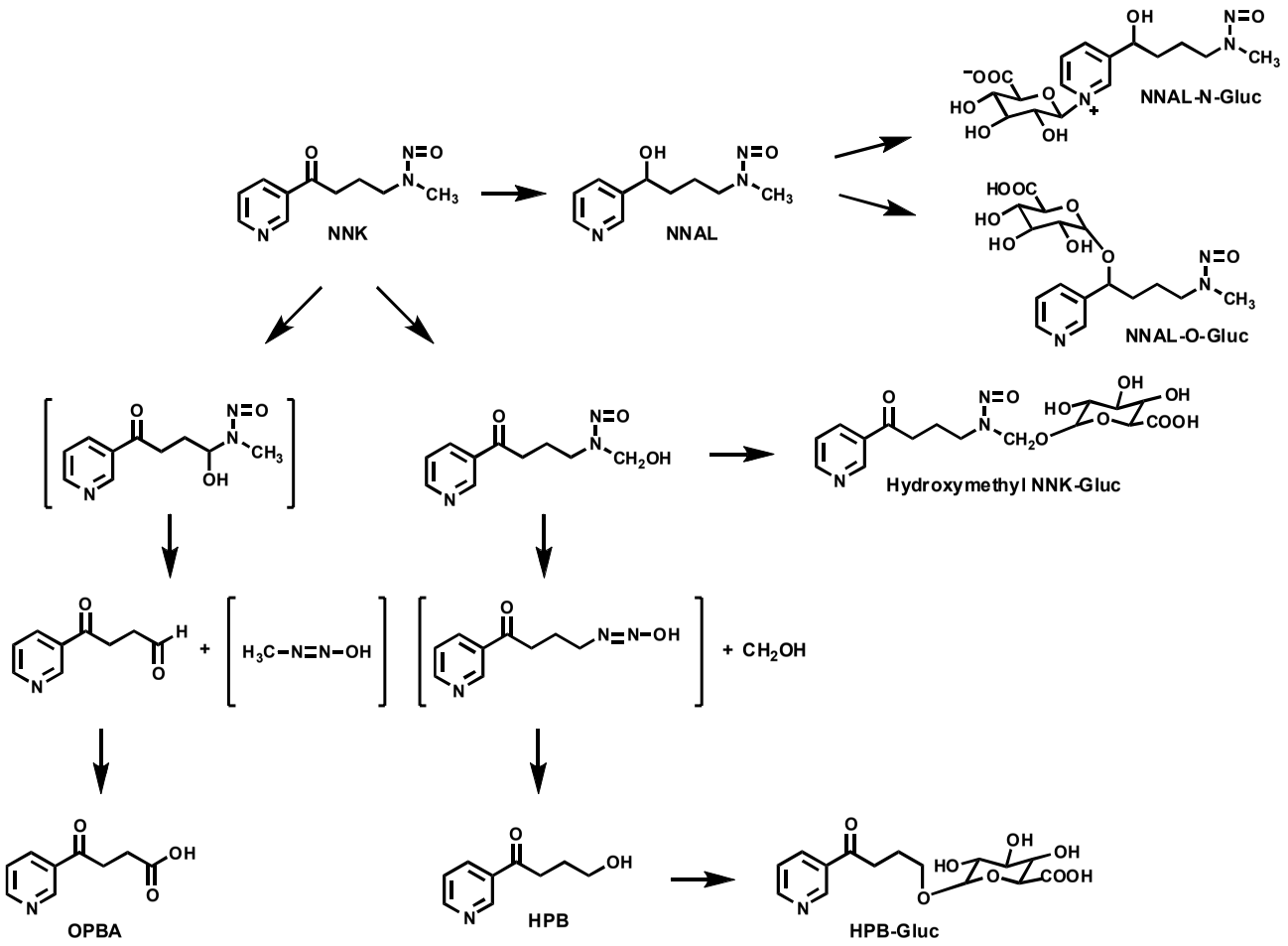

7.2 Methods

7.2.1 Metabolism by primary human hepatocytes

Primary human hepatocytes (Cellzdirect) in 12-well plates with matrigel overlay were incubated with 2 μM coumarin or 1-10 μM 3H-NNK, 3H-nicotine, or 3H-NNAL in Williams E media supplemented with insulin, transferrin, selenium, +/- dexamethasone. Coumarin metabolites in the media at 0.5, 1, 2, 6, and 12 hours were analyzed by fluorescence HPLC and compared to authentic standards (212). 3H-NNK, 3H-nicotine, and 3H-NNAL metabolites in the media at 6, 12, and 24 hours were analyzed by radioflow HPLC with co-injection of available authentic standards (200). β-glucuronidase treatment was used to evaluate the presence of glucuronide metabolites.

7.2.2 Enzyme sources

Human liver microsomes were previously prepared from human liver tissue provided by Dr. F. P. Guengerich, Vanderbilt University (163). *E.Coli*-expressed, purified P450 2A13 and *E.Coli*-expressed rat P450 oxidoreductase were prepared as described (206). UGT2B17 supersomes were purchased from BD biosciences. Cell lysate from UGT1A4 and UGT2B7 was from expressed in HEK293 cells. All enzymes were stored in aliquots at -80˚C until use.

7.2.3 Co-expression of CYP2A13 and UGT2B7

P450 2A13 was transferred from the pCW vector to pBUDCE4.1 (Invitrogen, Carlsbad, CA) between the EcoI and NotI multiple cloning sites and placed under control of the EF-1 promoter. HEK293 cells expressing UGT2B7 were transfected with CYP2A13pBUD using calcium phosphate precipitation (219). UGT2B7 and P450 2A13 were under continuous selection using G418 and zeocin, respectively. Enzyme activity was evaluated in whole cells and cell lysate use with coumarin, 7-hydroxycoumarin, and p-nitrophenol (163;212).

7.2.4 Incubations with ^{3}H-NNK, ^{3}H-NNAL, and ^{3}H-HPB

Incubations were performed with 2-100 μM coumarin, 50-500 μM ^{3}H-NNK, 100 μM ^{3}H-NNAL, and 100 μM ^{3}H-HPB and UDPGA (0.1 – 2.5 mM). For incubations with purified P450 2A13, a reconstitution including P450 2A13 (40 pmol), 1:4 P450:oxidoreductase, and 0.2μg/pmol DLPC was prepared on ice and incubated for 30 minute prior to addition of UGT enzyme (0.5-2 mg/ml final concentration) which was then incubated for an additional 15 minutes. The reaction mix was prepared in 50 mM Tris buffer, pH 7.4, 5 mM $MgCl_2$, +/- 0.1mg/ml alamethicin, and reactions were initiated at 37 ˚C with NADPH generating system and/or UDPGA. Incubations time was 80 minutes. Products were analyzed by fluorescence HPLC (coumarin) or by radioflow HPLC (200;212). The presence of glucuronide conjugates was tested by treatment with β-glucuronidase followed by HPLC analysis.

7.2.5 LC/MS analysis of glucuronide metabolites

NNK metabolites were analyzed by LC/MS using electrospray ionization (ESI) with positive ion detection using a Thermo Finnigan TSQ Discovery (200). Metabolites (1-8 µl) were separated on a Phenomenex Luna capillary flow system using a gradient with 10 mM ammonium acetate buffer, pH 6.7 and acetonitrile. Metabolites of NNK metabolism, authentic standards, and metabolite standards previously collected from rat urine or rat hepatocytes were analyzed. The monitored *m/z* range was 150 – 420 amu, and metabolites standards were detected, $[MH^+ + 1]$: HPB-glucuronide, 342; NNAL-O-glucuronide, 386; α-hydroxymethyl NNK glucuronide, 400.

7.3 Results

7.3.1 Coumarin metabolism by primary human hepatocytes

Primary human hepatocytes incubated with 2 µM coumarin formed 7-hydroxycoumarin and 7-hydroxycoumarin glucuronide, and the glucuronide conjugate was the major metabolite that accumulated in media (Figure 7-2). Coumarin metabolites, 7-hyroxycoumarin and 7-hydroxycoumarin glucuronide were detected directly using fluorescence HPLC. The 7-hydroxycoumarin glucuronide was quantified as free and total 7-hydroxycoumarin following treatment with β-glucuronidase. The peak concentration of 7-hydroxycoumarin was 60 minutes while the glucuronide

accumulated in the media over 12 hours. The glucuronide conjugate was also detected at 15 minutes, the earliest timepoint measured.

Figure 7-2. Coumarin metabolism by primary human hepatocytes

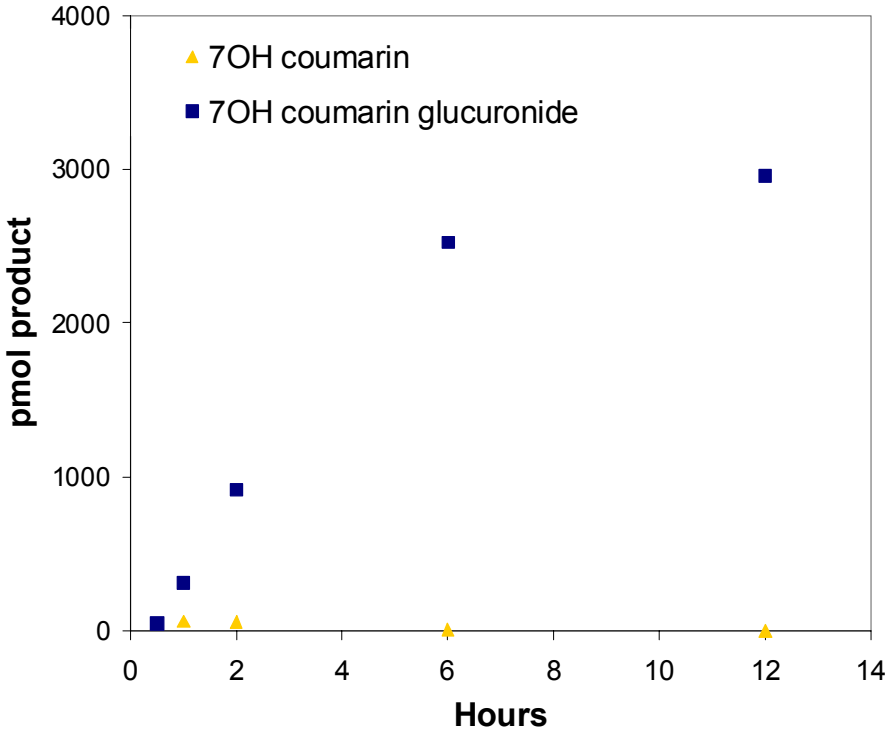

Figure 7-2. Primary human hepatocytes were incubated with 2 µM coumarin. The products 7OH coumarin and its *O*-glucuronide were quantified by fluorescence HPLC. Pmol product formed represents the mean product formation per incubation with ~$1x10^6$ cells (n=2-5 donors per time point).

7.3.2 ^{3}H-NNK metabolism by hepatocyte cultures

Primary human hepatocytes were incubated with 1 or 10 μM ^{3}H-NNK and metabolites were analyzed by radioflow HPLC (Figure 7-3). NNAL was the earliest detected and most abundant metabolite, present at levels greater than 80% of total metabolism at 24 hours. NNAL was further metabolized by glucuronidation and α-hydroxylation at a mean ratio of 1.3:1 respectively, and the products of each pathway accumulated to 1-10% of total metabolism (Table 7-1). Significant NNK α-hydroxylation was not observed. Also, there was no evidence of appreciable *N*-oxidation.

7.3.3 Coumarin metabolism by mixed or co-expressed P450 enzyme and UGTs

When P450 enzyme was co-incubated or co-expressed with UGT enzyme, coumarin was rapidly hydroxylated and glucuronidated to 7-hydroxycoumarin glucuronide (Figure 7-3). For instance, when purified P450 2A6 was incubated with UGT1A9 cell lysate and 5 μM coumarin, 7-hydroxycoumarin glucuronide was detected within 1 minute of incubation. Human liver microsomes had substantially higher glucuronidation activity. Co-expressed incubations had the lowest hydroxylation and glucuronidation activity.

Figure 7-3. ^{3}H-NNK metabolism by primary hepatocytes

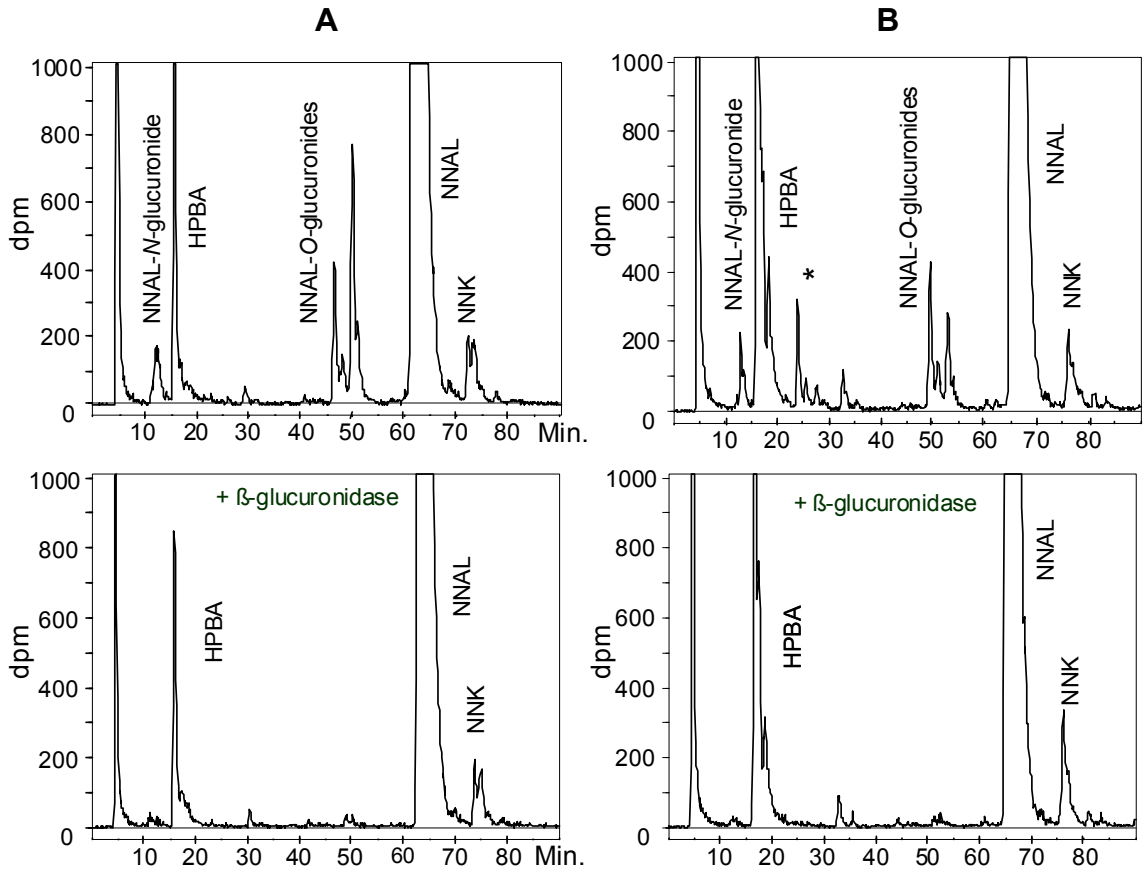

Figure 7-3. Human hepatocytes were incubated with 1 or 10 µM ^{3}H-NNK and media was removed at 6, 12, and 24 hours for analysis by radioflow HPLC. Represenative HPLC analyses of media at 24 hours, 1µM ^{3}H-NNK, are presented. * Unidentified peaks that disappear with β-glucuronidase treatment.

Table 7-1. Product ratios from 3H-NNK metabolism by human hepatocytes

Metabolism Product Ratios	Mean (n = 8)	Range
Glucuronidation : Hydroxylation	1.3	0.3 – 1.8
NNAL-*O*-gluc : NNAL-*N*-gluc	4.2	1.0 – 7.7
(S)-NNAL-*O*-gluc : (*R*)-NNAL-*O*-gluc	2.2	0.7 – 2.9

Figure 7-4. Coumarin metabolism by mixed P450 and UGT

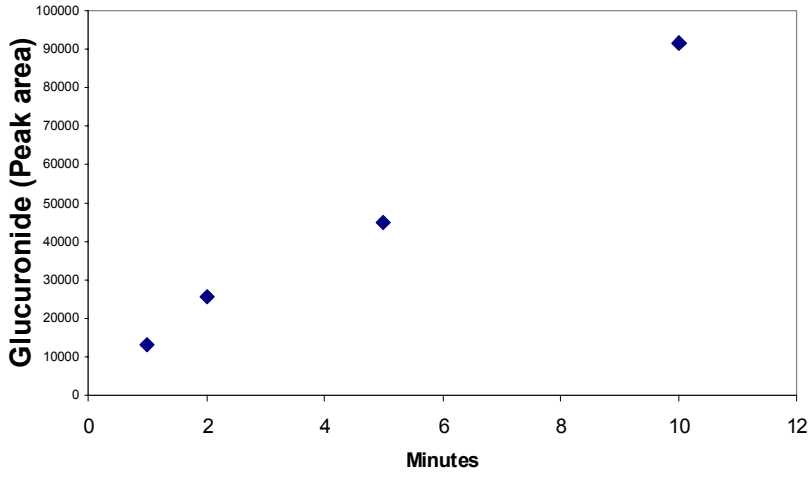

Figure 7-4. Purified P450 2A6 was incubated with lysate from HEK cells expressing UGT1A9 and 5 μM coumarin in the prescence of NADPH and UDPGA (2 mM). Coumarin was rapidly hydroxylated and glucuronidated to 7OH coumarin glucuronide.

The glucuronide product was detected directly by fluorescence HPLC (λ_{ex}= 320, λ_{em}= 375).

7.3.4 Nitrosamine metabolism by mixed P450 2A13 and UGT2B7 or HLMs

Glucuronide metabolites were detected following co-incubation of P450s and UGTs with ^{3}H-NNAL, ^{3}H-HPB, or ^{3}H-NNK. In the absence of NADPH generating system, but with UDPGA, ^{3}H-NNAL O-glucuronide and ^{3}H-HPB glucuronide were observed; no glucuronide metabolite of ^{3}H-NNK was detected. β-glucuronidase treatment released the starting substrate. In the presence of NADPH generating system and no UDPGA cosubstrate, α-hydroxylation products of ^{3}H-NNAL and ^{3}H-NNK were detected in the usual amount and distribution. However, in the presence of NADPH and UDPGA a new product peak is formed when P450 2A13 is co-incubated with UGT2B7, UGT1A9, or human liver microsomes (Figure 7-5). In addition, another product peak co-elutes with OPBA. β-glucuronidase treatment results in a decrease but not disappearance of the peak that eluted at 41 minutes. An increase in ^{3}H-HPB is observed when the reaction mix from an incubation with ^{3}H-NNK is treated with β-glucuronidase (Figure 7-6). The formation of NNAL *O*-glucuronide and HPB *O*-glucuronide has been confirmed by analysis of the reaction mix by LC/MS. No α-hyroxymethyl NNK glucuronide was detected in one reaction mix that was analyzed by LC/MS. Collected product has not been analyzed by LC/MS.

Figure 7-5. ^{3}H-NNAL and ^{3}H-NNK metabolism by mixed P450 2A13 and UGT2B7

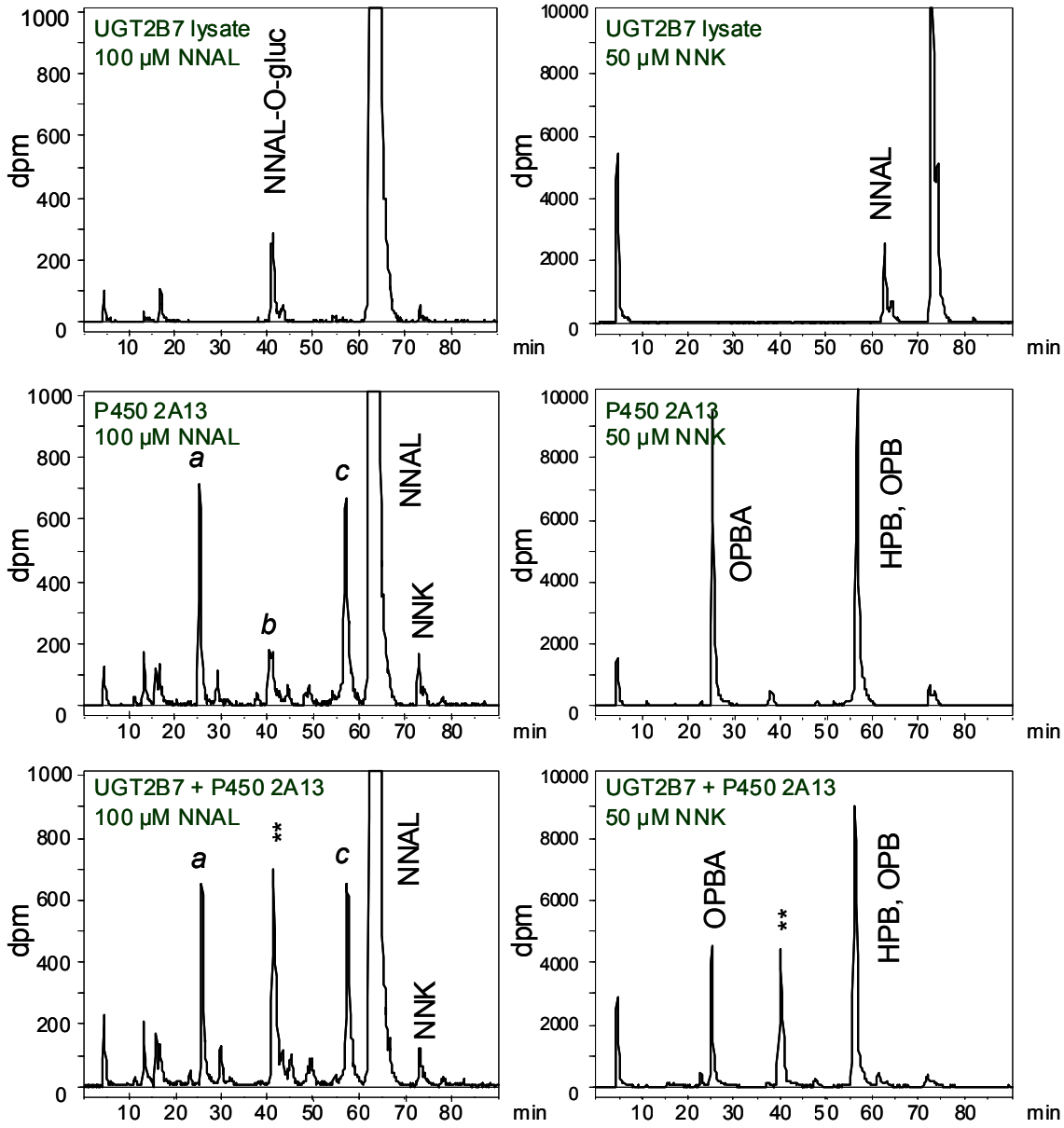

Figure 7-3. Purified P450 2A13 and lysate of HEK cells expressing UGT2B7 were incubated with ^{3}H-NNAL (generated from 3H-NNK with human liver cytosol) or ^{3}H-

NNK in the presence of NADPH and UDPGA (2.5 mM). Co-elution of metabolite peaks with authentic standards: *a*. OPBA, *b*. diol (an NNAL hydroxylation product), *c*. HPB, OPB, lactol (an NNAL hydroxylation product). ** A peak that is generated only in the presence of P450 2A13 and UGT2B7.

Figure 7-6. Detection of an HPB-releasing glucuronide

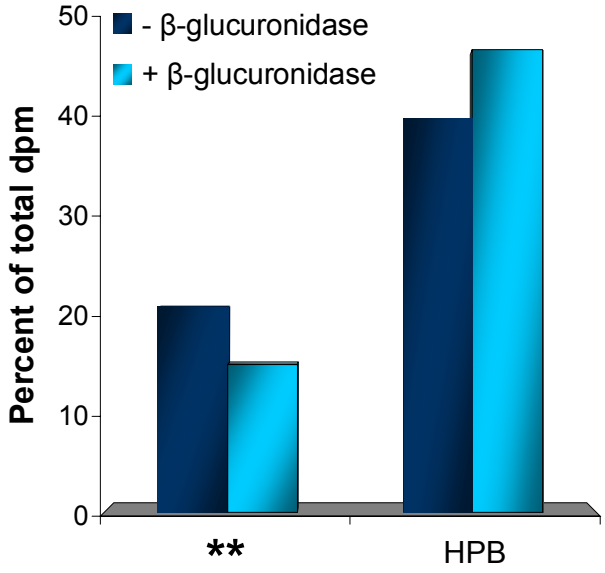

Figure 7-6. β-glucuronidase treatment of the reaction of ^{3}H-NNK incubated with mixed P450 2A13 and UGT2B7 resulted in a 6 % total dpm decrease in the unknown peak and a 7 % total dpm increase in the peak that co-eluted with HPB, which would be consistent with a glucuronide metabolite that is formed only when ^{3}H-NNK is hydroxylated.

7.4 Discussion

Primary human hepatocytes formed both *N*- and *O*-linked glucuronides of the NNK metabolite, NNAL. This is constent with data from incubations with human liver microsomes and the detection of both glucuronides in the urine of smokers. We predicted the distribution of (S)-NNAL glucuronide to (R)-NNAL glucuronide based on the retention time of metabolites compared to standard. Confirming the identity of these enantiomers and the distribution of (S)- and (R-) NNAL formed from NNK carbonyl reduction would be interesting as (S)-NNAL is more carcinogenic in laboratory animals.

NNAL was the predominant metabolite of NNK. Compared to incubations with rat primary hepatocytes, we observed less total α-hydroxylation and glucuronidation. It is unclear how experimental conditions directly or indirectly (e.g. dexamethasone,) influenced the metabolism of NNK. The viability of the hepatocyte cultures was varied, though a few cultures had > 80 % viability at 24 hours. Differences in expression of carbonyl reductases and transporters may have contributed to the observed difference between rat and human hepatocytes. In regards to α-hydroxylation, the P450s in human liver that can catalyze NNK and NNAL α-hydroxylation are quite inefficient. However, in human smokers who received deuterated NNK, α-hydroxylation products account for more than 80 % of total metabolites excreted in urine. The relative contribution of

hepatic and extrahepatic (e.g. P450 2A13-catalyzed) enzymes to *in vivo* NNK metabolism is unknown.

Co-incubation of P450s and UGTs is a useful system to evaluate two-step metabolism by P450s and UGTs. We observed rapid hydroxylation and glucuronidation of coumarin even at low substrate concentration (5 μM). Starting from NNK, we were able to detect HPB-glucuronide in reactions where P450 2A13 was co-incubated with UGT2B7, UGT1A9, or human liver microsomes. This experimental approach will be used to generate the unstable subtrate, α-hydroxymethyl NNK, with the potential for rapid glucuronidation by UGTs present in the reaction mix. Unfortunately, the activity of co-expressed P450 and UGT in HEK cells is low. Finel *et al.* reported 100-fold lower product formation by HEK-expressed UGTs compared to HLMs. Therefore, a comparison of inividual UGTs as potential catalysts of α-hydroxymethyl NNK glucuronide formation will be challenging and will require highly sensitive product detection.

7.5 Conclusion

A possible detoxification product of NNK in humans is α-hydroxymethyl NNK glucuronide, but this has not been demonstrated. Since the half-life of α-hydroxymethyl NNK is in the order of seconds it is a difficult to study the metabolism of this substrate. Primary human hepatocyte cultures are not a good *in vitro* system to study the potential metabolism of NNK to α-hydroxymethyl NNK glucuronide as little NNK α-

hydroxylation was observed. Co-incubation of P4502A13 and HLMs represents a promising approach to study *in vitro* glucuronide conjugation of α-hydroxymethyl NNK by human liver microsomes.

7.6 Acknowledgements

Many thanks to Dr. Stephen Hecht for kindly sharing cultures of primary human hepatocytes and NNK metabolites standards. Thanks also to the Blazer lab for allowing me to use their incubators for the primary human hepatocyte experiments.

CHAPTER 8

Concluding remarks

The goals of this thesis were to better understand the role of specific enzymes in nicotine and NNK metabolism, to consider metabolic flux through more than one enzymatic pathway, and to improve the scientific basis of using selected tobacco biomarkers. Towards these goals, the major findings achieved were:

(1) In P450 2A13, the most efficient human catalyst of NNK hydroxylation, we demonstrated that Asn297 influences the orientation of substrates that can form a hydrogen bond wth Asn297 in the active site, including NNK and coumarin. Mutation of Asn297 to Ala resulted in altered substrate binding, and in the case of coumarin, a shift in product distribution. In designing a P450 2A13 inhibitor, it may be useful to take advantage of this potential hydrogen bonding residue to facilitate orientation of the inhibitor in a desirable position.

(2) We identified that UGT2B10 contributes to *in vivo* nicotine metabolism, since individuals who were heterozygous for UGT2B10 Asp67Tyr, an allele previously

shown to decrease *in vitro* glucuronidation, had decreased excretion of nicotine and cotinine as their glucuronide conjugates in urine. Furthermore, the ratio of cotinine glucuronide to cotinine was a useful biomarker of glucuronidation phenotype. We established that this ratio should be adjusted for nicotine equivalents. Surprisingly, we observed that individuals who had the UGT2B10 Asp67Tyr allele had lower nicotine equivalents, which is an indication that this gene influences nicotine intake analogous to variation in CYP2A6, which catalyzes C-oxidation.

(3) In two studies of nicotine metabolism, focusing on the effect of ethnicity or UGT2B10 genotype, we found that nicotine equivalents is a superior biomarker of tobacco exposure than cotinine, as it is less sensitive to variation in individual metabolic pathways. Nicotine equivalents are also a reasonable biomarker from a cost and time standpoint, as advancements in LC/MS permit rapid and high throughput quantification. As a biomarker, nicotine equivalents could provide a useful estimate of typical daily tobacco exposure, which is critical for many cancer epidemiology and etiology studies.

Variation in the metabolism of nicotine may influence smoking and consequently exposure to the tobacco carcinogen NNK (Figure 8-1). Risk of lung cancer is likely affected not only by cummulative NNK exposure but also by the relative contribution of activation and detoxification to total metabolism. An important gap is whether or not an α-hydroxyNNK-linked glucuronide is formed in humans as it is in rats. Overall, the majority of smokers will not develop lung cancer, but it would be useful to identify smokers that are at high risk so that more intensive smoking cessation interventions,

chemoprevention, and lung cancer screening could be targeted to this group. A prospective study could address the utility of such an approach, wherein smokers would be characterized by nicotine and NNK metabolism by phenotype and selected genotypes. Enzyme induction and inhibition may also influence level of smoking or cancer risk, and understanding the mechanisms of induction and inhibition could be applied to developing chemopreventive and smoking cessation pharmaceuticals.

Figure 8-1. The influence of nicotine and NNK on lung cancer risk

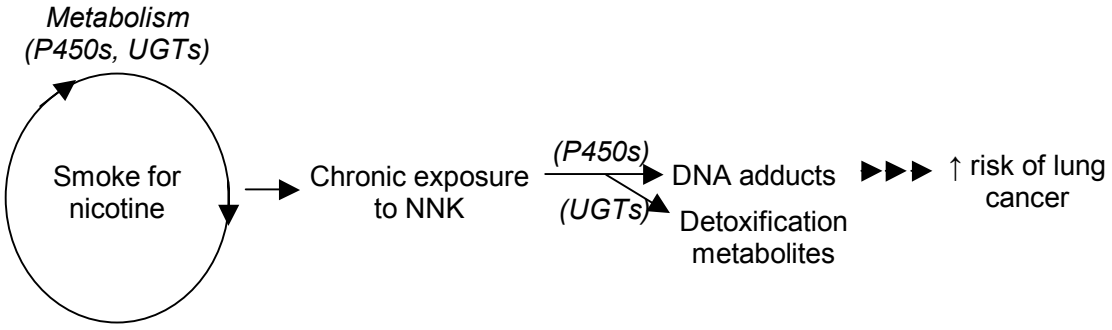

A number of genetic factors that have not been identified yet likely contribute to variation in nicotine intake, and a broader view should be adopted to identify involved genes. To date polymorphisms in CYP2A6, the nicotinic acetylcholine receptor A subunits 3 and 5 (CHRNA3 andCHRNA5), and now UGT2B10 have been linked to variation in nicotine intake. Beyond genes directly connected to nicotine, variation may be due to differences in transcription factors, translational control proteins, and other regulatory proteins. Progress in identifying such genes may result either from large

genome surveys of smokers or initially from a basic science approach (e.g. *in vitro* systems like hepatocyte cultures, or animal models).

In the past, an important application of quantifying nicotine and NNK metabolites was to demonstrate exposure in smokers and secondhand exposure in nonsmokers to promote anti-smoking public health policies. In the future, knowledge of nicotine and NNK metabolism could be increasingly employed to design other effective smoking cessation and chemoprevention strategies.

References

(1) [Anon]. WHO report on the global tobacco epidemic, 2008: The MPOWER package. Population and Development Review 2008; 34(3):581.

(2) CDC. The health consequences of smoking: a report of the Surgeon General. 2004. Atlanta, US Department of Health and Human Services.

(3) Centers for Disease Control. The Health Benefits of Smoking Cessation. 1990. Atlanta, GA, US Department of Health and Human Services.

(4) Miller M. NCI monograph links secondhand smoke to cancer and other diseases. J Natl Cancer Inst 2000; 92(1):14.

(5) International Agency for Research on Cancer. Tobacco Smoke and Involuntary Smoking. IARC Monographs on the Evaluation of Carcinogenic Risks to Humans. Lyon, FR: IARC, 2004: 1179-1187.

(6) McCay J, Ericksen M. The Tobacco Atlas. Geneva: World Health Organization, 2002.

(7) Centers for Disease Control. Behavioral Risk Factor Surveillance System (BRFSS): Prevalence of tobacco use. 2008. US Department of Health and Human Services.

(8) [Anon]. Cigarette use among high school students - United Sstates, 1991-2007 (Reprinted from MMWR, vol 57, pg 686-688, 2008). Jama-Journal of the American Medical Association 2008; 300(11):1292-1293.

(9) Messer K, Trinidad DR, Al Delaimy WK, Pierce JP. Smoking cessation rates in the United States: A comparison of young adult and older smokers. Am J Public Health 2008; 98(2):317-322.

(10) Centers for Disease Control. Cigarette smoking among adults--United States, 2002. MMWR Morb Mortal Wkly Rep 2004; 53(20):427-431.

(11) Centers for Disease Control. 1994 Surgeon General's Report—Preventing Tobacco Use Among Young People. Atlanta: US Department of Health and Human Services, 1994.

(12) Steinberg MB, Schmelzer AC, Richardson DL, Foulds J. The case for treating tobacco dependence as a chronic disease. Ann Intern Med 2008; 148(7):554-556.

(13) International Agency for Research on Cancer. IARC Monographs on the Evaluation of the Carcinogenic Risk of Chemicals to Humans: Tobacco Smoke and involuntary smoking. Lyon: World health Organization, 2002.

(14) Hecht SS. Tobacco carcinogens, their biomarkers, and tobacco-induced cancer. Nature Rev Cancer 2003; 3:733-744.

(15) Jemal A, Thun MJ, Ries LAG, Howe HL, Weir HK, Center MM et al. Annual Report to the Nation on the Status of Cancer, 1975-2005, Featuring Trends in Lung Cancer, Tobacco Use, and Tobacco Control. Journal of the National Cancer Institute 2008; 100(23):1672-1694.

(16) Thun MJ, Henley SJ, Calle EE. Tobacco use and cancer: an epidemiologic perspective for geneticists. Oncogene 2002; 21(48):7307-7325.

(17) Crispo A, Brennan P, Jockel KH, Schaffrath-Rosario A, Wichmann HE, Nyberg F et al. The cumulative risk of lung cancer among current, ex- and never-smokers in European men. Br J Cancer 2004; 91(7):1280-1286.

(18) Gallup AM, Newport F. U.S. smoking habits have come a long way. The Gallup Poll: public opinion 2004. Rowman & Littlefield, 2006, 2004: 417.

(19) Hoffman D, Hoffman I. Chemistry and Toxicology. Cigars: Health Effects and Trends. NCI Tobacco Control Monograph 9. National Cancer Institute, 1998: 55-104.

(20) Department of Health and Human Service US. The health consequences of smoking: nicotine addiction. Washington, DC: Government Printing Office, 1988.

(21) Picciotto MR. Common aspects of the action of nicotine and other drugs of abuse. Drug Alcohol Depend 1998; 51(1-2):165-172.

(22) Henningfield JE, Miyasato K, Jasinski DR. Cigarette Smokers Self-Administer Intravenous Nicotine. Pharmacology Biochemistry and Behavior 1983; 19(5):887-890.

(23) Ashton H, Stepney R, Thompson JW. Self-Titration by Cigarette Smokers. British Medical Journal 1979; 2(6186):357-360.

(24) Djordjevic MV, Hoffmann D, Hoffmann I. Nicotine regulates smoking patterns. Prev Med 1997; 26(4):435-440.

(25) Benowitz NL, Dains KM, Hall SM, Stewart S, Wilson M, Dempsey D et al. Progressive Commercial Cigarette Yield Reduction: Biochemical Exposure and Behavioral Assessment. Cancer Epidemiol Biomarkers Prev 2009; 18(3):876-883.

(26) Fiore MC, Bailey MC, Cohen SJ. Treating Tobacco Use and Depedence. Clinical Practice Guideline. Rockville, MD: U.S. Department of Health and Human Services, Public Health Service, 2003.

(27) Benowitz NL. Clinical pharmacology of inhaled drugs of abuse: implications in understanding nicotine dependence. Research findings on smoking of abused substances. [99], 12-29. 1990. Washington, DC, Superintendent of Documents. NIDA Research Monograph. Chiang, C. N. and Hawke, R. L.

(28) Laviolette SR, van der KD. The neurobiology of nicotine addiction: bridging the gap from molecules to behaviour. Nat Rev Neurosci 2004; 5(1):55-65.

(29) Benowitz NL. Nicotine pharmacology and addiction. In: Benowitz NL, editor. Nicotine Safety and Toxicity. New york: Oxford University Press, 1998: 3-16.

(30) Benowitz NL. The human pharmacology of nicotine. Research Advances in Alcohol Drug Problems 1986; 9:1-52.

(31) Gervot L, Rochat B, Gautier JC, Bohnenstengel F, Kroemer H, de B, V et al. Human CYP2B6: expression, inducibility and catalytic activities. Pharmacogenetics 1999; 9(3):295-306.

(32) Benowitz NL, Jacob P, III, Fong I, Gupta S. Nicotine metabolic profile in man: comparison of cigarette smoking and transdermal nicotine. J Pharmacol Exp Ther 1994; 268:296-303.

(33) Benowitz NL, Perez-Stable EJ, Herrera B, Jacob P, III. Slower metabolism and reduced intake of nicotine from cigarette smoking in Chinese-Americans. J Natl Cancer Inst 2002; 94(2):108-115.

(34) Jalas JR, Hecht SS, Murphy SE. Cytochrome P450 enzymes as catalysts of metabolism of 4-(methylnitrosamino)-1-(3-pyridyl)-1-butanone (NNK), a tobacco-specific carcinogen. Chem Res Toxicol 2005; 18:95-110.

(35) Hecht SS. Biochemistry, biology, and carcinogenicity of tobacco-specific *N*-nitrosamines. Chem Res Toxicol 1998; 11:559-603.

(36) Anderson KE, Kliris J, Murphy L, Carmella SG, Han S, Link C et al. Metabolites of a tobacco-specific lung carcinogen in nonsmoking casino patrons. Cancer Epidemiol Biomarkers Prev 2003; 12(12):1544-1546.

(37) Stepanov I, Hecht SS, Lindgren B, Jacob P, III, Wilson M, Benowitz NL. Relationship of human toenail nicotine, cotinine, and 4-(methylnitrosamino)-1-(3-pyridyl)-1-butanol to levels of these biomarkers in plasma and urine. Cancer Epidemiol Biomarkers Prev 2007; 16(7):1382-1386.

(38) Hecht SS, Carmella SG, Le KA, Murphy SE, Boettcher AJ, Le C et al. 4-(methylnitrosamino)-1-(3-pyridyl)-1-butanol and its glucuronides in the urine of infants exposed to environmental tobacco smoke. Cancer Epidemiol Biomarkers Prev 2006; 15(5):988-992.

(39) Hecht SS, Carmella SG, Chen M, Koch JFD, Miller AT, Murphy SE et al. Quantitation of urinary metabolites of a tobacco-specific lung carcinogen after smoking cessation. Cancer Res 1999; 59:590-596.

(40) Schloebe DHDREaTAR. Determination of tobacco specific nitrosamin hemoglobin and lung DNA adducts. Proc Am Assoc Cancer Res 2002; 43:346.

(41) Wagenknecht LE, Cutter GR, Haley NJ, Sidney S, Manolio TA, Hughes GH et al. Racial differences in serum cotinine levels among smokers in the Coronary Artery Risk Development in (Young) Adults study. Am J Public Health 1990; 80(9):1053-1056.

(42) Kreslake JM, Wayne GF, Alpert HR, Koh HK, Connolly GN. Tobacco industry control of menthol in cigarettes and targeting of adolescents and young adults. Am J Public Health 2008; 98(9):1685-1692.

(43) Landi MT, Zocchetti C, Bernucci I, Kadlubar FF, Tannenbaum S, Skipper P et al. Cytochrome P4501A2: Enzyme induction and genetic control in determining 4-aminobiphenyl-hemoglobin adduct levels. Cancer Epidemiol Biomarkers Prev 1996; 5(9):693-698.

(44) Khojasteh-Bakht SC, Koenigs LL, Peter RM, Trager WF, Nelson SD. (R)-(+)-Menthofuran is a potent, mechanism-based inactivator of human liver cytochrome P450 2A6. Drug Metab Dispos 1998; 26(7):701-704.

(45) von Weymarn LB, Brown KM, Murphy SE. Inactivation of CYP2A6 and CYP2A13 during nicotine metabolism. J Pharmacol Exp Ther 2006; 316:295-303.

(46) Hecht SS. Tobacco smoke carcinogens and lung cancer. J Natl Cancer Inst 1999; 91:1194-1210.

(47) Nebert DW, Russell DW. Clinical importance of the cytochromes P450. Lancet 2002; 360(9340):1155-1162.

(48) Guengerich FP. Common and uncommon cytochrome P450 reactions related to metabolism and chemical toxicity. Chem Res Toxicol 2001; 14(6):611-650.

(49) Lewis DFV, Watson E, Lake BG. Evolution of the cytochrome P450 superfamily: sequence alignments and pharmacogenetics. Mutat Res 1998; 410:245-270.

(50) Bair SR, Mellon SH. Deletion of the mouse P450c17 gene causes early embryonic lethality. Mol Cell Biol 2004; 24(12):5383-5390.

(51) Raunio H, Rautio A, Gullsten H, Pelkonen O. Polymorphisms of CYP2A6 and its practical consequences. Br J Clin Pharmacol 2001; 52(4):357-363.

(52) Nebert DW, Dalton TP. The role of cytochrome P450 enzymes in endogenous signalling pathways and environmental carcinogenesis. Nature Reviews Cancer 2006; 6(12):947-960.

(53) Nelson DR, Zeldin DC, Hoffman SM, Maltais LJ, Wain HM, Nebert DW. Comparison of cytochrome P450 (*CYP*) genes from the mouse and human genomes, including nomenclature recommendations for genes, pseudogenes and alternative-splice variants. Pharmacogenetics 2004; 14(1):1-18.

(54) Hoffman SM, Nelson DR, Keeney DS. Organization, structure and evolution of the CYP2 gene cluster on human chromosome 19. Pharmacogenetics 2001; 11(8):687-698.

(55) Guengerich FP. Human Cytochrome P450 Enzymes. In: Ortiz de Montellano PR, editor. Cytochrome P450: Structure, Mechanism, and Biochemistry. New York: Kluwer Academic/Plenum Publishers, 2005: 377-530.

(56) Tirona RG, Lee W, Leake BF, Lan LB, Cline CB, Lamba V et al. The orphan nuclear receptor HNF4alpha determines PXR- and CAR-mediated xenobiotic induction of CYP3A4. Nat Med 2003; 9(2):220-224.

(57) Finel M, Li X, Gardner-Stephen D, Bratton S, Mackenzie PI, Radominska-Pandya A. Human UDP-glucuronosyltransferase 1A5: identification, expression, and activity. J Pharmacol Exp Ther 2005; 315(3):1143-1149.

(58) Williams SN, Dunham E., and Bradfield C.A. Induction of cytochrome P450 enzymes. In: De Montellano PO, editor. Cytochrome P450 Structure, Mechanism, and Biochemistry. New York: Kluwer Academic, 2005: 323-346.

(59) Galijatovic A, Beaton D, Nguyen N, Chen S, Bonzo J, Johnson R et al. The human CYP1A1 gene is regulated in a developmental and tissue-specific fashion in transgenic mice. J Biol Chem 2004; 279(23):23969-23976.

(60) Evans WE, Relling MV. Pharmacogenomics: Translating functional genomics into rational therapeutics. Science 1999; 286(5439):487-491.

(61) Omura T, Sato R. The carbon monoxide-binding pigment of liver microsomes. I. evidence for its hemoprotein nature. J Biol Chem 1964; 239:2370-2378.

(62) Jefcoate CR. Measurement of substrate and inhibitor binding to microsomal cytochrome P450 by optical-difference spectroscopy. Methods Enzymol 1978; 52:258-279.

(63) Guengerich FP. Mechanisms of cytochrome p450 substrate oxidation: MiniReview. Journal of Biochemical and Molecular Toxicology 2007; 21(4):163-168.

(64) Isin EM, Guengerich FP. Complex reactions catalyzed by cytochrome P450 enzymes. Biochimica et Biophysica Acta-General Subjects 2007; 1770(3):314-329.

(65) Schenkman JB, Remmer H, Estabrook RW. Spectral studies of drug interaction with hepatic microsomal cytochrome. Mol Pharmacol 1967; 3(2):113-123.

(66) Yang ML, Kabulski JL, Wollenberg L, Chen XQ, Subramanian M, Tracy TS et al. Electrocatalytic Drug Metabolism by CYP2C9 Bonded to A Self-Assembled Monolayer-Modified Electrode. Drug Metab Dispos 2009; 37(4):892-899.

(67) Yun CH, Kim KH, Calcutt MW, Guengerich FP. Kinetic analysis of oxidation of coumarins by human cytochrome P450 2A6. J Biol Chem 2005; 280(13):12279-12291.

(68) Isin EM, Guengerich FP. Kinetics and thermodynamics of ligand binding by cytochrome P450 3A4. J Biol Chem 2006; 281(14):9127-9136.

(69) Makris TM, Denisov I, Schlichting I, Sligar SG. Activation of molecular oxygen by cytochrome P450. In: De Montellano PO, editor. Cytochrome P450: Structure, Mechanism, and Biochemistry. New York: Kluwer Academic/Plenum Publishers, 2005: 149-182.

(70) Groves JT. Models and mechanisms of cytochrome P450 action. In: De Montellano PO, editor. Cytochrome P450: Structure, Mechanism, and Biochemistry. New York: Kluwer Academic/Plenum Publishers, 2005: 1-43.

(71) Bock KW. Vertebrate UDP-glucuronosyltransferases: functional and evolutionary aspects. Biochem Pharmacol 2003; 66(5):691-696.

(72) Campbell JA, Davies GJ, Bulone V, Henrissat B. A classification of nucleotide-diphospho-sugar glycosyltransferases based on amino acid sequence similarities. Biochem J 1997; 326:929-939.

(73) Mackenzie PI, Walter BK, Burchell B, Guillemette C, Ikushiro S, Iyanagi T et al. Nomenclature update for the mammalian UDP glycosyltransferase (UGT) gene superfamily. Pharmacogenet Genomics 2005; 15(10):677-685.

(74) Coutinho PM, Deleury E, Davies GJ, Henrissat B. An evolving hierarchical family classification for glycosyltransferases. J Mol Biol 2003; 328(2):307-317.

(75) Gong QH, Cho JW, Huang T, Potter C, Gholami N, Basu NK et al. Thirteen UDPglucuronosyltransferase genes are encoded at the human *UGT1* gene complex locus. Pharmacogenetics 2001; 11(4):357-368.

(76) Miley MJ, Zielinska AK, Keenan JE, Bratton SM, Radominska-Pandya A, Redinbo MR. Crystal structure of the cofactor-binding domain of the human phase II drug-metabolism enzyme UDP-glucuronosyltransferase 2B7. J Mol Biol 2007; 369(2):498-511.

(77) Luukkanen L, Taskinen J, Kurkela M, Kostiainen R, Hirvonen J, Finel M. Kinetic characterization of the 1A subfamily of recombinant human UDP-glucuronosyltransferases. Drug Metab Dispos 2005; 33(7):1017-1026.

(78) King CD, Rios GR, Green MD, Tephly TR. UDP-glucuronosyltransferases. Curr Drug Metab 2000; 1(2):143-161.

(79) Guillemette C. Pharmacogenomics of human UDP-glucuronosyltransferase enzymes. Pharmacogenomics J 2003; 3(3):136-158.

(80) Guengerich FP. Cytochrome P450S and other enzymes in drug metabolism and toxicity. AAPS J 2006; 8(220905):E101-E111.

(81) Tukey RH, Strassburg CP. Human UDP-glucuronosyltransferases: Metabolism, expression, and disease. Annu Rev Pharmacol Toxicol 2000; 40:581-616.

(82) Kiang TK, Ensom MH, Chang TK. UDP-glucuronosyltransferases and clinical drug-drug interactions. Pharmacol Ther 2005; 106(1):97-132.

(83) Radominska-Pandya A, Czernik PJ, Little JM, Battaglia E, Mackenzie PI. Structural and functional studies of UDP-glucuronosyltransferases. Drug Metab Rev 1999; 31(4):817-899.

(84) Patana AS, Kurkela M, Finel M, Goldman A. Mutation analysis in UGT1A9 suggests a relationship between substrate and catalytic residues in UDP-glucuronosyltransferases. Protein Engineering Design & Selection 2008; 21(9):537-543.

(85) Ouzzine M, Magdalou J, Burchell B, Fournel-Gigleux S. An internal signal sequence mediates the targeting and retention of the human UDP-glucuronosyltransferase 1A6 to the endoplasmic reticulum. J Biol Chem 1999; 274(44):31401-31409.

(86) Kurkela M, Morsky S, Hirvonen J, Kostiainen R, Finel M. An active and water-soluble truncation mutant of the human UDP-glucuronosyltransferase 1A9. Mol Pharmacol 2004; 65(4):826-831.

(87) Kaivosaari S, Toivonen P, Hesse LM, Koskinen M, Court MH, Finel M. Nicotine Glucuronidation and the Human UDP-Glucuronosyltransferase UGT2B10. Mol Pharmacol 2007; 72(3):761-768.

(88) Nakajima M, Yokoi T. Interindividual variability in nicotine metabolism: C-oxidation and glucuronidation. Drug Metab Pharmacokinet 2005; 20(4):227-235.

(89) Mitchell SC. Flavin mono-oxygenase (FMO) - The 'other' oxidase. CURRENT DRUG METABOLISM 2008; 9(4):280-284.

(90) Phillips IR, Shephard EA. Flavin-containing monooxygenases: mutations, disease and drug response. Trends Pharmacol Sci 2008; 29(6):294-301.

(91) Ziegler DM. An overview of the mechanism, substrate specificities, and structure of FMOs. Drug Metab Rev 2002; 34(3):503-511.

(92) Cashman JR, Zhang J. Human flavin-containing monooxygenases. Annu Rev Pharmacol Toxicol 2006; 46:65-100.

(93) Jones KC, Ballou DP. Reactions of the 4A-Hydroperoxide of Liver Microsomal Flavin-Containing Monooxygenase with Nucleophilic and Electrophilic Substrates. J Biol Chem 1986; 261(6):2553-2559.

(94) Kim YM, Ziegler DM. Size limits of thiocarbamides accepted as substrates by human flavin-containing monooxygenase 1. Drug Metab Dispos 2000; 28(8):1003-1006.

(95) Cashman JR. Some distinctions between flavin-containing and cytochrome P450 monooxygenases. Biochem Biophys Res Commun 2005; 338(1):599-604.

(96) Krueger SK, Williams DE. Mammalian flavin-containing monooxygenases: structure/function, genetic polymorphisms and role in drug metabolism. Pharmacol Ther 2005; 106(3):357-387.

(97) Kitchell BB, Rauckman EJ, Rosen GM. Effect of Temperature on Mixed-Function Amine Oxidase Intrinsic Fluorescence and Oxidative Activity. Mol Pharmacol 1978; 14(6):1092-1098.

(98) Senekeo-Effenberger K, Chen S, Brace-Sinnokrak E, Bonzo JA, Yueh MF, Argikar U et al. Expression of the human UGT1 locus in transgenic mice by 4-chloro-6-(2,3-xylidino)-2-pyrimidinylthioacetic acid (WY-14643) and implications on drug metabolism through peroxisome proliferator-activated receptor alpha activation. Drug Metab Dispos 2007; 35(3):419-427.

(99) Yueh MF, Bonzo JA, Tukey RH. The role of Ah receptor in induction of human UDP-glucuronosyltransferase 1A1. Methods Enzymol 2005; 400:75-91.

(100) Machemer DE, Tukey RH. The role of protein kinase C in regulation of TCDD-mediated CYP1A1 gene expression. Toxicol Sci 2005; 87(1):27-37.

(101) Gardner-Stephen D, Heydel JM, Goyal A, Lu Y, Xie W, Lindblom T et al. Human PXR variants and their differential effects on the regulation of human UDP-glucuronosyltransferase gene expression. Drug Metab Dispos 2004; 32(3):340-347.

(102) Arpiainen S, Raffalli-Mathieu F, Lang MA, Pelkonen O, Hakkola J. Regulation of the Cyp2a5 gene involves an aryl hydrocarbon receptor-dependent pathway. Mol Pharmacol 2005; 67(4):1325-1333.

(103) Kim JH, Sherman ME, Curriero FC, Guengerich FP, Strickland PT, Sutter TR. Expression of cytochromes P450 1A1 and 1B1 in human lung from smokers, non-smokers, and ex-smokers. Toxicol Appl Pharmacol 2004; 199(3):210-219.

(104) Haiman CA, Stram DO, Wilkens LR, Pike MC, Kolonel LN, Henderson BE et al. Ethnic and racial differences in the smoking-related risk of lung cancer. N Engl J Med 2006; 354(4):333-342.

(105) Stellman SD, Chen Y, Muscat JE, Djordjevic MV, Richie JP, Jr., Lazarus P et al. Lung cancer risk in white and black Americans. Ann Epidemiol 2003; 13(4):294-302.

(106) Caraballo RS, Giovino GA, Pechacek TF, Mowery PD, Richter PA, Strauss WJ et al. Racial and ethnic differences in serum cotinine levels of cigarette smokers - Third National Health and Nutrition Examination Survey, 1988-1991. J Am Med Assoc 1998; 280(2):135-139.

(107) Perez-Stable EJ, Herrera B, Jacob P, III, Benowitz NL. Nicotine metabolism and intake in black and white smokers. JAMA 1998; 280(2):152-156.

(108) Kandel DB, Hu MC, Schaffran C, Udry JR, Benowitz NL. Urine nicotine metabolites and smoking behavior in a multiracial/multiethnic national sample of young adults. Am J Epidemiol 2007; 165(8):901-910.

(109) Pirkle JL, Flegal KM, Bernert JT, Brody DJ, Etzel RA, Maurer KR. Exposure of the US population to environmental tobacco smoke: the Third National Health

and Nutrition Examination Survey, 1988 to 1991. JAMA 1996; 275(16):1233-1240.

(110) Cashman JR, Park SB, Yang ZC, Wrighton SA, Jacob P, III, Benowitz NL. Metabolism of nicotine by human liver microsomes: stereoselective formation of *trans*-nicotine *N*'-oxide. Chem Res Toxicol 1992; 5:639-646.

(111) Byrd GD, Chang KM, Greene JM, deBethizy JD. Evidence for urinary excretion of glucuronide conjugates of nicotine, cotinine, and *trans*-3'-hydroxycotinine in smokers. Drug Metab Dispos 1992; 20:192-197.

(112) Murphy SE, Link CA, Jensen J, Le C, Puumala S, Hecht SS et al. A comparison of urinary biomarkers of tobacco and carcinogen exposure in smokers. Cancer Epidemiol Biomarkers Prev 2004; 13:1617-1623.

(113) Benowitz NL, Kuyt F, Jacob P, III, Jones RT, Osman AL. Cotinine disposition and effects. Clin Pharmacol Ther 1983; 34:604-611.

(114) Davis RA, Curvall M. Determination of nicotine and its metabolites in biological fluids:*in vivo* studies. In: Gorrod JW, Jacob P, III, editors. Analytical Determination of Nicotine and Related Compounds and Their Metabolites. Amsterdam: Elsevier Science, 1999: 583-643.

(115) Benowitz NL, Swan GE, Jacob P, III, Lessov-Schlaggar CN, Tyndale RF. CYP2A6 genotype and the metabolism and disposition kinetics of nicotine. Clin Pharmacol Ther 2006; 80(5):457-467.

(116) Siegmund B, Leitner E, Pfannhauser W. Determination of the nicotine content of various edible nightshades (Solanaceae) and their products and estimation of the associated dietary nicotine intake. J Agric Food Chem 1999; 47(8):3113-3120.

(117) Benowitz NL. Cotinine as a biomarker of environmental tobacco smoke exposure. Epidemiol Rev 1996; 18:188-204.

(118) Yamanaka H, Nakajima M, Nishimura K, Yoshida R, Fukami T, Katoh M et al. Metabolic profile of nicotine in subjects whose CYP2A6 gene is deleted. Eur J Pharm Sci 2004; 22(5):419-425.

(119) Meger M, Meger-Kossien I, Schuler-Metz A, Janket D, Scherer G. Simultaneous determination of nicotine and eight nicotine metabolites in urine of smokers using liquid chromatography-tandem mass spectrometry. J Chromatogr B Analyt Technol Biomed Life Sci 2002; 778(1-2):251-261.

(120) Scherer G, Engl J, Urban M, Gilch G, Janket D, Riedel K. Relationship between machine-derived smoke yields and biomarkers in cigarette smokers in Germany. Regul Toxicol Pharmacol 2007; 47(2):171-183.

(121) Andersson G, Björnberg G, Curvali M. Oral mucosal changes and nicotine disposition in users of Swedish smokeless tobacco products: a comparative study. J Oral Pathol Med 1994; 23:161-167.

(122) Byrd GD, Robinson JH, Caldwell WS, deBethizy JD. Comparison of Measured and Ftc-Predicted Nicotine Uptake in Smokers. Psychopharmacology 1995; 122(2):95-103.

(123) Murphy SE, Raulinaitis V, Brown KM. Nicotine 5'-oxidation and methyl oxidation by P450 2A enzymes. Drug Metab Dispos 2005; 13:1166-1173.

(124) Murphy PJ. Enzymatic oxidation of nicotine to nicotine delta$^{1'(5')}$ iminium ion. J Biol Chem 1973; 248:2796-2800.

(125) Gorrod JW, Hibberd AR. The metabolism of nicotine-delta 1'(5')-iminium ion, *in vivo* and *in vitro*. Eur J Drug Metab Pharmacokinet 1982; 7:293-298.

(126) Kitagawa K, Kunugita N, Katoh T, Yang MH, Kawamoto T. The significance of the homozygous CYP2A6 deletion on nicotine metabolism: A new genotyping method of CYP2A6 using a single PCR-RFLP. Biochem Biophys Res Commun 1999; 262(1):146-151.

(127) Dicke K, Skrlin S, Murphy SE. Nicotine and 4-(methylnitrosamino)-1-(3-pyridyl)-butanone (NNK) metabolism by P450 2B6. Drug Metab Dispos 2005; 33:1760-1764.

(128) Wong HL, Zhang X, Zhang QY, Gu J, Ding X, Hecht SS et al. Metabolic activation of the tobacco carcinogen 4-(methylnitrosamino)-(3-pyridyl)-1-butanone by cytochrome p450 2A13 in human fetal nasal microsomes. Chem Res Toxicol 2005; 18:913-918.

(129) Zhang X, D'Agostino J, Wu H, Zhang QY, von Weymarn L, Murphy SE et al. CYP2A13: variable expression and role in human lung microsomal metabolic activation of the tobacco-specific carcinogen 4-(methylnitrosamino)-1-(3-pyridyl)-1-butanone. J Pharmacol Exp Ther 2007; 323(2):570-578.

(130) Neurath GB, Dunger M, Krenz O, Orth D, Pein FG. Trans-3'-hydroxycotinine - a main metabolite in smokers. Klin Wochenschr 1988; 66:2-4.

(131) Mwenifumbo JC, Sellers EM, Tyndale RF. Nicotine metabolism and CYP2A6 activity in a population of black African descent: impact of gender and light smoking. Drug Alcohol Depend 2007; 89(1):24-33.

(132) Le Marchand L, Derby KS, Murphy SE, Hecht SS, Hatsukami D, Carmella SG et al. Smokers with the CHRNA lung cancer-associated variants are exposed to higher levels of nicotine equivalents and a carcinogenic tobacco-specific nitrosamine. Cancer Res 2008; 68(22):9137-9140.

(133) Derby KS, Cuthrell K, Caberto C, Carmella SG, Franke AA, Hecht SS et al. Nicotine metabolism in three ethnic/racial groups with different risks of lung cancer. Cancer Epidemiol Biomarkers & Prev 2008; 17:3526-3535.

(134) Malaiyandi V, Lerman C, Benowitz NL, Jepson C, Patterson F, Tyndale RF. Impact of CYP2A6 genotype on pretreatment smoking behaviour and nicotine levels from and usage of nicotine replacement therapy. Mol Psychiatry 2006; 11(4):400-409.

(135) Benowitz NL, Pomerleau OF, Pomerleau CS, Jacob P, III. Nicotine metabolite ratio as a predictor of cigarette consumption. Nicotine Tob Res 2003; 5(5):621-624.

(136) Malaiyandi V, Sellers EM, Tyndale RF. Implications of CYP2A6 genetic variation for smoking behaviors and nicotine dependence. Clin Pharmacol Ther 2005; 77(3):145-158.

(137) Strasser AA, Malaiyandi V, Hoffmann E, Tyndale RF, Lerman C. An association of CYP2A6 genotype and smoking topography. Nicotine Tob Res 2007; 9(4):511-518.

(138) Mwenifumbo JC, Al Koudsi N, Ho MK, Zhou Q, Hoffmann EB, Sellers EM et al. Novel and established CYP2A6 alleles impair in vivo nicotine metabolism in a population of Black African descent. Hum Mutat 2008; 29(5):679-688.

(139) Benowitz NL, Jacob P, III, Sachs DP. Deficient C-oxidation of nicotine. Clin Pharmacol Ther 1995; 57(5):590-594.

(140) Nakajima M, Yamamoto T, Nunoya K, Yokoi T, Nagashima K, Inoue K et al. Role of human cytochrome P4502A6 in c-oxidation of nicotine. Drug Metab Dispos 1996; 24:1212-1217.

(141) Berkman CE, Park SB, Wrighton SA, Cashman JR. In vitro-in vivo correlations of human (S)-nicotine metabolism. Biochem Pharmacol 1995; 50(4):565-570.

(142) Brown KM, von Weymarn LB, Murphy SE. Identification of N-(hydroxymethyl)-norcotinine as a major product of cytochrome P450 2A6, but not cytochrome P450 2A13-catalyzed cotinine metabolism. Chem Res Toxicol 2005; 18:1792-1798.

(143) Chen G, Blevins-Primeau AS, Dellinger RW, Muscat JE, Lazarus P. Glucuronidation of nicotine and cotinine by UGT2B10: loss of function by the UGT2B10 Codon 67 (Asp>Tyr) polymorphism. Cancer Res 2007; 67(19):9024-9029.

(144) Kuehl GE, Murphy SE. *N*-Glucuronidation of t*rans*-3′-hydroxycotinine by human liver microsomes. Chem Res Toxicol 2003; 16:1502-1506.

(145) Benowitz NL, Perez-Stable EJ, Fong I, Modin G, Herrera B, Jacob P, III. Ethnic differences in N-glucuronidation of nicotine and cotinine. J Pharmacol Exp Ther 1999; 291(3):1196-1203.

(146) Yamano S, Tatsuno J, Gonzalez FJ. The CYP2A3 gene product catalyzes coumarin 7-hydroxylation in human liver microsomes. Biochemistry 1990; 29:1322-1329.

(147) Inoue K, Yamazaki H, Shimada T. CYP2A6 genetic polymorphisms and liver microsomal coumarin and nicotine oxidation activities in Japanese and Caucasians. Arch Toxicol 2000; 73(10-11):532-539.

(148) Hadidi H, Irshaid Y, Vagbo CB, Brunsvik A, Cholerton S, Zahlsen K et al. Variability of coumarin 7- and 3-hydroxylation in a Jordanian population is suggestive of a functional polymorphism in cytochrome P450 CYP2A6. European Journal of Clinical Pharmacoloy 1998; 54:437-441.

(149) Ho MK, Mwenifumbo JC, Zhao B, Gillam EM, Tyndale RF. A novel CYP2A6 allele, CYP2A6*23, impairs enzyme function in vitro and in vivo and decreases smoking in a population of Black-African descent. Pharmacogenet Genomics 2008; 18(1):67-75.

(150) Ho M, Mwenifumbo JC, Al Koudsi N, Okuyemi K, Ahluwalia J, Benowitz NL et al. Association of Nicotine Metabolite Ratio and CYP2A6 Genotype With Smoking Cessation Treatment in African-American Light Smokers. Clin Pharmacol Ther 2009.

(151) Mwenifumbo JC, Tyndale RF. Genetic variability in CYP2A6 and the pharmacokinetics of nicotine. Pharmacogenomics 2007; 8(10):1385-1402.

(152) Saeki M, Saito Y, Jinno H, Sai K, Hachisuka A, Kaniwa N et al. Genetic variations and haplotypes of UGT1A4 in a Japanese population. Drug Metab Pharmacokinet 2005; 20(2):144-151.

(153) Ehmer U, Vogel A, Schutte JK, Krone B, Manns MP, Strassburg CP. Variation of hepatic glucuronidation: Novel functional polymorphisms of the UDP-glucuronosyltransferase UGT1A4. Hepatology 2004; 39(4):970-977.

(154) Hecht SS, Carmella SG, Murphy SE. Effects of watercress consumption on urinary metabolites of nicotine in smokers. Cancer Epidemiol Biomarkers Prev 1999; 8:907-913.

(155) Gelal A, Jacob P, III, Yu L, Benowitz NL. Disposition kinetics and effects of menthol. Clin Pharmacol Ther 1999; 66(2):128-135.

(156) Swan GE, Lessov-Schlaggar CN, Bergen AW, He Y, Tyndale R, Benowitz NL. Genetic and environmental influences on the ratio of 3'hydroxycotinine to cotinine in plasma and urine. Pharmacogenetics 2009; 19(5):388-398.

(157) Benowitz NL, Bernert JT, Caraballo RS, Holiday DB, Wang J. Optimal serum cotinine levels for distinguishing cigarette smokers and nonsmokers within different racial/ethnic groups in the United States between 1999 and 2004. Am J Epidemiol 2009; 169(2):236-248.

(158) Benowitz NL. Pharmacology of Nicotine: Addiction, Smoking-Induced Disease, and Therapeutics. Annu Rev Pharmacol Toxicol 2009; 49:57-71.

(159) Hukkanen J, Jacob P, III, Benowitz NL. Metabolism and disposition kinetics of nicotine. Pharmacol Rev 2005; 57(1):79-115.

(160) Schoedel KA, Hoffmann EB, Rao Y, Sellers EM, Tyndale RF. Ethnic variation in CYP2A6 and association of genetically slow nicotine metabolism and smoking in adult Caucasians. Pharmacogenetics 2004; 14(9):615-626.

(161) Benowitz NL. Nicotine addiction. Prim Care 1999; 26(3):611-631.

(162) Caldwell WS, Greene JM, Byrd GD, Chang KM, Uhrig MS, deBethizy JD et al. Characterization of the glucuronide conjugate of cotinine: a previously unidentified major metabolite of nicotine in smokers' urine. Chem Res Toxicol 1992; 5:280-285.

(163) Kuehl GE, Murphy SE. *N*-Glucuronidation of Nicotine and Cotinine by human liver microsomes and Heterologously-Expressed UDP-glucuronosyltransferases. Drug Metab Dispos 2003; 31:1361-1368.

(164) Turgeon D, Chouinard S, Belanger P, Picard S, Labbe JF, Borgeat P et al. Glucuronidation of arachidonic and linoleic acid metabolites by human UDP-glucuronosyltransferases. J Lipid Res 2003; 44(6):1182-1191.

(165) Green MD, Tephly TR. Glucuronidation of amine substrates by purified and expressed UDP- glucuronosyltransferase proteins. Drug Metab Dispos 1998; 26:860-867.

(166) Kaivosaari S, Salonen JS, Taskinen J. *N*-Glucuronidation of some 4-arylalkyl-1*H*-imidazoles by rat, dog, and human liver microsomes. Drug Metab Dispos 2002; 30(3):295-300.

(167) Zenser TV, Lakshmi VM, Hsu FF, Davis BB. Metabolism of N-acetylbenzidine and initiation of bladder cancer. Mutat Res 2002; 506-507:29-40.

(168) Rowland A, Elliot DJ, Williams JA, Mackenzie PI, Dickinson RG, Miners JO. In vitro characterization of lamotrigine N2-glucuronidation and the lamotrigine-valproic acid interaction. Drug Metab Dispos 2006; 34(6):1055-1062.

(169) Staines AG, Coughtrie MWH, Burchell B. N-glucuronidation of carbamazepine in human tissues is mediated by UGT2B7. J Pharmacol Exp Ther 2004; 311(3):1131-1137.

(170) Omura K, Nakazawa T, Sato T, Iwanaga T, Nagata O. Characterization of N-glucuronidation of 4-(5-Pyridin-4-yl-1H[1,2,4]triazol-3-yl) pyridine-2-carbonitrile (FYX-051): A new xanthine oxidoreductase inhibitor. Drug Metab Dispos 2007; 35(12):2143-2148.

(171) Murphy SE, Kuehl GE. Nicotine, cotinine, and trans 3'-hydroxycotinine glucuronidation by UDP-glucuronosyltransferases 1A3, 1A4 and 1A9. 9th Annual Meeting of the Society for Research on Nicotine and Tobacco, New Orleans, Louisiana, February 19-22, 2003 2003.

(172) Jin CJ, Miners JO, Lillywhite KJ, Mackenzie PI. Cdna Cloning and Expression of 2 New Members of the Human Liver Udp-Glucuronosyltransferase-2B Subfamily. Biochem Biophys Res Commun 1993; 194(1):496-503.

(173) Girard H, Thibaudeau J, Court MH, Fortier LC, Villeneuve L, Carom P et al. UGT1A1 polymorphisms are important determinants of dietary carcinogen detoxification in the liver. Hepatology 2005; 42(2):448-457.

(174) Girard H, Levesque E, Bellemare J, Journault K, Caillier B, Guillemette C. Genetic diversity at the UGT1 locus is amplified by a novel 3' alternative splicing mechanism leading to nine additional UGT1A proteins that act as regulators of glucuronidation activity. Pharmacogenet Genomics 2007; 17(12):1077-1089.

(175) Mori A, Maruo Y, Iwai M, Sato H, Takeuchi Y. UDP-glucuronosyltransferase 1A4 polymorphisms in a Japanese population and kinetics of clozapine glucuronidation. Drug Metab Dispos 2005; 33(5):672-675.

(176) Wiener D, Fang JL, Dossett N, Lazarus P. Correlation between UDP-glucuronosyltransferase genotypes and 4-(methylnitrosamino)-1-(3-pyridyl)-1-butanone glucuronidation phenotype in human liver microsomes. Cancer Res 2004; 64(3):1190-1196.

(177) Chen G, Dellinger RW, Gallagher CJ, Sun D, Lazarus P. Identification of a prevalent functional missense polymorphism in the UGT2B10 gene and its association with UGT2B10 inactivation against tobacco-specific nitrosamines. Pharmacogenet Genomics 2008; 18(3):181-191.

(178) Hecht SS, Murphy SE, Carmella SG, Zimmerman CL, Losey L, Kramarczuk I et al. Effects of reduced cigarette smoking on the uptake of a tobacco-specific lung carcinogen. J Natl Cancer Inst 2004; 96(2):107-115.

(179) Fowler BA, Kleinow KM, Squibb KS, Lucier GW, Hayes WA. Organelles as Tools in Toxicology. In: A.Wallace Hayes, editor. Principles and Methods of Toxicology. New York: Raven Press, 1994: 1267-1268.

(180) Kaivosaari S, Toivonen P, Aitio O, Sipila J, Koskinen M, Salonen JS et al. Regio- and stereospecific N-glucuronidation of medetomidine: the differences between UDP glucuronosyltransferase (UGT) 1A4 and UGT2B10 account for the complex kinetics of human liver microsomes. Drug Metab Dispos 2008; 36(8):1529-1537.

(181) Lazarus P, Zheng Y, Aaron RE, Muscat JE, Wiener D. Genotype-phenotype correlation between the polymorphic UGT2B17 gene deletion and NNAL glucuronidation activities in human liver microsomes. Pharmacogenet Genomics 2005; 15(11):769-778.

(182) Boffetta P, Clark S, Shen M, Gislefoss R, Peto R, Andersen A. Serum cotinine level as predictor of lung cancer risk. Cancer Epidemiol Biomarkers Prev 2006; 15(6):1184-1188.

(183) Vaccarella S, Herrero R, Snijders PJF, Dai M, Thomas JO, Hieu NT et al. Smoking and human papillomavirus infection: pooled analysis of the International Agency for Research on Cancer HPV Prevalence Surveys. Int J Epidemiol 2008; 37(3):536-546.

(184) Nieters A, Rohrmann S, Becker N, Linseisen J, Ruediger T, Overvad K et al. Smoking and lymphoma risk in the european prospective investigation into cancer and nutrition. Am J Epidemiol 2008; 167(9):1081-1089.

(185) Benowitz NL. Biomarkers of environmental tobacco smoke exposure. Environ Health Perspect 1999; 107:349-355.

(186) Etter JF, Perneger TV. Measurement of self reported active exposure to cigarette smoke. J Epidemiol Community Health 2001; 55(9):674-680.

(187) Strasser AA, Pickworth WB, Patterson F, Lerman C. Smoking topography predicts abstinence following treatment with nicotine replacement therapy. Cancer Epidemiol Biomarkers Prev 2004; 13(11 Pt 1):1800-1804.

(188) Zinggeler J, Mason J, Hatsukami DK, Murphy SE. Variation in nicotine and cotinine N-glucuronidation among African American and Caucasians on the nicotine patch. J Pharmacol Exp Ther 2009.

(189) Ho MK, Tyndale RF. Overview of the pharmacogenomics of cigarette smoking. Pharmacogenomics Journal 2007; 7(2):81-98.

(190) Gu DF, Hinks LJ, Morton NE, Day IN. The use of long PCR to confirm three common alleles at the CYP2A6 locus and the relationship between genotype and smoking habit. Ann Hum Genet 2000; 64(Pt 5):383-390.

(191) Kiyotani K, Yamazaki H, Fujieda M, Iwano S, Matsumura K, Satarug S et al. Decreased coumarin 7-hydroxylase activities and CYP2A6 expression levels in humans caused by genetic polymorphism in CYP2A6 promoter region (CYP2A6*9). Pharmacogenetics 2003; 13(11):689-695.

(192) Haberl M, Anwald B, Klein K, Weil R, Fuss C, Gepdiremen A et al. Three haplotypes associated with CYP2A6 phenotypes in Caucasians. Pharmacogenet Genomics 2005; 15(9):609-624.

(193) Hecht SS. Cigarette smoking: cancer risks, carcinogens, and mechanisms. Langenbecks Archives of Surgery 2006; 391(6):603-613.

(194) Jalas JR, Ding X, Murphy SE. Comparative metabolism of the tobacco-specific nitrosamines 4-(methylnitrosamino)-1-(3-pyridyl)-1-butanone (NNK) and 4-(methylnitrosamino)-1-(3-pyridyl)-1-butanol (NNAL) by rat cytochrome P450 2A3 and human cytochrome P450 2A13. Drug Metabol Dispos 2003; 31:1199-1202.

(195) Upadhyaya P, Kalscheuer S, Hochalter B, Villalta PW, Hecht SS. Quantitation of pyridylhydroxybutyl-DNA adducts in liver and lung of F-344 rats treated with 4-(methylnitrosamino)-1-(3-pyridyl)-1-butanone and enantiomers of its metabolite 4-(methylnitrosamino)-1-(3-pyridyl)-1-butanol. Chem Res Toxicol 2008; in press.

(196) Hecht SS, Carmella SG, Stepanov I, Jensen J, Anderson A, Hatsukami DK. Metabolism of the tobacco-specific carcinogen 4-(methylnitrosamino)-1-(3-pyridyl)-1-butanone to its biomarker total NNAL in smokeless tobacco users. Cancer Epidemiol Biomarkers Prev 2008; 17(3):732-735.

(197) Tulunay OE, Hecht SS, Carmella SG, Zhang Y, Lemmonds C, Murphy S et al. Urinary metabolites of a tobacco-specific lung carcinogen in nonsmoking hospitality workers. Cancer Epidemiol Biomarkers Prev 2005; 14(5):1283-1286.

(198) Stepanov I, Upadhyaya P, Feuer R, Jensen J, Hatsukami DK, Hecht SS. Extensive metabolic activation of the tobacco-specific carcinogen 4-(methylnitrosamino)-1-(3-pyridyl)-1-butanone in smokers. Cancer Epidemiol Biomarkers & Prev 2008; submitted.

(199) Murphy SE, Palomino A, Hecht SS, Hoffmann D. Dose-response study of DNA and hemoglobin adduct formation by 4-(methylnitrosamino)-1-(3-pyridyl)-1-butanone in F344 rats. Cancer Res 1990; 50:5446-5452.

(200) Murphy SE, Nunes MG, Hatala MA. Effects of phenobarbital and 3-methylcholanthrene induction on the formation of three glucuronide metabolites of 4-(methylnitrosamino)-1-(3-pyridyl)-1-butanone, NNK. Chemical Biological Interactions 1997; 103:153-166.

(201) Peterson LA, Hecht SS. O^6-Methylguanine is a critical determinant of 4-(methylnitrosamino)-1-(3-pyridyl)-1-butanone tumorigenesis in A/J mouse lung. Cancer Res 1991; 51:5557-5564.

(202) Lao Y, Yu N, Kassie F, Villalta PW, Hecht SS. Formation and Accumulation of Pyridyloxobutyl DNA Adducts in F344 Rats Chronically Treated with 4-(Methylnitrosamino)-1-(3-pyridyl)-1-butanone and Enantiomers of Its Metabolite, 4-(Methylnitrosamino)-1-(3-pyridyl)-1-butanol. Chem Res Toxicol 2007; 20(2):235-245.

(203) Peterson LA, Matthew R, Murphy SE, Trushin N, Hecht SS. *In vivo* and *in vitro* persistence of pyridyloxobutyl DNA adducts from 4-(methylnitrosamino)-1-(3-pyridyl)-1-butanone. Carcinogenesis 1991; 12:2069-2072.

(204) Weng Y, Fang C, Turesky RJ, Behr M, Kaminsky LS, Ding X. Determination of the role of target tissue metabolism in lung carcinogenesis using conditional cytochrome P450 reductase-null mice. Cancer Res 2007; 67(16):7825-7832.

(205) Smith BD, Sanders JL, Porubsky PR, Lushington GH, Stout CD, Scott EE. Structure of the human lung cytochrome P450 2A13. J Biol Chem 2007; 282(23):17306-17313.

(206) Schlicht KE, Zinggeler-Berg J, Murphy SE. Effect of CYP2A13 Active Site Mutation Asn297Ala on Metabolism of Coumarin and Tobacco-specific Nitrosamines. Drug Metab Dispos 2008; in press.

(207) Guengerich FP, Wu ZL, Bartleson CJ. Function of human cytochrome P450s: characterization of the orphans. Biochem Biophys Res Commun 2005; 338(1):465-469.

(208) Oscarson M, McLellan RA, Asp V, Ledesma M, Ruiz ML, Sinues B et al. Characterization of a novel CYP2A7/CYP2A6 hybrid allele (CYP2A6*12) that causes reduced CYP2A6 activity. Hum Mutat 2002; 20(4):275-283.

(209) Koskela S, Hakkola J, Hukkanen J, Pelkonen O, Sorri M, Saranen A et al. Expression of CYP2A genes in human liver and extrahepatic tissues. Biochem Pharmacol 1999; 57(12):1407-1413.

(210) Su T, Bao Z, Zhang QY, Smith TJ, Hong JY, Ding X. Human cytochrome P 450 CYP2A13: Predominant expression in the respiratory tract and in high efficiency metabolic activation of a tobacco-specific carcinogen, 4-(methylnitrosamino)-1-(3-pyridyl)-1-butanone. Cancer Res 2000; 60:5074-5079.

(211) Patten CJ, Smith TJ, Murphy SE, Wang MH, Lee J, Tynes RE et al. Kinetic analysis of activation of 4-(methylnitrosamino)-1-(3-pyridyl)-1-butanone by heterologously expressed human P450 enzymes, and the effect of P450 specific chemical inhibitors on this activation in human liver microsomes. Arch Biochem Biophys 1996; 333:127-138.

(212) von Weymarn LB, Murphy SE. CYP 2A13-catalyzed coumarin metabolism, comparison to CYP2A5 and CYP2A6. Xenobiotica 2003; 33:73-81.

(213) Ding S, Lake BG, Friedberg T, Wolf CR. Expression and alternative splicing of the cytochrome P450 CYP2A6. Biochem J 1995; 306:161-166.

(214) Boyd GW, Coombs MM, Baird WM. The presence of a trifluoromethyl rather than a methyl substituent in the bay-region greatly decreases the DNA-binding and tumour-initiating activity of the cyclopenta[*a*]phenanthren-17-ones. Carcinogenesis 1995; 16:2543-2547.

(215) Oscarson M. Genetic polymorphisms in the cytochrome P450 2A6 (CYP2A6) gene: implications for interindividual differences in nicotine metabolism. Drug Metab Dispos 2001; 29(2):91-95.

(216) Mwenifumbo JC, Lessov-Schlaggar CN, Zhou Q, Krasnow RE, Swan GE, Benowitz NL et al. Identification of Novel CYP2A6*1B Variants: The CYP2A6*1B Allele is Associated With Faster In Vivo Nicotine Metabolism. Clin Pharmacol Ther 2008; 83(1):115-121.

(217) Tyndale RF, Sellers EM. Genetic variation in CYP2A6-mediated nicotine metabolism alters smoking behavior. Ther Drug Monit 2002; 24(1):163-171.

(218) von Weymarn LB, Sridar C, Hollenberg PF. Identification of Amino Acid Residues Involved in the Inactivation of Cytochrome P450 2B1 by Two Acetylenic Compounds: The Role of Three Residues in Non-Substrate Recognition Sites. J Pharmacol Exp Ther 2004.

(219) Jordan M, Schallhorn A, Wurm FM. Transfecting mammalian cells: Optimization of critical parameters affecting calcium-phosphate precipitate formation. Nucleic Acids Res 1996; 24(4):596-601.

(220) von Weymarn LB, Felicia ND, Ding X, Murphy SE. *N*-Nitrosobenzylmethylamine α-hydroxylation and coumarin 7-hydroxylation by rat esophageal microsomes and cytochrome P450 2A3 and 2A6 enzymes. Chem Res Toxicol 1999; 12:1254-1261.

(221) Cox SK, Hamner T, Bartges J. Determination of 6-hydroxychlorzoxazone and chlorzoxazone in porcine microsome samples. Journal of Chromatography B-Analytical Technologies in the Biomedical and Life Sciences 2003; 784(1):111-116.

(222) Larson JR, Coon MJ, Porter TD. Purification and Properties of A Shortened Form of Cytochrome-P-450 2E1 - Deletion of the Nh2-Terminal Membrane-Insertion Signal Peptide Does Not Alter the Catalytic Activities. Proc Natl Acad Sci U S A 1991; 88(20):9141-9145.

(223) International Agency for Research on Cancer. IARC monographs programme finds smokeless tobacco is carcinogenic to humans. IARC Press Release No 154 2005.

(224) Zhu LR, Thomas PE, Lu G, Reuhl KR, Yang GY, Wang LD et al. CYP2A13 in human respiratory tissues and lung cancers: an immunohistochemical study with a new peptide-specific antibody. Drug Metab Dispos 2006; 34(10):1672-1676.

(225) Yano JK, Hsu MH, Griffin KJ, Stout CD, Johnson EF. Structures of human microsomal cytochrome P450 2A6 complexed with coumarin and methoxsalen. Nat Struct Mol Biol 2005; 12(9):822-823.

(226) Honkakoski P, Negishi M. The structure, function, and regulation of cytochrome P450 2A enzymes. Drug Metab Rev 1997; 29:977-996.

(227) Born SL, Rodriguez PA, Eddy CL, Lehmann-McKeeman LD. Synthesis and reactivity of coumarin 3,4-epoxide. Drug Metab Dispos 1997; 25:1318-1323.

(228) Vassallo JD, Hicks SM, Born SL, Daston GP. Roles for epoxidation and detoxification of coumarin in determining species differences in clara cell toxicity. Toxicol Sci 2004; 82(1):26-33.

(229) von Weymarn LB, Zhang QY, Ding X, Hollenberg PF. Effects of 8-methoxypsoralen on cytochrome P450 2A13. Carcinogenesis 2005; 26(3):621-629.

(230) von Weymarn LB, Blobaum AL, Hollenberg PF. The mechanism-based inactivation of p450 2B4 by tert-butyl 1-methyl-2-propynyl ether: structural determination of the adducts to the p450 heme. Arch Biochem Biophys 2004; 425(1):95-105.

(231) Shultz MA, Choudary PV, Buckpitt AR. Role of murine cytochrome P-4502F2 in metabolic activation of naphthalene and metabolism of other xenobiotics. J Pharmacol Exp Ther 1999; 290(1):281-288.

(232) Vassallo JD, Morrall SW, Fliter KL, Curry SM, Daston GP, Lehman-McKeeman LD. Liquid chromatographic determination of the glutathione

conjugate and ring-opened metabolites formed from coumarin epoxidation. J Chromatogr B Analyt Technol Biomed Life Sci 2003; 794(2):257-271.

(233) Nakamura K, Hanna IH, Cai HL, Nishimura Y, Williams KM, Guengerich FP. Coumarin substrates for cytochrome P450 2D6 fluorescence assays. Analytical Biochemistry 292[2], 280-286. 5-15-2001.
Ref Type: Journal (Full)

(234) Sansen S, Hsu MH, Stout CD, Johnson EF. Structural insight into the altered substrate specificity of human cytochrome P450 2A6 mutants. Arch Biochem Biophys 2007; 464(2):197-206.

(235) Upadhyaya P, Kenney PMJ, Hochalter JB, Wang M, Hecht SS. Tumorigenicity and metabolism of 4-(methylnitrosamino)-1-(3-pyridyl)-1-butanol (NNAL) enantiomers and metabolites in the A/J mouse. Carcinogenesis 1999; 20:1577-1582.

(236) Human UDP-glucuronosyltransferases 1A7 and 1A9 form N- and N-OH linked glucuronides from procarcinogens. 2000.

(237) Carmella SG, Le KA, Upadhyaya P, Hecht SS. Analysis of N- and O-glucuronides of 4-(methylnitrosamino)-1-(3- pyridyl)-1-butanol (NNAL) in human urine. Chem Res Toxicol 2002; 15:545-550.